International
Progress Report

IPR-03-13

Äspö Hard Rock Laboratory

Äspö Task Force on modelling of groundwater flow and transport of solutes

Task 6c

A semi-synthetic model of block scale conductive structures at the Äspö HRL

William Dershowitz, Golder Associates Inc
Anders Winberg, Conterra AB
Jan Hermanson, Golder Associates AB
Johan Byegård, GEOSIGMA AB
Eva-Lena Tullborg, Terralogica AB
Peter Andersson, GEOSIGMA AB
Martin Mazurek, University of Bern

March 2003

Svensk Kärnbränslehantering AB
Swedish Nuclear Fuel
and Waste Management Co
Box 5864
SE-102 40 Stockholm Sweden
Tel +46 8 459 84 00
Fax +46 8 661 57 19

Äspö Hard Rock Laboratory

Report no.
IPR-03-13
No.
F65K
Author
Bill Dershowitz
Anders Winberg
Jan Hermanson
Johan Byegård
Eva-Lena Tullborg
Peter Andersson
Martin Mazurek
Date
Mars 2003
Checked by
Jan-Olof Selroos
Date
Mars 2003
Approved
Christer Svemar
Date

Äspö Hard Rock Laboratory

Äspö Task Force on modelling of groundwater flow and transport of solutes

Task 6c

A semi-synthetic model of block scale conductive structures at the Äspö HRL

William Dershowitz, Golder Associates Inc
Anders Winberg, Conterra AB
Jan Hermanson, Golder Associates AB
Johan Byegård, GEOSIGMA AB
Eva-Lena Tullborg, Terralogica AB
Peter Andersson, GEOSIGMA AB
Martin Mazurek, University of Bern

March 2003

Keywords: Block scale, micro-structural, model, PA, retention, semi-synthetic

Foreword

This report presents the information needed to construct a semi-synthetic, fractured granite hydrostructural model for use in the Äspö Task Force Task 6 PASC Project (Performance Assessment Modelling using Site Characterisation data). The information supports two scales of model construction — a 200 m block-scale model and a 2000 m site-scale model. Studies of flow and transport performed as part of Task 6 will use the deterministic 200 m scale hydrostructural models as a common modelling framework. The 2000-m Site Scale model is defined primarily to provide a context for assignment of boundary conditions to the 200 m scale model.

Abstract

A semi-synthetic hydrostructural model was developed based on conditions at the TRUE Block scale site in the south-west of the Äspö Hard Rock Laboratory. This model was built through a combination of deterministic and stochastic analyses of hydraulically significant structural features at scales from millimetres to kilometres. The 200-m scale hydrostructural model combines features of 0 to 20 m ("Background Fractures"), 20 to 200 m ("100 m structures") and 200 to 2000-m ("1000 m Structures") length scales. At each scale, structures are described with regards to their geometric, hydraulic, and transport properties. Microstructural models are provided for the structures at each scale, including fault gouge, altered wall rock, and fracture coating.

Sammanfattning

En delvis syntetisk modell av konduktiva strukturer konstruerades med utgångspunkt från de geologiska och hydrogeologiska förhållandena i TRUE Block Scale siten i Äspölaboratoriet. Denna modell togs fram med hjälp av en kombination av deterministisk och stokastisk analys av hydrauliskt signifikanta strukturer över en rumslig skala med spännvidd från millimeter till kilometer. Modellen som kontruerats i 200 m skala kombinerar bergmassans normala sprickighet (background fractures, med spricklängder upp till 20 m) med "100 m strukturer" (20-200 m) och "1000 m strukturer" (200-2000 m). För varje rumslig skala ges en beskrivning vad avser ingående strukturers geometri och egenskaper som bestämmer flöde och transport. Modeller som beskriver mikrostruktur ges på varje skala och inkluderar bl a beskrivning av okonsoliderade sprickfylllnader (fault gouge), omvandlat sidoberg och sprickmineralbeläggning.

Executive Summary

A semi-synthetic hydrostructural model was developed based on conditions at the TRUE-Block scale region in the south-west of the Äspö Hard Rock Laboratory. This model was built using both deterministic and stochastic analyses of hydraulically significant structural features at scales from millimetres to kilometres.

The 200x200x200-m Task 6C hydrostructural model is based on the March 2000 TRUE Block Scale hydrostructural model, with adjustments based on additional analyses. The 200-m scale model is set within the context of a 2000-m scale "Site Scale model". Both models are formed as a combination of 1000-m and 100-m scale structures and background fractures. At each scale, structures are described based on their geometric, hydraulic, and transport properties. Microstructural models are provided for the structures at each scale, including fault gouge, altered wall rock and fracture coating.

The difference compared to previously developed hydrostructural models of Äspö island and its environs is that the Task 6C models attempts to interpolate both between scales and within space to produce a model that honours both available data and provides a realistic picture of conditions where characterisation data are absent. This extrapolation is made using classical discrete feature network (DFN) analysis techniques, combined with empirical data from structural geology and geochemistry.

The structures identified are attributed to two basic geological structure types; "Fault" (Type 1) and "Non-fault" (Type 2). A basic description and visualisation of the two types and their characteristic components (including intact unaltered wall rock, altered zone, cataclasite, fault gouge and fracture coating) are provided. Geometric (thickness/extent) and transport (porosity, formation factor and K_d) parameters are assigned to the two types.

Scaling laws are derived to assign geological structure type, hydraulic, and transport properties to structures of all scales.

Contents

1	**Introduction**	**17**
1.1	Purpose of Report	17
1.2	Context of Sub-Task 6C within Modelling Task 6	18
1.3	Temporal scales, spatial scales, and boundary conditions	20
1.4	Data sources and candidate Task 6C prototypes	21
1.4.1	TRUE-1	22
1.4.2	Prototype Repository	22
1.4.3	TRUE Block Scale	23
1.4.4	Fracture Characterisation and Classification	23
1.4.5	Site scale models	24
1.5	Selection of a prototype for the Task 6C semi-synthetic hydrostructural model	24
1.6	Outline of detailed approach to Task 6C	25
1.7	Disclaimer	26
2	**Micro-structural Elements of Hydrostructural Model**	**27**
2.1	Available database	29
2.2	Definition of micro-structural models	29
2.2.1	Concept	29
2.2.2	Base case Geological Structure Types	29
2.2.3	Mineralogy	32
2.2.4	Porosity	37
2.2.5	Formation factor	37
2.2.6	Effective diffusivity D_e	38
2.2.7	Volumetric distribution coefficient K_d	38
2.2.8	Surface sorption coefficient K_a	40
2.2.9	Groundwater composition	40
2.2.10	Potential influence of heterogeneity, surface diffusion and anion exclusion	41
3	**Structures and Background Fractures**	**47**
3.1	Available database	47
3.2	Background fractures	47
3.3	100-m Scale Structures	52
3.3.1	TRUE Block Scale Structures	52
3.3.2	Synthetic 100-m Structures	55
3.4	1000-m Scale Structures	56
3.5	Structure heterogeneity	57

4 Approach for assignment of properties to synthetic structures 61
4.1 Overview 61
4.2 Structure geometry 61
4.3 Hydraulic properties 62
4.4 Microstructural model 64
4.4.1 Geological Structure Type 65
4.4.2 Structure Complexity 69
4.4.3 Scaling of parameters of Microstructural models 78

5 Semi-synthetic hydrostructural models 81
5.1 Block scale (200-m) Semi-Synthetic Hydrostructural Model 81
5.2 Site scale (2000-m) Semi Synthetic Hydrostructural Model 89

6 Boundary Conditions 97
6.1 Block Scale (200-m) 97
6.2 Site scale (2000-m) 98
6.3 Block Scale tracer tests 99

7 Discussion and recommendations 101

8 References 103

Appendix A – Scaling rules 110
A.1 Size 111
A.2 Geological Width 113
A.3 Size and Transmissivity 115
A.4 Transport Properties 116
A.5 Geological Structure Type and Complexity Factor 117

Appendix B: Example assignment of properties to synthetic structures 123
B.1 Overview 123
B.2 Structure Length 123
B.3 Hydraulic and transport properties 124
B.4 Geological and Microstructural Properties 125
B.5 Microstructural Model Parameters 126

List of Figures

Figure 2-1. Flow chart showing the basic simplifications used for the micro/macro semi-synthetic structure model. 28

Figure 2-2. Illustration of the Geological Structure Type 1 (Fault). 30

Figure 2-3. Illustration of Geological Structure Type 2 (Non-fault). 31

Figure 2-4. Influence of the water composition on the sorption coefficients. Examples are given for the contact with fault gouge material (top) with a CEC estimated to 90 μeq/g together with the intact unaltered wall rock (bottom) with a CEC estimated to 5.7 μeq/g. 35

Figure 2-5. Comparisons of calculated and experimentally determined K_d for intact unaltered wall rock (top) and cataclasite (bottom). The calculated K_d values are based on the TRUE Block Scale water composition, which is very similar to the TRUE-1 water composition used in the laboratory experiments (cf. Byegård et al. 1998). 36

Figure 2-6. Histogram of porosity as mapped on the surface (top, left) for intact unaltered Äspö diorite, measured from autoradiographs of ^{14}C-PMMA impregnation (middle, right). The line corresponds to a fitted log-normal distribution of the porosity, $\varepsilon=10^{(-2.75\pm0.44)}$. A photograph of the rock sample is also shown (upper, right). An experimentally determined penetration profile for Cs^+ in Äspö diorite, contact time 472 d, is also presented (bottom). In this graph, comparisons are made with a fitted penetration profile using a porosity distribution model (solid line) and to the results of a calculation using a homogeneous single porosity model with the retention parameters recommended in this report (dashed line). 44

Figure 2-7. Histogram of porosity as mapped on the surface (top, left) for altered diorite/mylonite, measured from autoradiographs of ^{14}C-PMMA impregnation (middle, right). The line corresponds to a fitted log-normal distribution of the porosity, $\varepsilon=10^{(-2.06\pm0.39)}$. A photograph of the rock sample is also shown (top, right). An experimentally determined penetration profile for Cs^+ in altered diorite/mylonite (contact time 1143 d) is also presented (bottom). In this graph, comparisons are made to a fitted penetration profile using a porosity distribution model (solid line) and the results of a calculation using a homogeneous single porosity model with the retention parameters recommended in this report (dashed line). 45

Figure 3-1. Orientations of background fractures throughout Äspö HRL. 47

Figure 3-2. Stereonet of "Background fracture set #2", cf. Table 3-1. 51

Figure 3-3. Stereonet of "Background fracture set #1", cf. Table 3-1. 51

Figure 3-4. Simplified representation of Structure #20 intersections with TRUE Block Scale boreholes. 57

Figure 3-5. Stochastic transmissivity field on Structure 20 (Holton, in prep.). 58

Figure 3-6. Stochastic field of hydraulic conductivity on structures (Gómez-Hernández et al., 2002). 58
Figure 4-1. Correlation between structure/fracture size and transmissivity. 63
Figure 4-2. Flow chart showing the basic simplifications used for the micro/macro semi-synthetic structure model. 64
Figure 4-3. Relationship used for assignment of Geological Structure Type to synthetic 100 m structures and background fractures. 67
Figure 4-4. Illustration of the areal coverage of the two different geological structure type concepts. The structures included in the Task 6C reference hydro-structural model contain different areal proportions of geological structure Type 1 and Type 2 along their extent. In the illustration these proportions are roughly 50% geological structure Type 1 and 50% Type 2 + Type 1. 70
Figure 4-5. Illustration of geological complexity and the assignment of models of geological structure type over length scales from cm scale to the 200 m reference case Task 6C hydrostructural model. 73
Figure 4-6. Relationship between Complexity Factor and structure size for TRUE Block Scale deterministic 100 m scale structures. 77
Figure 5-1. Deterministic 100 m scale structures in the 200-m scale model region. 84
Figure 5-2. Synthetic 100-m Structures (Blue) with Deterministic 100-m Structures (Red) in 200-m Scale Model. 84
Figure 5-3. Deterministic 100 m scale structures coloured according to transmissivity. 85
Figure 5-4. Horizontal section (trace map) through the deterministic 100 m structures of the 200 m model at Z= –450 masl. 85
Figure 5-5. Background fractures coloured by set, Shallow set (blue), NNW (yellow). 88
Figure 5-6. Background fractures coloured by transmissivity (log scale). 89
Figure 5-7. 1000-m Scale Structures. 90
Figure 5-8. 1000 m scale structures in the 2000 m scale model coloured according to their transmissivity. 95
Figure 5-9. Synthetic 100 m scale structures in the 2000 m scale model. 95
Figure 5-10. Plan view trace map of synthetic 100 m scale structures in the 2000 m scale model at Z= –450-masl. 96
Figure 5-11. Visualisation of background fractures in the 2000 m model. Size cut-off employed : L>10m. 96
Figure 6-1. Boundary Conditions on 200-m model block (NB not conditioned to measure hydraulic head in boreholes). 97
Figure 6-2. Fresh-water hydraulic head (m) at the top of the 2000-m model. 99
Figure 6-3. Test C2 injection functions for Re-186, Ca-47, Ba-131, and Cs-137. 100

List of Tables

Table 1-1. Spatial scales considered within the scope of Task 6C. 20
Table 2-1. Properties of 100-m Scale Geological Structure Type 1 (Fault) 32
Table 2-2. Properties of 100-m Scale Geological Structure Type 2 (Non-fault) 32
Table 2-3. Mineralogical composition combined with the calculation of the cation exchange capacity of the rock types used in the concept applied to Task 6C. 33
Table 2-4. Calculated K_d for the different materials in contact with the different types of groundwater c.f. Section 2.2.6. 34
Table 2-5. Calculated formation factors for relevant geological materials. 37
Table 2-6. Effective diffusivities for the different tracers in contact with the different types of geologic material. The diffusivities has calculated using the formation factor, F, (cf. Section 2.2.5) and the tabulated water diffusivities, Dw 38
Table 2-7. Sorption coefficients for Ra^{2+} estimated according to the procedure outlined in the text above. 40
Table 2-8. Composition of groundwaters used for calculations of K_d values. 41
Table 2-9. Complementary data on diffusivity for the different tracers in contact with the different types of geologic material in a fresh groundwater environment, i.e., the anion exclusion and surface diffusion processes have been addressed. Values are only presented for those tracers for which the diffusivities can be a subject to correction for the surface diffusion and anion exclusion according to the concept given in the text. For the diffusivities for the other groundwater environments and for the other tracers, reference is made to Table 2-6. 43
Table 3-1. Parameters of a DFN model of conductive background fractures in the TRUE Block Scale tracer test area (Andersson et al., 2002a). 48
Table 3-2. Compilation of analyses of size of conductive background fracture population. 49
Table 3-3. Transmissivity and intensity of conductive background fracture population. 50
Table 3-4. Corner coordinates of interpreted deterministic structures of the TRUE Block Scale 200-m model (Hermanson and Doe, 2000). 53
Table 3-5. Summary of transmissivity established for the interpreted TRUE Block Scale deterministic structures. Example values of transmissivity (m^2/s) and hydraulic conductivity (m/s) are given for reference for the calibrated TRUE Block Scale numerical 3D flow models. 54
Table 3-6. Attribution of geologic categorisation to 100 m scale deterministic structures (based on information in Andersson et al., (2002a). 55
Table 3-7. Statistical properties for 100-m scale synthetic structures. 56
Table 3-8. Properties of generated geostatistical stochastic fields of hydraulic material property data 59

Table 4-1. Geological Structure Type assigned to 100-m Scale deterministic structures 66
Table 4-2. Geological Structure Type assigned to 1000-m Scale deterministic structures 66
Table 4-3. Geological Structure Type assigned to synthetic 100 m structures. 68
Table 4-4. Geological Structure Type assigned to synthetic background fractures (Sample of N=5648 background fractures in 200 m model) 69
Table 4-5. Definition of Complexity Factor assigned to modelled synthetic structures (cf. Table 4-3 for application to 100 m scale synthetic structures). 71
Table 4-6. Complexity Factor assigned to 100 m scale deterministic structures. 71
Table 4-7. Complexity Factor assigned to deterministic 1000-m Scale structures 72
Table 4-8. Detailed Assignment of "Overall Complexity" to the deterministic TRUE Block Scale100-m Scale Structures 75
Table 4-9. Probability of a given complexity factor for typical scales of synthetic structures. 76
Table 4-10. Scaled geometrical properties of the microstructural model related to Geological Structure Type 1 attributed to their occurrence at different length scales, ranging in length. Geometrical properties are specified per discrete feature within the structure. 79
Table 4-11. Scaled geometrical properties of the microstructural model related to Geological Structure Type 2 attributed to their occurrence at different length scales, ranging in length from 0.5 m fractures to >1000 m fracture zones. Geometrical properties are specified per discrete feature within the structure. 79
Table 5-1. Deterministic structures of the Task 6C reference case 200 m semi-synthetic hydrostructural model (based on Hermanson and Doe, 2000). 82
Table 5-2. Stochastic 100m scale structures in the Task 6C reference case 200 m scale semi-synthetic hydrostructural model. 83
Table 5-3. Example sample (20 Fractures) from background fracture realisation used in Task 6C reference case semi-synthetic hydrostructural models 87
Table 5-4. Example sample of synthetic background fractures in Task 6C reference case semi-synthetic 2000 m hydrostructural models. 91
Table 5-5. Synthetic 100 m scale structures the Task 6C reference case semi-synthetic 2000 m hydrostructural model. 92
Table 5-6. Geometric properties of 1000 m scale structures employed in Task 6C reference case semi-synthetic hydrostructural models (data from Rhén et al., 1997) 93
Table 5-7. Hydrogeological properties 1000 m scale structures included in Task 6C reference case semi-synthetic hydrostructural models - (data from Rhén et al., 1997). 94
Table 6-1. Hydraulic head boundary conditions on the 200 m model rock block faces (Example). 98
Table 6-2. Net fluxes on the faces of 2000 m scale model rock block. 99
Table 6-3. Experimental specifics for TRUE Block Scale Phase C tracer injection C2 (primarily based on Andersson et al., 2002b). 100
Table 6-4. Measured and estimated Test C2 injection activity. 100

1 Introduction

1.1 Purpose of Report

This report presents the information needed to construct a semi-synthetic, fractured granite hydrostructural model for use in the Task 6 PASC project (Performance Assessment modelling using Site Characterisation data). The information supports two scales of model construction — a 200 m block-scale model and a 2000 m site-scale model. Task 6 studies of flow and transport codes will use the 200-m scale hydrostructural models as a common modelling framework (Tasks 6D and 6E). The 2000-m Site-Scale model is defined primarily to provide context for the 200-m scale model.

Data from several programs at the Äspö Hard Rock Laboratory provide the bases for constructing the Task 6C hydrostructural model. Although the intent is not to simulate a specific site, the models employ the networks of major conductive features that were identified in the Äspö TRUE Block Scale experiment (Andersson et al., 2002a) and the Äspö site-scale characterisation programs (Rhén et al., 1997). In addition to the identified features from the Äspö Hard Rock Laboratory, the models also contain synthetic fracture networks that have been generated based on geometric statistics from the TRUE Block-Scale program. Because the models contain both interpreted deterministic and synthesised features, the term *semi-synthetic* is applied to describe the models developed as part of this work.

The developed semi-synthetic models provide a common basis for comparing different numerical models of flow and transport. The hydrostructural models in this report support the efforts of Modelling Task 6 of the Äspö Modelling Task Force. Task 6 is an effort to compare and integrate flow and transport codes that are used for site characterisation (SC) with codes that are used in performance assessment (PA).

This report completes Task 6C, the third of five Task 6 tasks, which is the development of the semi-synthetic hydrostructural model. Benabderrahmane et al. (2000) define the objectives and scope of Task 6C as the following:

> *… to "develop a 50-100m block scale synthesised structural model using data from the Prototype Repository, TRUE Block Scale, TRUE-1 and FCC. The structural model should also be complemented with a hydraulic parameterisation. It is suggested that a deterministic rather than a stochastic model is constructed so that the differences between models will be results of variations in assumptions, simplifications, and implementation rather than in the structural framework. The structural model will include sufficient elements of the TRUE Block Scale experiment to make it possible to reproduce a TRUE Block Scale tracer experiment as part of Task 6D. It is also suggested that Task 6C is performed by a single group led by SKB in order to provide a structural model that fulfils the needs of all modelling teams*".

The following is a reading guide to the material contained in this report:

Chapter 1 provides the background to Task 6C and presents the objectives of the work and the basic work approach.

Chapters 2 and 3 present the development of the individual elements that make up the hydrostructural model. Chapter 2 derives the micro-structural elements and Chapter 3 derives background fractures and larger conductive structures.

Chapter 4 derives and describes the procedure used to apply hydraulic, transport, and micro structural properties to structures.

Chapter 5 presents the development of hydrostructural models at the 200-m and 2000-m scales.

Chapter 6 defines the boundary conditions for the models at the two scales and also provides description of boundary conditions for a select set of block scale tracer tests.

Chapter 7 presents a discussion of the Task 6C hydrostructural model, and recommendations for its application.

Appendix A present a compilation of the scaling rules applied in the present work.

Appendix B provides an example assignment to an arbitrary synthetic structure.

1.2 Context of Sub-Task 6C within Modelling Task 6

Although site characterisation codes and performance assessment codes use similar physical concepts, their constructions differ due to their different purposes. Site characterisation codes represent the entire flow system of a volume of rock. The models include full three-dimensional representations of the major conducting features, either as discrete features or stochastic continua. The boundary conditions attempt to be detailed and realistic. Site characterisation codes are used to design, predict, and analyse experimental activities. They are used to test conceptual models of the hydrostructural framework, and to develop realistic flow and transport parameters.

Site characterisation codes, because of their detail, require significant effort in their construction and execution. Site characterisation codes often require extensive and time-consuming calibration to available field data.

Performance assessment codes have different purposes than site characterisation codes. Performance assessment codes consider a wide range of scenarios for the projected post-closure life of a repository. These problems often include all relevant features, events, and processes with all their attendant uncertainties. Hence, a performance assessment code must be capable of producing many realisations by being very fast and flexible. Due to their detail and complexity, site characterisation codes are generally not practical for direct application to performance assessment problems where many parameters must be systematically varied, or many different scenarios must be tested.

Performance assessment codes respond to these requirements by simplifying the description of the flow system and abstracting the natural system to one-dimensional pathways or networks of one-dimensional pathways. These pathways and their associated properties may be extracted from the results of site characterisation codes. With these simple models, one can run many scenarios and variations over the long time scales that are required for performance assessment calculations.

The process of simplification from site characterisation data to performance assessment codes should involve an extraction of the critical aspects of the site characterisation information. The extraction requires the reduction of a detailed site characterisation model to simple features with properties and geometries that produce equivalent flow and transport behaviours. The effectiveness of the procedure for performing these extractions from site characterisation to performance assessment is a critical issue for repository development.

Äspö Task Force Task 6 consists of a set of numerical experiments that use on a common set of hydrostructural models to test performance assessment codes and site characterisation codes. The comparison of the results of these simulations serves several objectives (Benabderrahmane et al, 2000):

1. Assessment of simplifications used in PA models.
2. Determination of how the experimental tracer and flow experiments can constrain the range of parameters used in PA models.
3. Support of the design of site characterisation programs to assure that the results have optimal value for performance assessment calculations.
4. Better understanding of site-specific flow and transport behaviour at different scales using site characterisation models.

The objectives of Task 6 are being met through an iterative process of SC model implementation, calibration to in situ experiments, PA type simulations, and sensitivity studies. In this process Task 6 will primarily focus on the 50 to 100 m block scale (Tasks 6D and 6E) which is the critical scale for geosphere retention for many repository assessment programs. However, in order to allow for a more direct comparison, initial simulations will be carried out using data from the TRUE-1 site at the 5 metre scale (Tasks 6A, 6B and 6BII). The latter three tasks have been worked upon during 2001-2002. Irrespective of scales of application the main purpose of the modelling is to assess how different conceptualisations at the two scales considered compare to each other.

Tasks 6D and 6E is preceded by Task 6C which involves construction of a semi-synthetic block scale model which integrates available information from the Äspö HRL and which will serve as a basis for the subsequent modelling phases. The current report presents the results of Task 6C.

1.3 Temporal scales, spatial scales, and boundary conditions

The comparison of SC and PA models will use a range of temporal and spatial scales. Flow and transport at the two (or optionally three) spatial scales will be analysed for both experimental boundary conditions and for PA relevant hydraulic boundary conditions and PA relevant time scales. Each modelling group may address four or more different combinations of spatial and temporal scales.

The time scales for simulations are:

- ***Tracer test time scale (Tracer test mode):*** Models will address the TRUE-1 and TRUE Block Scale tracer experiments, which ran for periods up to a few months to a few years. Tracer test time scale modelling provides means for a calibration of PA models to in situ measurement data.
- ***PA time scale (PA mode):*** Radionuclide and/or sorbing tracer transport modelling with PA type boundary conditions will be performed over performance assessment time scales, which are set at different times by each national repository program. Typical time scales involve a few thousand to tens of thousands of years.

The spatial scales for simulation include:

- ***Detailed spatial scale***: Transport is considered on the detailed scale of a single conducting feature that provides a pathway from a canister to a network of fractures. This scale was the focus of the experiments of the TRUE-1 program (Winberg et al., 2000).
- ***Block spatial scale***: Transport is considered from a single, TRUE-1 type fracture to a major conductive structures through a network of fractures and structures similar to those defined by the TRUE Block Scale project (Andersson et al., 2002a, Hermanson and Doe, 2000), or the Prototype Repository project (Patel and Dahlström, in prep, Rhén et al., in prep.).
- ***Site spatial scale (optional):*** This scale extends from the block scale to the biosphere through major structural features such as those defined in the Äspö HRL site descriptive model (Rhén et al. 1997, Mazurek et al., 1997)). For this option, geochemical data may also be utilised similar to Task 5 (i.e., models may be tested using data on current geochemical conditions).

Table 1-1. Spatial scales considered within the scope of Task 6C.

Scale	L (m)	Data source: Project/model
Detailed scale	L < 20	TRUE-1 Long-term Diffusion Experiment (Prototype Repository) FCC-III
Block Scale	20 < L <200	TRUE Block Scale Prototype Repository FCC-II (TRUE-1)
Site scale	200 < L < 2000	Äspö site conceptual model FCC-II

The hydraulic boundary conditions will include both SC and PA types. SC boundary conditions are those that exist during the experimental programs and include the underground excavations as sinks. The SC boundary conditions entail high hydraulic gradients and relatively rapid groundwater velocities compared with those produced by PA boundary conditions.

PA boundary conditions are either those conditions that existed before underground excavation or those that are restored following repository closure. The PA boundary condition will produce low hydraulic gradients and low groundwater velocities.

One objective of using both the SC and PA hydraulic boundary conditions is to investigate the relative roles of different transport and retention processes under the different conditions. For example, matrix-fracture interactions should become more pronounced during the lower groundwater flow velocities resulting from applied PA boundary conditions. On the other hand, advective transport will be a stronger process under the boundary conditions applied during the TRUE tracer tests, which are governed by more extreme hydraulic boundary conditions.

1.4 Data sources and candidate Task 6C prototypes

The experiments performed at the Äspö HRL relate to different aspects of geological disposal. Among the experimental categories are the following:

- demonstration of disposal technology and retrieval
- evaluation of engineered barrier systems(including prototype disposal)
- evaluation of natural barriers (radionuclide migration, microbial effects, two phase flow effects)

The three groups of projects require different types and amounts of characterisation. The disposal technology and engineered barrier projects require mechanical and hydraulic information on a detailed scale (< 20m)[1]. The natural barrier experiments, on the other hand, require more extensive, larger-scale geological, hydraulic and chemical characterisation. Furthermore, defining the boundary conditions for an experiment may require characterisation from boreholes covering volumes in the order of 70-100 10^6 m^3 (for example, the TRUE Block Scale experiment, Winberg, 1997, Andersson et al, 2002a). Detailed scale natural barrier experiments may also require knowledge from block scale characterisation, e.g. the TRUE-1 experiment (Winberg et al., 2000).

The following sections briefly describe the experiments at the Äspö Hard Rock Laboratory that provide information for building semi-synthetic hydrostructural models.

[1] The Prototype Experiment, which is partly funded by the European Commission (REF), is an exception in requiring larger scale geoscientific information of highly variable character in addition to the detailed-scale information.

1.4.1 TRUE-1

The TRUE-1 experiment (Winberg et al., 2000) involved a detailed characterisation of a feature that was interpreted as a single fracture. The characterisation effort collected geological and hydraulic information using a borehole array covering a 50x20x20-m volume. Additional information was also obtained from the access tunnel and nearby boreholes that were drilled as part of other experiments. The TRUE-1 program collected only limited data on retention and transport parameters (Byegård et al, 1998, Byegård et al, 2001).

Descriptive and conceptual models of the TRUE-1 site are presented by Winberg et al. (2000), Mazurek et al (2002) and Neretnieks (2002). The experiment has not resolved whether the apparent retention that was observed in tracer tests could be attributed to

- fracture-rock matrix interactions in a single fracture (Cvetkovic et al., 2000), or
- multiple pathways with retention occurring in fine-grained fault gouge (Mazurek et al, 2002, Jacob et al, 2002), or
- 3-D flow effects (increased WL/q) (Neretnieks, 2002).

Elert (1999) and Elert and Svensson (2001) present accounts of the modelling work performed on the TRUE-1 experiments within the context of the Äspö Task Force.

The characterisation activities did not determine whether the investigated feature made up of one single continuous fracture or a series of near parallel interconnected fractures. Neither was presence of erodable infilling materials, such as fault gouge, certified. To resolve the uncertainties related to the origin of retention effects, the site will be injected with epoxy resin to identify open-fracture space and preserve infilling materials. Then the fracture will be overcored. This injection will be preceded by a series of complementary hydraulic and tracer tests (including tracer dilution).

1.4.2 Prototype Repository

The Prototype Repository project has a draft hydraulic descriptive model (Rhén and Forsmark, in prep.). A corresponding geological model is in preparation (Patel and Dahlström, in prep.). The plans for the project specify integrating the two models into a common hydrostructural model. In addition, a number of numerical models are available. Svensson (2002, in press.) has produces a site characterisation model (100x175x100-m) that includes the deterministic structures from both the Prototype Repository area and the TRUE Block Scale rock volume. A discrete fracture network (DFN) model of stochastically generated fractures has been prepared on the scale of a 100-m cube (Stigsson et al., 2001). The SC model includes boundary conditions obtained from a larger scale "laboratory model" (Svensson, 1999), which in turn obtains boundary conditions from an even larger-scale site model of the Äspö site (Svensson, 1997). The DFN models are assigned either synthetic boundary conditions or boundary conditions obtained from the SC "laboratory model".

1.4.3 TRUE Block Scale

A descriptive hydrostructural model and several numerical and analytical models of flow and transport have been developed for the TRUE Block Scale rock volume (Hermanson and Doe, 2000, Andersson et al. 2002a). The developed numerical flow models (Poteri et al., in prep.) account for the major deterministic structures that are interpreted to dominate flow in the investigated rock block. Information is also available on the background fracture population. Boundary conditions have either been obtained from a site-scale DFN model developed within the project, or from an existing site-scale SC model (Svensson, 1997).

Tracer experimentation at the site has been conducted at various times during the characterisation. The tracer experiments were conducted in stages, first to demonstrate test feasibility of running block scale tracer tests, then to select the best source and sink locations (Andersson et al., 2000a, 2000b), and finally to run a series of radioactive sorbing tracer tests (Andersson et al., 2001, 2002).

The field experiments were complemented by mineralogical and structural descriptions of some of the key conducting features (Andersson et al., 2002a). Laboratory studies have investigated the porosity distributions of material from fracture wall rock and breccia fragments (Kelokaski et al., 2001). Hydrochemistry data collected from packed-off borehole intervals have been used jointly with hydraulic head data and ambient groundwater flow data to corroborate the developed hydrostructural model (Andersson et al., 2002a).

During the course of the TRUE Block Scale project, flow and transport models have been used to design and predict performed experiments (hydraulic and tracer experiments). This work has intensified towards the end of the project. The modelling work performed include modelling based on AD, SC, DFN, CN, LaSAR and the POSIVA stream-tube approaches (Poteri et al, 2002).

Winberg et al. (2002) provide an overall synthesis of the work performed. The project will have an extension that will provide for longer term data collection and analysis of tracer breakthrough data.

1.4.4 Fracture Characterisation and Classification

The Phase II of the Fracture Characterisation and Classification project (FCC) included field examinations of conductive structures in the access tunnel (Mazurek et al, 1997). The work produced detailed geometrical and structural descriptions of a number of structures along the tunnel and also on the land surface. The investigations span a range of scales from microscopic to site-scale. Supporting data include mineralogical analyses and epoxy resin injections.

Phase III of the FCC (Bossart et al., 2001) presented an alternative interpretation of TRUE-1 site where the investigated rock block is interpreted to be a dense network of open fractures with a superimposed lattice of mylonitic fracture components (Mazurek et al., 2002).

1.4.5 Site scale models

Site scale hydrostructural models of the Äspö HRL have been documented by Rhén et al. (1997). Complementary studies are presented by Munier and Hermanson (1994) and Mazurek et al. (1997)

An ongoing project (GEOMOD) initiated by SKB will serve to provide an update of the descriptive model of Äspö in the fields of geology, geology, hydrogeology and chemistry.

Numerical modelling of site scale flow and transport has been performed in different contexts including evaluation of the construction phase (Svensson, 1997) (stochastic continuum), the alternative modelling project (AMP); Gylling et al. (1999) (channel network), Dershowitz et al. (1999) (DFN), Widén and Walker (1999) (SC) and in other contexts; Painter (1999) (stochastic continuum), Svensson (1999) (stochastic continuum), and Outters and Shuttle (2000) (DFN). The Äspö International Cooperation Report (ICR) series documents the earlier site-scale modelling activities of Modelling Task Force through Tasks 1, 3 and 5.

1.5 Selection of a prototype for the Task 6C semi-synthetic hydrostructural model

Two experimental areas of the Äspö HRL were candidates for the Task 6 semi-synthetic model. These regions include the Prototype Repository and TRUE Block Scale projects, both of which are located in the southwest part of the laboratory.

The database of the Prototype Repository project includes ten high quality cross-hole interference tests involving some 60 observation sections in boreholes drilled from the Prototype Repository Tunnel. No tracer tests have been performed at the site (Rhén, pers. comm.) At present the deterministic hydrostructural model consists of only 2-3 subparallel, vertical structures. These three structures are insufficient to form a conducting network of deterministic features; hence block-scale connectivity can only be achieved using stochastic background fractures. This condition is inconsistent with the premises for Task 6C, which require a basic network of deterministic features.

The TRUE Block Scale rock volume offers a relatively robust hydrostructural model of connected major deterministic structures. The block has a comprehensive database including tracer tests, and it has been the subject of numerous numerical flow and transport models. The TRUE Block Scale database includes the cross-hole hydraulic interference, tracer dilution and tracer tests that Task 6D requires for calibration purposes.

The Äspö Modelling Task Force Meeting in Goslar in September 2001 produced the following decisions and guidelines for the Task 6 project:

- Focus on a rock volume 200x200x200-m in size centred on TRUE Block Scale rock volume (larger volume included for completeness),
- Account for observed compartmentalisation/length scale of connectivity for the included deterministic structures,

- Generate structures based on available statistics (based on statistics of deterministic and background fracturing)

- Retain elements of site scale model of Äspö HRL (e.g. NE-2, EW-3, NW-1 etc.).

- Update report disposition (emphasise integration of information presently distributed in various reports, unification of terminology, production of series of clarifying figures, conceptual figures, and tables).

The further work was discussed at a workshop at Thoresta Herrgård, March 14-15, 2002. The results of the discussions at this workshop and subsequent analysis and model development form the basis for the current report.

1.6 Outline of detailed approach to Task 6C

The Task 6C semi-synthetic hydrostructural model is founded primarily on the March 2000 TRUE Block Scale hydrostructural model. The size of the model is 200x200x200-m. The semi-synthetic model fills in the uninformed parts of the 200 m scale model, and extends this 200 m scale model throughout a 2000 m scale model based on the Äspö Task 5 hydrostructural model. In the present report basic properties/characteristics related to the structures at various scales are derived, tabulated and visualised.

Boundary conditions for both 200-m and 2000-m scale models are defined. These boundary conditions are proposed to use hydraulic head boundary conditions such that explicit geometric modelling of tunnels and shafts can be avoided. Boundary conditions are also provided for selected reference tracer experiments carried out within the context of the TRUE Block Scale project.

The structures identified in the 200-m model are defined as a combination of multiple discrete features, with superimposed variations in characteristics in the plane of the features. These variations include detailed specification of the microstructural elements that are interpreted to have a strong influence on solute retention characteristics.

This report defines two types of microstructural models for conductive features in conductive structures — those that indicate of faulting/shearing (Geological Structure Type 1) or those that do not (Geological Structure Type 2). Type 1 microstructural models include features associated with faulting such as fault gouge, cataclasite and/ or mineral coatings. Based on the descriptions of conducting structures in the TRUE Block Scale rock volume, a heterogeneous distribution of geological structure types and associated properties within conducting structures is proposed. The Type 2 microstructural models, not associated with faulting, consist of intact wall rock with some alteration. Hence, an individual structure may contain a combination of geological structure types at different locations within a given conductive structure.

Chapter 2 provides basic descriptions and visualisations of the detailed components of flowing structures such as intact unaltered wall rock, altered zone, cataclasite, fault gouge, and fracture coating). Chapter 2 also assigns typical geometric descriptors of thickness and areal extent as well as transport parameters (porosity, formation factor and Kd) to the two basic microstructural models. An empirical "complexity factor" is introduced to quantify the variation in Geological Structure Type and in the number of fractures or features which make up a structure at a given scale. Since both the number of fractures and the portions of each structure that contains Type 1 or Type 2 characteristics are assumed to vary with structure size, the complexity factor is also scale dependent. Background fractures are assumed to be dominated by Type 2 features. Major structures that have extents of hundreds of metres are mainly Type 1. While a given structure of any size may contain portions of either Type 1 or Type 2, the basic approach for building the semi-synthetic models assumes that the portion of Type 2 material is greater in smaller features, and Type 1 material is more likely to occur in larger structures.

1.7 Disclaimer

The present report presents a possible methodology for abstraction of information from Äspö HRL related studies at different scales and attribution of properties to generated synthetic structures of variable sizes. The generated numerical values of various properties are intended for use in the context of Task 6. The data should not be used indiscriminately in a safety and/or performance assessment context without reviewing the underlying data, underlying uncertainties and assumptions made.

2 Micro-structural Elements of Hydrostructural Model

Radionuclide migration in the geosphere will be retarded by, sorption on mineral surfaces, diffusion/sorption in geological materials, diffusion into stagnant pore volumes and immobilisation due to precipitation and incorporation in mineral lattices. Two of these processes (sorption and matrix diffusion) are usually used in performance assessment. These two processes will interact in a complex way depending on variations in flow velocity, available "flow wetted surface area" ($2WL/q$, β), sorption capacities of the materials along the flow path and the texture and frequency of micro pores.

From different geological/structural studies at Äspö it has been pointed out that mineral assemblages in the fractures, coatings on the fracture walls and the altered wall rock deviate substantially from that of the intact unaltered bedrock (Mazurek et al., 1997, Winberg et al., 2000, Andersson et al., 2002a). Most of the fractures and fracture zones at Äspö HRL were formed early in the geologic history and hydrothermal alteration along the conductive features/structures is common. The alteration usually includes chloritisation of the biotite, saussuritisation of the plagioclase (resulting in formation of albite + epidote + sericite), and more or less extensive oxidation of magnetite to hematite. Very importantly, a low-temperature alteration is also present in faults and results in the presence of clay minerals, including swelling species, in fault rock zones and their immediate surroundings. Usually, the alteration has caused increased porosity of the wall rock. A high proportion of the water conducting structures is faults. These faults usually show traces of ductile as well as brittle deformation (mylonites as well as breccia and fault gouge formation). The microstructural models will therefore include a number of components, each having different properties with regards to radionuclide retention.

Studies of radionuclide retention at Äspö HRL include laboratory studies (sorption capacities determined by batch sorption experiments and diffusivities determined in diffusion cells). In addition *in situ* retention data of selected radionuclides are available from tracer experiments performed along specific flow paths (usually over distances from a few metres up to a maximum of 100 metres).

Both approaches, however, yield limited information about the retention effects over long time scales and at slow groundwater flow. Determination of sorption capacities applicable to longer time scales may however be determined with higher precision. On the other hand, the many variables involved in the sorption processes make the number of measurements required very large. This while not only each radionuclide should be tested with each mineral assemblage, but also using different groundwater compositions, the latter accounting for different scenarios. There are obvious shortcomings in the available laboratory sorption database (too few measurements on representative materials from mylonites/cataclasite/altered wall rock and no relevant measurements on fault gouge). Furthermore, one large challenge that remains is to determine the structure of the interconnected pore space from the fracture coating, through the altered zone into intact unaltered rock. In addition there is a need to assess the *in situ* porosity of the fault gouge in fault rock zones.

The subsequent sections describe the development of the micro-structural components of the hydrostructural model and attribution of retention parameters. These components in combination will be assigned to each conductive structure/feature within the developed semi-synthetic models. The basic approach is outlined in Figure 2-1 and is detailed in the subsequent sections.

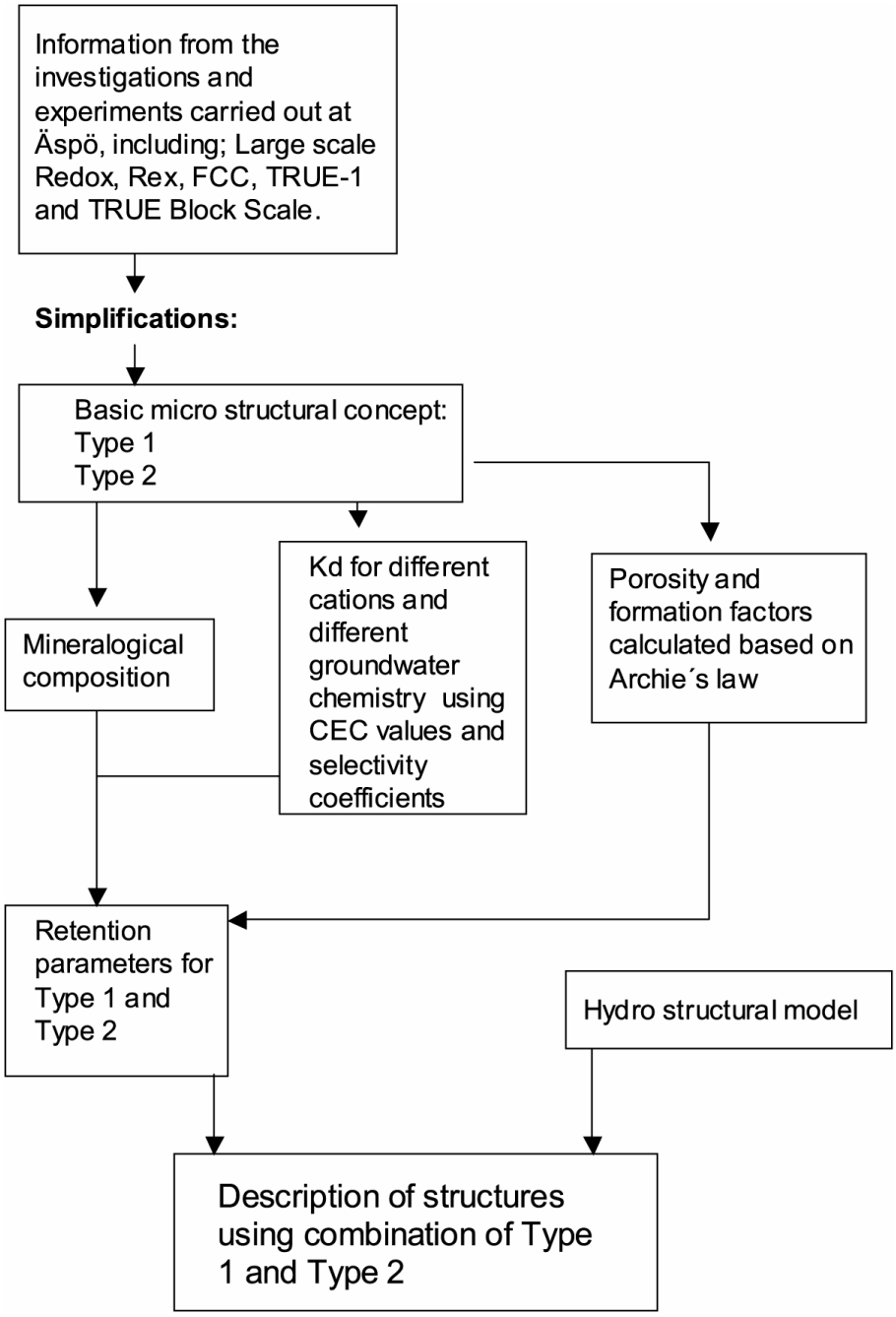

Figure 2-1. *Flow chart showing the basic simplifications used for the micro/macro semi-synthetic structure model.*

2.1 Available database

Unaltered and undeformed rock material from Äspö, including fresh samples of Äspö diorite and fine grained granite have been used for laboratory sorption experiments carried out on crushed and sieved material of different grain sizes. Through-diffusion measurements have been carried out on drill core discs of different thickness (1 to 4 centimetres in thickness) and porosity values have been measured using different techniques. Also the texture and distributional form of the porosity has been studied using ^{14}C –PMMA. The results are presented in Byegård et al. (1998) and Johansson (2000).

Samples of altered wall rock, cataclasite, and mylonite representative for the TRUE-1 site have been used for similar batch experiments as the generic rock samples. There are, however, relatively few experiments done and the available amounts are very limited (results reported in Byegård et al., 1998 and Byegård et al., 2001).

Fault gouge material has not been included in any laboratory sorption studies so far.

2.2 Definition of micro-structural models

2.2.1 Concept

Detailed studies (such as Eliasson 1993, Mazurek et al., 1997, Andersson et al., 2002a) of different faults and fractures have shown large variability in extent of alteration, presence of mylonite, cataclasite, thickness of coatings, and amounts and composition of fault gouge material. The variations are significant not only between different structures but also along single faults or fractures.

The aim of subtask 6C is to provide data for a semi-synthetic rock block (with similarities to the Äspö case). Since the retention database is limited, as are the detailed studies of the fractures and faults, an approach using radical simplifications is needed. It was therefore agreed that transport parameters should be given for two main types of structures (denoted “Faults” and “Non-faults”). These two structure types, to be regarded as two end members of a spectrum of possible structure compositions in the real system, are described in terms of presence and extent of the following entities: cataclasite association, mineralogy assembly, infillings (fine-grained fault gouge), porosity, aperture and transmissivity.

2.2.2 Base case Geological Structure Types

The identified conceptual models include two basic types (representing end members of a spectrum of possible conductive features):

- Faults (Geological Structure Type 1)
- Non-faults (Geological Structure Type 2)

The two types of type structure can be illustrated as shown in Figure 2-2 and Figure 2-3, respectively. Type 1 is characterised by a significant shear movement along one main fault plane. The structure contains a ductile precursor (mylonite) which has been reactivated forming a brittle fault filled with mineralizations, cataclasite and fault gouge. The host rock around the structure has been altered by hydrothermal solutions. It is often accompanied by sub-parallel fractures in the cataclasite and in the altered zone. Alternative combinations (occurrences) using the defined building blocks of the presented Geological Structure Type 1 include eg.; a) cataclasite + fault gouge, b) fault gouge, c) cataclasite + mylonite, d) mylonite + fault gouge.

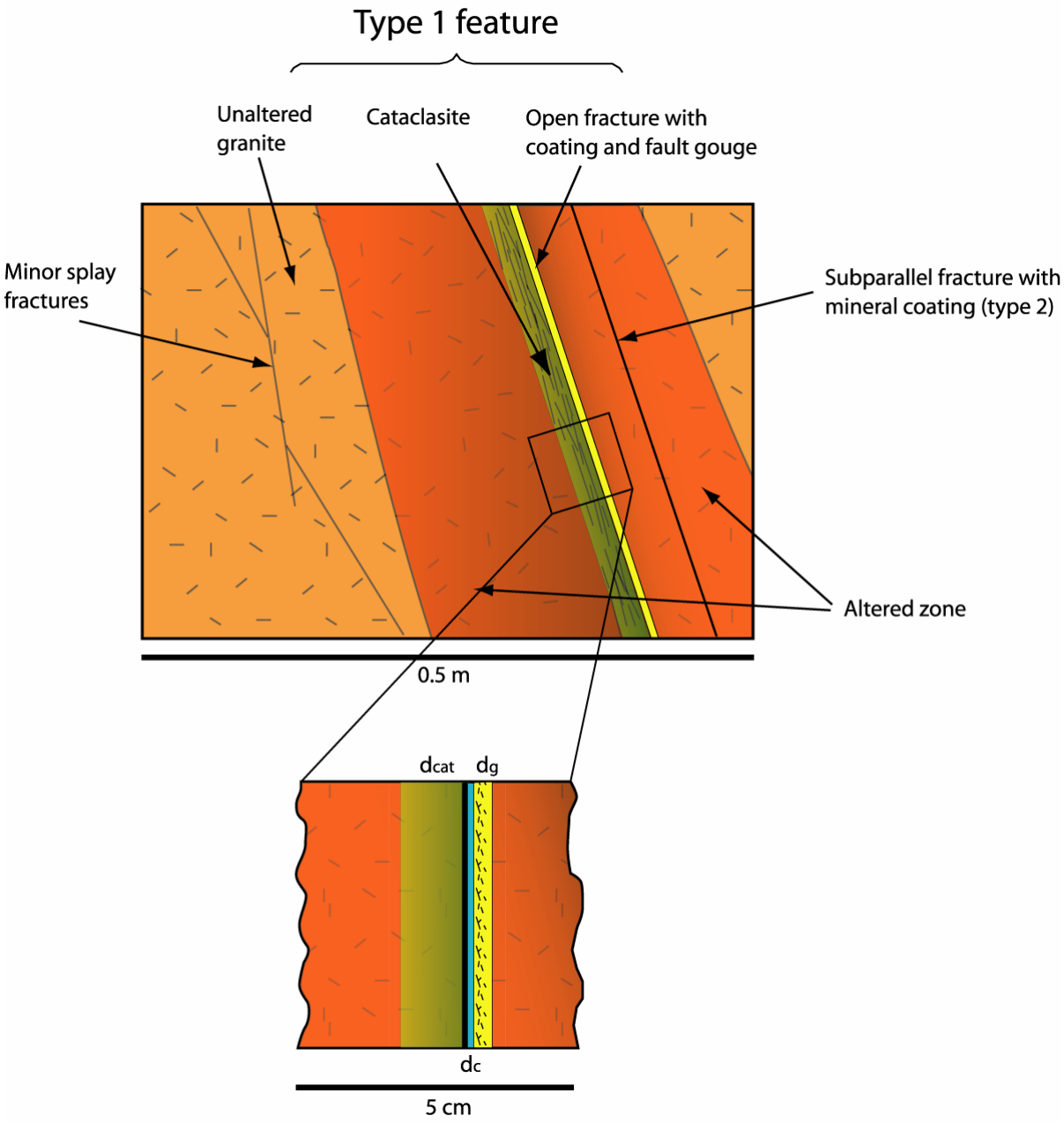

Figure 2-2. *Illustration of the Geological Structure Type 1 (Fault).*

Geological Structure Type 2 is characterised by a fracture without typical shear indicators. The fracture is formed without any plastic precursor and contains fracture mineralisations only. There is a significant zone of alteration around the open fracture plane and it is often accompanied by sub-parallel fractures of the same type.

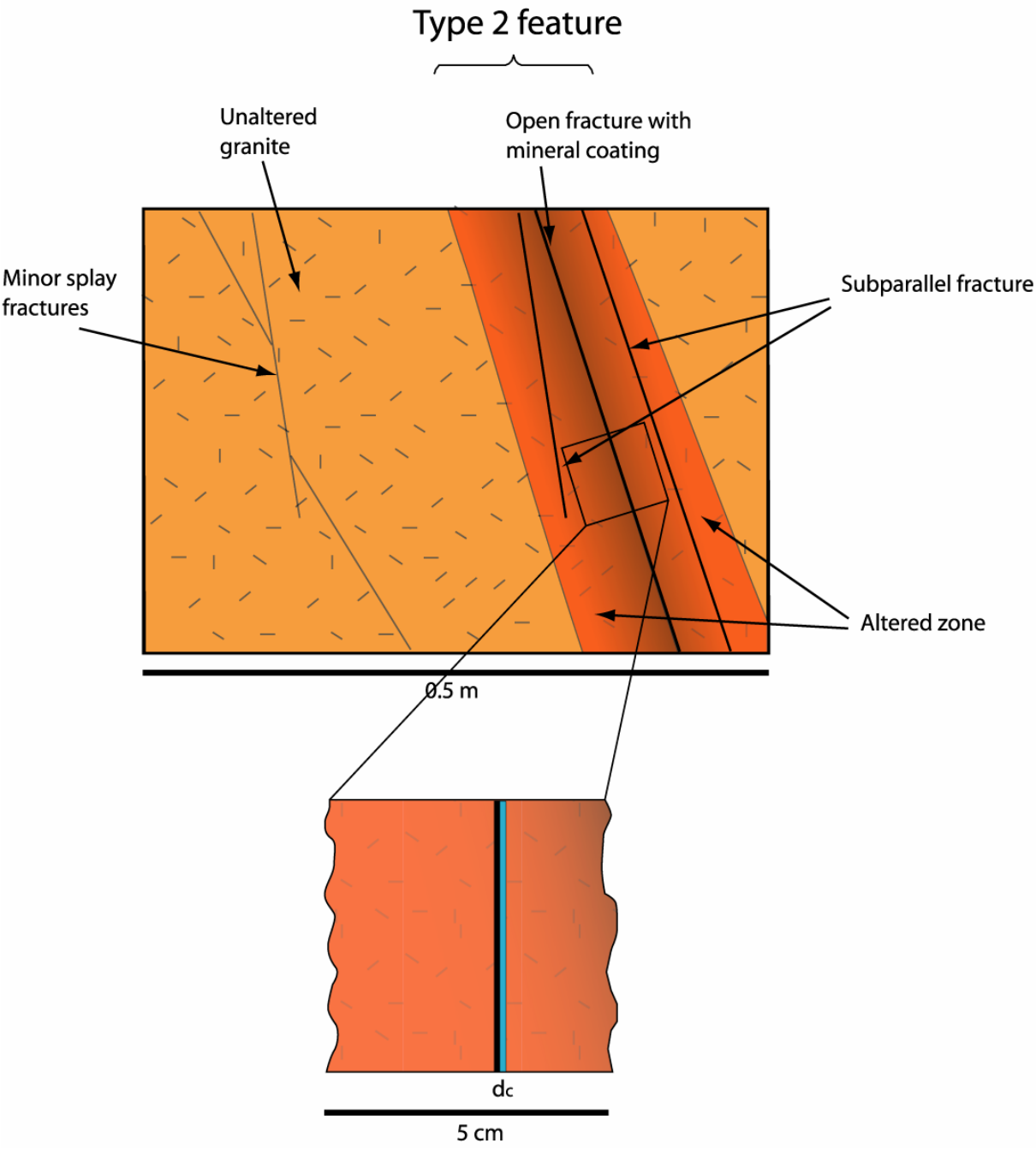

Figure 2-3. *Illustration of Geological Structure Type 2 (Non-fault).*

The micro-structural models for Geological Structure Type 1 and Type 2 are quantified in terms of the thickness of each of the geometrically defined (immobile) zones, and the porosity and formation factor of those zones. Since both Type 1 and Type 2 structures can be made up of multiple discrete features, the representative thickness provided of each of the zones is **per feature/fracture**. Larger structures tend to be made up of more features/fractures, and will consequently have a greater total thickness of each zone. In addition, the thickness of each zone can be scale dependent. The properties of the Geological Structure Type 1 and Type 2 are provided in Table 2-1and Table 2-2, respectively. These values are based on evaluation of the TRUE Block Scale deterministic 100 m structures as intersected in site characterisation boreholes. The variation of the values with the scale of structures is discussed in Section 4.4.3 below.

Table 2-1. Properties of 100-m Scale Geological Structure Type 1 (Fault)

Rock type	Extent (cm)	Porosity (%)	Formation factor (−)
Intact wall rock	−	0.3	7.E-5
Altered zone	20	0.6	2.E-4
Cataclasite d_{cat}	2	1	5.E-4
Fault gouge d_g	0.5	20	5.E-2
Fracture coating d_c	0.05	5	6.E-3

Table 2-2. Properties of 100-m Scale Geological Structure Type 2 (Non-fault)

Rock type	Extent (cm)	Porosity (%)	Formation factor (−)
Intact wall rock	−	0.3	7.E-5
Altered zone	10	0.6	2.E-4
Fracture coating d_c	0.05	5	6.E-3

2.2.3 Mineralogy

The Mineralogical compositions for fresh and altered Äspö diorite, cataclasite, fracture coating and fault gouge material are given in Table 2-3. The compositions for the cataclasite, altered zone and intact wall rock given are taken from Byegård et al. (1998) and belong to samples from the TRUE-1 site. The composition for the fault gouge is associated with samples from the TRUE Block Scale site (Andersson et al. 2002a) and the composition given for the fracture coating is based on the composition given by Mazurek et al., (1997). The samples representing fault gouge were chosen since they have been used for laboratory sorption measurements, but also because they are regarded as representative for Äspö HRL (similar compositions were also reported by e.g. Mazurek et al, 1997). For the Task 6C application no retention properties have been given for mylonite. The mylonite represents a low porosity material with less amount of clay that would promote lower retention compared to the cataclasite. For simplicity the somewhat complex interplay between mylonite and cataclasite occurrence in nature has been reduced to only include the situation where only cataclasite cohabits with fault gouge. This simplification is mainly due to the lack of data but also not to overly complicate modelling. It is emphasised that the Type 1 structure type selected should be regarded as an extreme that promotes radionuclide retention.

Table 2-3. Mineralogical composition combined with the calculation of the cation exchange capacity of the rock types used in the concept applied to Task 6C.

Rock type Reference		**Fracture Coating** Mazurek et al. 1997, interpretation by Tullborg (2002)		**Fault Gouge** Average composition of material[A)] described in Andersson et al. (2002a)		**Cataclasite** TRUE-1, intercept of Feature A in KXTT2, Byegård et al. (1998)		**Altered Zone** TRUE-1, Altered Äspö diorite in interception Feature A and KXTT3, Byegård et al. (1998)		**Intact wall rock** Äspö diorite, Byegård et al. (1998)	
Mineral	**CEC_{min}[B)] (μeq/g)**	**n_{min}·100 (%)**	**n_{min}·CEC_{min} (μeq/g)**	**n_{min}·100 (%)**	**n_{min}·CEC_{min} (μeq/g)**	**n_{min}·100 (%)**	**N_{min}·CEC_{min} (μeq/g)**	**n_{min}·100 (%)**	**n_{min}·CEC_{min} (μeq/g)**	**n_{min}·100 (%)**	**n_{min}·CEC_{min} (μeq/g)**
Smectite	800	-	-	4	32	-	-	-	-	-	-
Illite	191[C)]	2.5	5	12	23	-	-	-	-	-	-
Mixed layer clay	252[D)]	2.5	6	8	20	-	-	-	-	-	-
Chlorite	50	35	18	25	12	6	3	15	7.5	-	-
Mica	35[E)]	-	-	7	2.4	-	-	-	-	-	-
Epidote	6	5	0.3	1	0.06	20	1	15	0.9	5	0.3
Plagioclase	4	-	-	12	0.5	10	0.8	-	-	47	2
K-feldspar	3.7	10	0.4	6	0.2	-	-	-	-	10	0.4
Sulphides	1.5	-	-	1	0.02	-	-	-	-	-	-
Calcite	0.2	35	0.07	8	0.02	-	-	-	-	-	-
Quartz	0.2	8	0.02	16	0.03	14	0.02	15	0.03	14	0.03
Biotite	17	-	-	-	-	3	-	-	-	18	3
Albite	3.7	-	-	-	-	40	1.5	38	1.4	-	-
Sericite	52[F)]	-	-	-	-	4	2.1	2	1	-	-
Magnetite	0.4	-	-	-	-	1.25	0.01	1.5	0.01	2	0.01
Hematite	0.5	1.5	0.01	-	-	0.5	0.01	0.5	0.01	-	-
Titanite	?[G)]	-	-	-	-	1.25	-	1.5	-	2	-
Apatite	0.5	-	-	-	-	1	0.01	1.5	0.01	2	0.01
Pyrite	1.5	0.5	0.01	-	-	-	-	-	-	-	-
Sum:		**100**	**30**	**100**	**90**	**100**	**8.5**	**100**	**11**	**100**	**5.7**

A) Average mineralogical composition from gouge material found at the found in the TRUE Block Scale project at the following borehole/fracture intercepts: KA2563A:154 m (#6), KI0025F02:133m (#19), KI0023B:69.9m (#20) and KI0025F02:66.7m (#22).

B) Allard et al. (1983), unless other notification.

C) Comans et al. 1991.

D) Estimated as 90% illite and 10% smectite.

E) Estimated as 50% biotite and 50% muscovite, biotite 17μeq/g, muscovite 52μeq/g, both from Allard et al. 1983.

F) Values for sericite taken from values given for muscovite 52μeq/g from Allard et al. 1983

G) Not investigated in Allard et al. 1983, the influence of titanite on the total CEC is therefore neglected.

Table 2-4. Calculated K_d for the different materials in contact with the different types of groundwater c.f. Section 2.2.6.

TRUE Block Scale groundwater:

	C (mg/l)	C (M)	K_c	Fracture Coating CEC=30 μeq/g K_d (m^3/kg)	Fault Gouge CEC=90 μeq/g K_d (m^3/kg)	Cataclasite CEC=8.5 μeq/g K_d (m^3/kg)	Altered Zone CEC=11 μeq/g K_d (m^3/kg)	Intact wall rock CEC=5.7 μeq/g K_d (m^3/kg)
Na^+	2065	9.0E-2	0.1[A]	3.7E-5	1.1E-4	1.1E-5	1.4E-5	7.1E-6
Mg^{2+}	42	1.7E-3	11[B]	2.5E-3	7.8E-3	7.4E-4	9.7E-4	4.9E-4
K^+	8	2.1E-4	66[B]	9.4E-4	2.9E-3	2.7E-4	3.6E-4	1.8E-4
Ca^{2+}	1485	3.7E-2	1	2.3E-4	7.1E-4	6.7E-5	8.8E-5	4.4E-5
Rb^+	0.03	3.5E-7	2.00E+03[A]	5.2E-3	1.6E-2	1.5E-3	2.0E-3	1.0E-3
Sr^{2+}	24	2.7E-4	1[A]	2.3E-4	7.1E-4	6.7E-5	8.8E-5	4.4E-5
Cs^+	0.002	1.8E-8	2.00E+05[A]	5.2E-2	1.6E-1	1.5E-2	2.0E-2	1.0E-2
Ba^{2+}	0.06	4.3E-7	20[A]	4.6E-3	1.4E-2	1.3E-3	1.8E-3	8.8E-4

Fresh groundwater:

	C (mg/l)	C (M)	K_c	Fracture Coating CEC=30 μeq/g K_d (m^3/kg)	Fault Gouge CEC=90 μeq/g K_d (m^3/kg)	Cataclasite CEC=8.5 μeq/g K_d (m^3/kg)	Altered Zone CEC=11 μeq/g K_d (m^3/kg)	Intact wall rock CEC=5.7 μeq/g K_d (m^3/kg)
Na^+	21.1	9.2E-4	0.1[A]	1.9E-4	5.9E-4	5.6E-5	7.3E-5	3.7E-5
Mg^{2+}	3.2	1.3E-4	11[B]	6.9E-2	2.1E-1	2.0E-2	2.6E-2	1.3E-2
K^+	1.7	4.4E-5	66[B]	4.9E-3	1.5E-2	1.4E-3	1.9E-3	9.5E-4
Ca^{2+}	34.5	8.6E-4	1	6.2E-3	1.9E-2	1.8E-3	2.4E-3	1.2E-3
Rb^+	0.03	3.4E-7	2.00E+03[A]	2.7E-2	8.4E-2	7.9E-3	1.0E-2	5.2E-3
Sr^{2+}	0.6	6.4E-6	1[A]	6.2E-3	1.9E-2	1.8E-3	2.4E-3	1.2E-3
Cs^+	0.002	1.8E-8	2.00E+05[A]	2.7E-1	8.4E-1	7.9E-2	1.0E-1	5.2E-2
Ba^{2+}	0.06	4.3E-7	20[A]	1.2E-1	3.8E-1	3.6E-2	4.8E-2	2.4E-2

Brine groundwater:

	C (mg/l)	C (M)	K_c	Fracture Coating CEC=30 μeq/g K_d (m^3/kg)	Fault Gouge CEC=90 μeq/g K_d (m^3/kg)	Cataclasite CEC=8.5 μeq/g K_d (m^3/kg)	Altered Zone CEC=11 μeq/g K_d (m^3/kg)	Intact wall rock CEC=5.7 μeq/g K_d (m^3/kg)
Na^+	8500	3.6E-1	0.1[A]	1.2E-5	3.8E-5	3.5E-6	4.7E-6	2.3E-6
Mg^{2+}	2.1	8.7E-5	11[B]	2.8E-4	8.6E-4	8.1E-5	1.1E-4	5.3E-5
K^+	46	1.2E-3	66[B]	3.1E-4	9.7E-4	9.1E-5	1.2E-4	6.0E-5
Ca^{2+}	19300	4.8E-1	1	2.5E-5	7.8E-5	7.3E-6	9.7E-6	4.8E-6
Rb^+	0.03	3.4E-7	2.00E+03[A]	1.7E-3	5.3E-3	5.0E-4	6.6E-4	3.3E-4
Sr^{2+}	313	3.6E-3	1[A]	2.5E-5	7.8E-5	7.3E-6	9.7E-6	4.8E-6
Cs^+	0.002	1.8E-8	2.00E+05[A]	1.7E-2	5.3E-2	5.0E-3	6.6E-3	3.3E-3
Ba^{2+}	0.06	4.3E-7	20[A]	5.0E-4	1.6E-3	1.5E-4	1.9E-4	9.7E-5

A Value from TRUE-1 investigation of altered Äspö diorite, sampled at KXTT2 15.1m (Byegård et al. 1998)
B Value from investigation of Finnsjön granodiorite (Byegård et al. 1995)

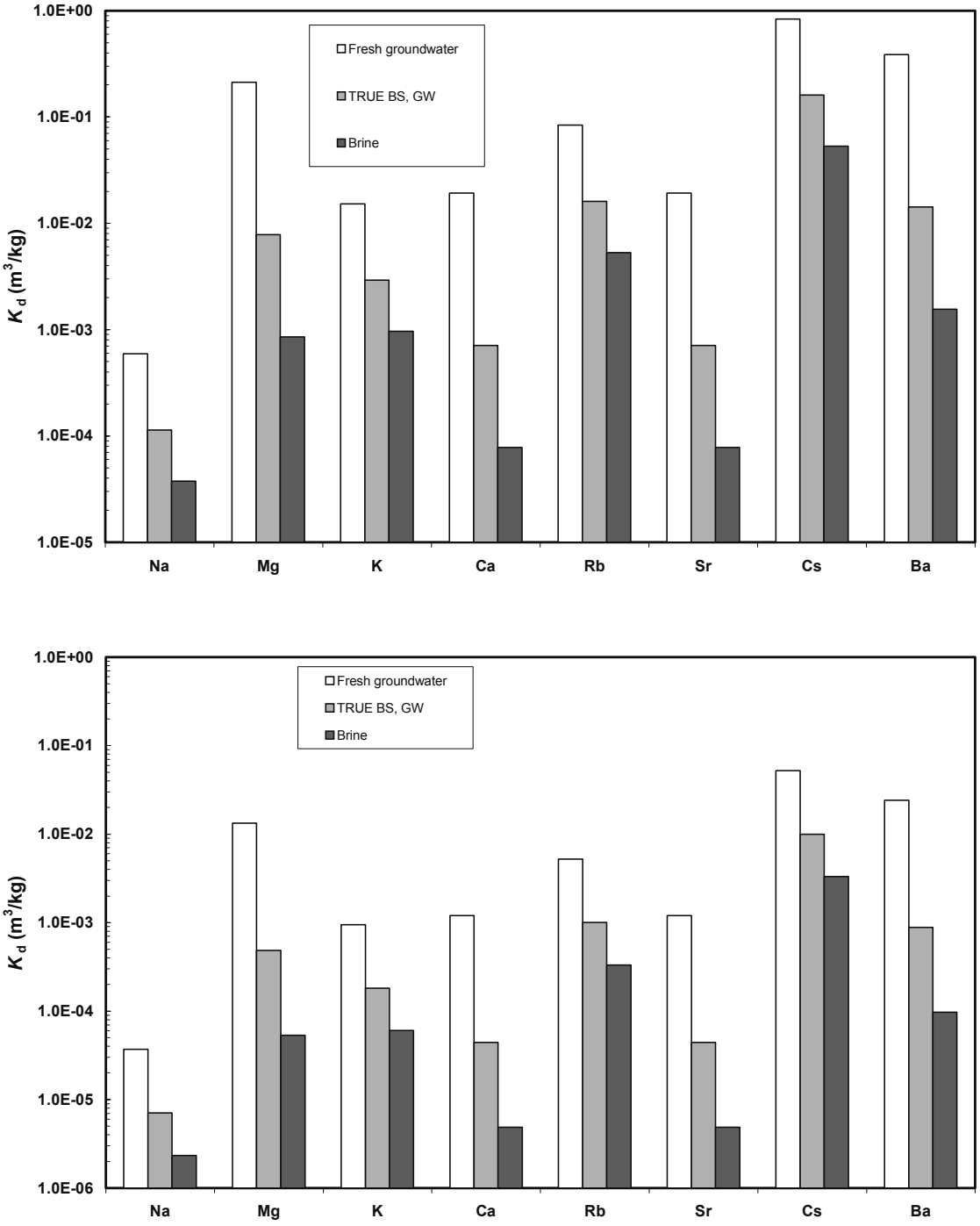

Figure 2-4. *Influence of the water composition on the sorption coefficients. Examples are given for the contact with fault gouge material (top) with a CEC estimated to 90 μeq/g together with the intact unaltered wall rock (bottom) with a CEC estimated to 5.7 μeq/g.*

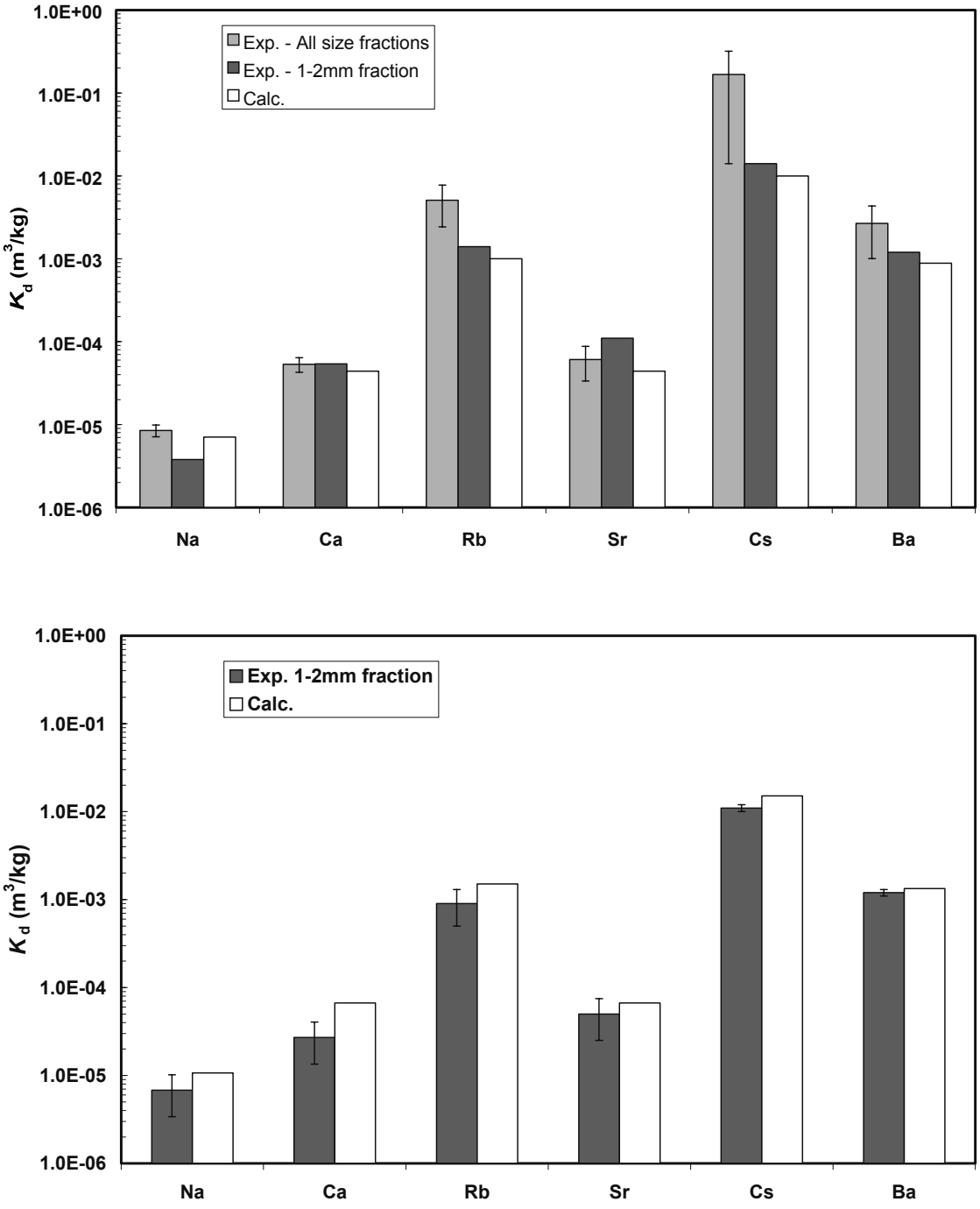

Figure 2-5. *Comparisons of calculated and experimentally determined K_d for intact unaltered wall rock (top) and cataclasite (bottom). The calculated K_d values are based on the TRUE Block Scale water composition, which is very similar to the TRUE-1 water composition used in the laboratory experiments (cf. Byegård et al. 1998).*

2.2.4 Porosity

The porosity values given in Table 2-1 and Table 2-2 are (except for the fracture coating and fault gouge parts) based on water saturation measurements carried out on drill core samples. These should be regarded as maximum values compared with values *in situ*. There are also indications of a decrease, not only in absolute porosity, but also in connectivity going from the fracture wall into the host rock, as shown in PMMA studies presented in Byegård et al. (1998; 2001) and Kelokaski et al. (2001).

The porosity of the fracture coating is estimated from PMMA and SEM studies. The porosity of the fault gouge material is projected based on impregnation studies reported by Mazurek et al., (1997).

Attempts to deal with the impact of heterogeneously-distributed porosity on diffusion and sorption have been presented by Byegård et al. (2001) and some implications of that report are included as a separate part in this report, cf. Section 2.2.10.

2.2.5 Formation factor

The values of the formation factor (equivalent to diffusivity, with tortousity and constrictivity not accounted for) are calculated using Archie's law (F=0.71·$\varepsilon^{1.58}$) using the porosity values in Table 2-1 and Table 2-2. The connected porosity in crystalline rock is mainly made up of micro fractures with some contribution from porous mineral phases (often secondary or altered minerals). Hence, the connectivity of the pores, the frequency, size and orientation of the micro fractures are crucial and large variation in diffusivity values on sample scale (cm) can be expected.

A decrease in diffusivity as a function of sample length has been demonstrated in several investigations on crystalline rocks such as Kumpulainen and Uusheimo (1989); Skagius (1986); Johansson (2000). This decrease is mainly attributed to higher effective porosity (connectivity of the pores) in short samples (1-2 cm) and better connectivity of the pores

Table 2-5. Calculated formation factors for relevant geological materials.

Material	Porosity ε (%)	Formation factor, *F*	
		Calc. from est. porosity + Archie's law	Comparison with experimentally determined value
Fracture coating	5	6.2E−3	-
Fault gouge	20	5.6E-2	-
Cataclasite	1	4.9E-4	4E-5 [A)]
Altered Zone	0.6	2.2E-4	7E-5 [B)]
Unaltered wall rock	0.3	7.3E-5	5E-5 [C)]

A. Determined in through diffusion experiment with HTO, sample from KXTT3 intersection with Feature A, average value of two samples, Byegård et al. (2001)
B. Determined in through diffusion experiment with HTO, sample from KXTT3 intersection with Feature A, value from one samples, Byegård et al. (2001)
C. Determined in through diffusion experiment with HTO, average from a large number of samples, Byegård et al. (1998)

over short distances and a decrease in effective porosity going from the fracture wall and into the wall rock (cf. Byegård et al., 2001). Also attempts to deal with the impact of heterogeneously distributed porosity on diffusion/sorption have been presented (Cvetkovic and Cheng, in press.).

2.2.6 Effective diffusivity D_e

The effective diffusivity is calculated according to

$$D_e = D_w \cdot F \tag{2.1}$$

where D_w is the water diffusivity for the tracer. The D_e calculated for the different tracers in contact with the different geologic materials is presented in Table 2-6.

Table 2-6. Effective diffusivities for the different tracers in contact with the different types of geologic material. The diffusivities has calculated using the formation factor, F, (cf. Section 2.2.5) and the tabulated water diffusivities, Dw

		Fracture Coating	Fault gouge	Cataclasite	Altered Zone	Unaltered wall rock
	Porosity (%)	5	20	1	0.6	0.3
	Formation factor, *F*	6.2E-03	5.6E-02	4.9E-04	2.2E-04	7.3E-05
	D_w (m^2/s)[A)]	D_e (m^2/s)	D_e (m^2/s)	D_e (m^2/s)	D_e (m^2/s)	D_e (m^2/s)
HTO	2.13E-09	1.3E-11	1.2E-10	1.0E-12	4.7E-13	1.6E-13
I^-	2.00E-09	1.2E-11	1.1E-10	9.8E-13	4.4E-13	1.5E-13
Na^+	1.33E-09	8.3E-12	7.4E-11	6.5E-13	2.9E-13	9.7E-14
Mg^{2+}	7.05E-10	4.4E-12	3.9E-11	3.5E-13	1.5E-13	5.2E-14
K^+	1.96E-09	1.2E-11	1.1E-10	9.6E-13	4.3E-13	1.4E-13
Ca^{2+}	7.93E-10	5.0E-12	4.4E-11	3.9E-13	1.7E-13	5.8E-14
Rb^+	2.06E-09	1.3E-11	1.2E-10	1.0E-12	4.5E-13	1.5E-13
Sr^{2+}	7.94E-10	5.0E-12	4.4E-11	3.9E-13	1.7E-13	5.8E-14
Cs^+	2.07E-09	1.3E-11	1.2E-10	1.0E-12	4.5E-13	1.5E-13
Ba^{2+}	8.48E-10	5.3E-12	4.7E-11	4.2E-13	1.9E-13	6.2E-14
Ra^{2+}	8.89E-10	5.6E-12	5.0E-11	4.4E-13	1.9E-13	6.5E-14
Am(III)	5.95E-10[B)]	3.7E-12	3.3E-11	2.9E-13	1.3E-13	4.4E-14
Tc(IV)	5.00E-10[C)]	3.1E-12	2.8E-11	2.5E-13	1.1E-13	3.7E-14

A. Values given in Li and Gregory (1974), unless other notification.
B. Mills and Lobo (1989), based on the Am^{3+} species
C. Estimated by Byegård and Widestrand (2003)

2.2.7 Volumetric distribution coefficient K_d

The values of K_d for interaction with the cation exchange sorbing tracers with the various units of the type conceptual models are calculated using existing cation exchange capacities (CEC) for the individual minerals, mineralogical analysis, selectivity coefficients and existing/inferred information on groundwater chemistry. The procedure used for estimation of the sorption coefficients is the same described by Andersson et al. (2002a).

The principal in-data for these calculations are:

1. Mineralogical analyses of the different geological materials
2. CEC determinations of pure mineral phases. The predominant part of the data is based on the investigation of Allard et al. (1983). In there work, the 0.044-0.063 mm size fraction of the minerals were saturated with >0.5M NaBr using contact times of 4 days.
3. Selectivity coefficients are mainly based on a batch sorption experiment with altered diorite sampled at the KXTT2 intercept with rim zone of the Feature A (TRUE-1) (Byegård et al., 1998). In this experiment, the 1-2 mm size fraction was contacted with synthetic groundwater (8.5ml water / 2g rock material) and the sorption was studied for a large number of alkali and alkaline earth metals. A sorption time of 10 days was applied.
4. Groundwater composition, cf. Section 2.2.9.

It should be noted that the presently used approach is founded on the following assumptions and simplifications:

1. It is assumed that all cation exchange sites of the different minerals have the same selectivity for the different cations; i.e., the K_d for the different cations will only vary with the total number of CEC that has been found for the different materials. For simplification purposes, no attempts have been made to include any mineral-specific selectivity coefficients.
2. The water is assumed to have the same composition in the fracture and in the different pores of the different materials. This assumption is questionable and data from the Matrix Fluid Chemistry project at the Äspö HRL, which are about to be published (Waber, in prep.), may give reason to update the data set.

The data used and the results of the calculation are given in Table 2-4. In Figure 2-4 the impact of the water composition of the estimated K_d are illustrated and comparisons of calculated and experimentally obtained values are given in Figure 2-5.

For the other radionuclides that are foreseen to be used in the PA calculations of the Task 6 project (i.e., I^-, Ra^{2+}, Tc(IV) and Am(III)), no work addressing their specific sorption properties in Äspö rock types has been done within the TRUE project. K_d-values have therefore been estimated according to the following procedures:

- I^- is considered as a conservative tracer and the K_d is set to 0. Support for this assumption is the non-sorbing behaviour of the $^{131}I^-$ tracer in the TRUE Block Scale Phase C test C4 (Andersson et al., 2001). This assumption is also in line with the SKB sorption database (Carbol and Engkvist , 1997) used for performance assessment.

- Sorption characteristics of Ra^{2+} in saline groundwater were addressed in the work of Kulmala and Hakanen (1995) who investigated and compared the sorption of Sr^{2+}, Ba^{2+} and Ra^{2+} for Finnish conditions. In this work two different groundwater compositions were used; saline groundwater from Olkiluoto (with Na^+ and Ca^{2+} as the dominating cations, 3070-mg/l and 2290-mg/l, respectively) and non-saline groundwater from Kivetty (Na^+ and Ca^{2+} concentrations of 17

mg/l and 10-mg/l, respectively). In the investigation, it is found that in the saline groundwater the K_d for $Ra^{2+}$is approximately a factor of 10 higher than the corresponding value for Ba^{2+}. However, for non-saline groundwater, the values are very similar. Based on these observations, K_d-values for Ra^{2+} in the brine groundwater and in the TRUE Block Scale groundwater are obtained by multiplying the corresponding K_d-value of Ba^{2+} with a factor of 10. For fresh groundwater environment, the K_d-values of Ra^{2+} is accordingly set equal to the K_d-values of Ba^{2+}.

- For Tc(IV) and Am(III) hydrolysis combined with surface complexation is considered to be the major sorption mechanism. The influence of different mineral types and different water compositions are considered to be minor. Therefore, the K_d-values based on the recommendations by Selroos and Elert (2001) are proposed to be used for all combinations of rock materials and water compositions, i.e., K_d = 0.2 m^3/kg for Tc(IV) and K_d =0.5 m^3/kg for Am(III).

Table 2-7. Sorption coefficients for Ra^{2+} estimated according to the procedure outlined in the text above.

Groundwater type	Fracture coating	Gouge material	Cataclasite	Altered Zone	Intact wall rock
TRUE Block Scale GW	4.6E-2	1.4E-1	1.3E-2	1.8E-2	8.8E-3
Fresh groundwater	1.2E-1	3.8E-1	3.6E-2	4.8E-2	2.4E-2
Brine	5.0E-3	1.6E-2	1.5E-3	1.9E-3	9.7E-5

2.2.8 Surface sorption coefficient K_a

For PA time scales, the surface sorption coefficient, K_a should use the K_d values that are specified for the fracture coatings. It should further be assumed (within the time perspective used in these calculations) that all of the sorption sites of this 0.5 mm thick fracture coating material are in immediate contact with the groundwater. K_a can thus be calculated from the K_d according to:

$$K_a = \left(K_d \rho + \varepsilon\right) \cdot d \tag{2.2}$$

where d is the thickness of the fracture coating (5×10^{-4} m), ε is the porosity (0.05) and ρ is the density of the fracture coating (~2600 kg/m^3).

For shorter time scales (e.g., time scales for *in situ* experiments) it is questionable if the more sorbing tracers will fully penetrate the 0.5 mm thick fracture coating. It is therefore recommended that the validity of the concept of transforming K_d for the fracture coatings to K_a be checked and verified by separate diffusion calculations.

2.2.9 Groundwater composition

A saline water (Na-Ca-Cl-SO4 type) with chlorine content around 6000 ppm was chosen as representative for the actual groundwater composition (see Table 2-8) and used for the K_d calculations. The composition was calculated as the average results from four sampled sections in boreholes KI0025F, KI0025F02 and KI0025F03 (Andersson et al. 2002a). Although, the groundwater chemistry in the far field is expected to remain

stable during the lifetime of the repository (cf. Puigdemenech, 2001) the changes in salinity and cation composition at repository depth maybe large enough to influence the K_d values significantly. For PA time scale, therefore, two groundwaters with extreme compositions were used in the K_d calculations: 1) fresh water (Ca-Na-HCO3 type): A component being increasingly important due to land uplift and as a result of a possible massive inflow of glacial melt water during later glacial stages. 2) brine type water (Ca-Na-Cl type): Waters with higher salinities are expected to occur during some glacial stages.

Table 2-8. Composition of groundwaters used for calculations of K_d values.

Sample groundwater	Cl (mg/l)	SO_4 (mg/l)	HCO_3 (mg/l)	Na (mg/l)	Ca (mg/l)	Mg (mg/l)	K (mg/l)
Repository depth present Mean from TRUE Block Scale analyses	5 970	400	15	2 067	1 485	42	8
Fresh water (HBH02)	13.5	24.3	137	21.1	34.5	3.2	1.7
Brine-type SGKLX02	47 200	906	14.1	8 500	19 300	2.1	45.5

2.2.10 Potential influence of heterogeneity, surface diffusion and anion exclusion

A general observation is that diffusion experiments with sorbing tracers give breakthrough results and/or penetration profiles that are not consistent with data from batch sorption experiment. Attempts to evaluate sorption coefficients from diffusion experiment have in most cases resulted in much lower K_d-values for diffusion experiments compared to corresponding batch sorption experiment. As an example, the interpretation of a penetration profile for Cs^+ in intact unaltered Äspö diorite with a homogeneous pore diffusion model resulted in K_d-values $\leq$ 8E-4 m^3/kg, while the corresponding batch sorption experiment gave K_d-values in the range 0.01-0.4 m^3/kg (Byegård et al. 1998). The large variation in K_d-values in the batch sorption experiments was found to follow a relationship with increasing K_d with decreasing particle size of the geologic material.

Attempts have been made (Byegård et al. 2001) to explain these inconsistencies using the assumption of heterogeneously distributed porosity in the crystalline rock. In this work, independently measured porosity distributions in 2D (PMMA-technique) were used as in-data and the diffusion in the rock was considered to take place in a system of non-connected parallel channels with a unique porosity. The frequency of each interval of porosity was set according to the PMMA measured porosity distribution. The porosity distribution was observed to follow a log-normal distribution very well. This work indicated that the shape of the penetration profile could be explained very well with a model of heterogeneous porosity. Furthermore, it is indicated that evaluation with a model of heterogeneously distributed porosity gives K_d-values that are more consistent with results from batch sorption experiments.

Porosity distributions for Äspö diorite (intact unaltered wall rock) and for a mixture of mylonite and altered wall rock are presented in Figure 2-6 and Figure 2-7. The experimental data for penetration profiles for Cs^+ are also presented. Two types of calculated penetration profiles are also presented; one which shows the best fit to the experimental data using a model of heterogeneously distributed porosity, and one where a penetration profile has been calculated using a homogeneous single porosity model combined with the retention parameters (K_d, D_e and ε) recommended in this report.

Another approach to explain the inconsistencies in the results between batch sorption experiments and diffusion experiments is to include a process consisting of mobility of the cations in the sorbed phase, i.e., surface diffusion. The surface diffusion concept has been thoroughly investigated by Ohlsson (2000). In their recommendations for diffusion data to be used in performance assessment, Ohlsson and Neretnieks (1997) proposed a multiplication factor of 10 of the effective diffusivities for alkali and alkaline earth metals in low ionic strength medium to account for the surface diffusion process. For groundwater with high ionic strengths as well as for cations not belonging to the alkali and alkaline earth metal group, Ohlsson and Neretnieks concluded that the influence of surface diffusion could be neglected. Following the concept of Ohlsson and Neretnieks, the effective diffusivities of alkali and alkaline earth metals in low ionic strength should thus be multiplied by a factor of 10. Ohlsson and Neretnieks also propose a multiplication of 0.1 of the effective diffusivities of anions in low ionic strength to account for the anion exclusion process. For the purpose of this report, surface diffusion and anion exclusion will thus only have an impact on the diffusivities in a fresh groundwater environment. The effective diffusivities with respect to these processes are presented in Table 2-9. It is furthermore assumed that the extra contribution of mobility in the sorbed phase will only play a significant part in the total effective diffusivities for intact unaltered crystalline rock. For fault gouge and fracture coating material, no increase of the effective diffusivity is introduced.

Table 2-9. Complementary data on diffusivity for the different tracers in contact with the different types of geologic material in a fresh groundwater environment, i.e., the anion exclusion and surface diffusion processes have been addressed. Values are only presented for those tracers for which the diffusivities can be a subject to correction for the surface diffusion and anion exclusion according to the concept given in the text. For the diffusivities for the other groundwater environments and for the other tracers, reference is made to Table 2-6.

		Fracture coating	Fault gouge	Cataclasite	Altered Zone	Unaltered wall rock
	Porosity (%)	5	20	1	0.6	0.3
	Formation factor, *F*	6.2E-03	5.6E-02	4.9E-04	2.2E-04	7.3E-05
	D_w (m^2/s)[A)]	D_e (m^2/s)	D_e (m^2/s)	D_e (m^2/s)	D_e (m^2/s)	D_e (m^2/s)
I^-	2.00E-09	1.2E-12	1.1E-11	9.8E-14	4.4E-14	1.5E-14
Na^+	1.33E-09			6.5E-12	2.9E-12	9.7E-13
Mg^{2+}	7.05E-10			3.5E-12	1.5E-12	5.2E-13
K^+	1.96E-09			9.6E-12	4.3E-12	1.4E-12
Ca^{2+}	7.93E-10			3.9E-12	1.7E-12	5.8E-13
Rb^+	2.06E-09			1.0E-11	4.5E-12	1.5E-12
Sr^{2+}	7.94E-10			3.9E-12	1.7E-12	5.8E-13
Cs^+	2.07E-09			1.0E-11	4.5E-12	1.5E-12
Ba^{2+}	8.48E-10			4.2E-12	1.9E-12	6.2E-13
Ra^{2+}	8.89E-10			4.4E-12	1.9E-13	6.5E-14

A. Values given by Li and Gregory (1974)

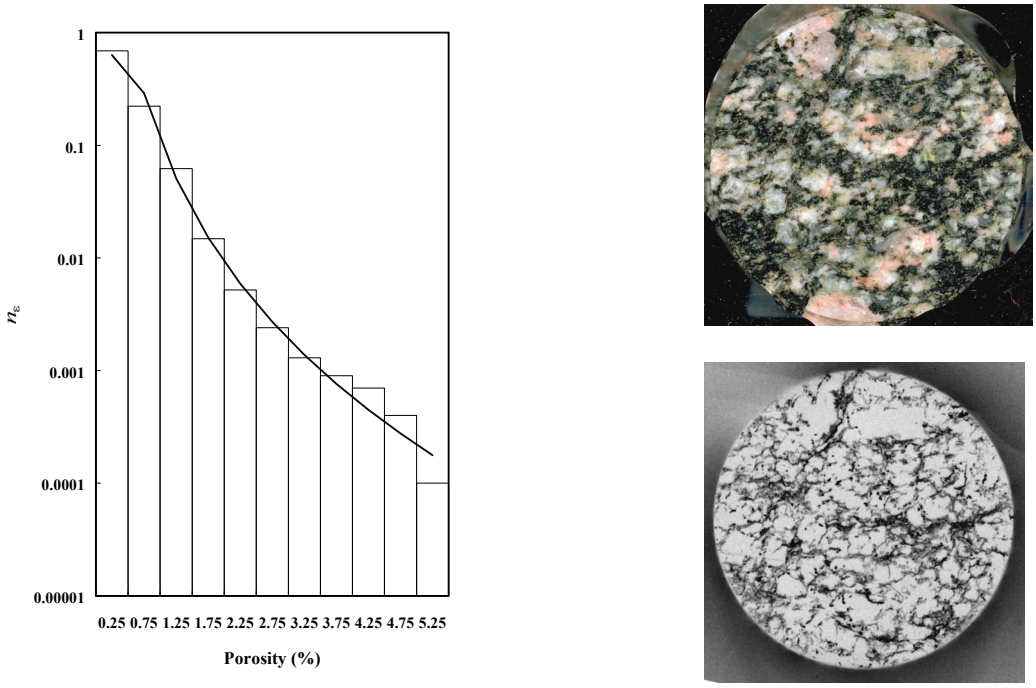

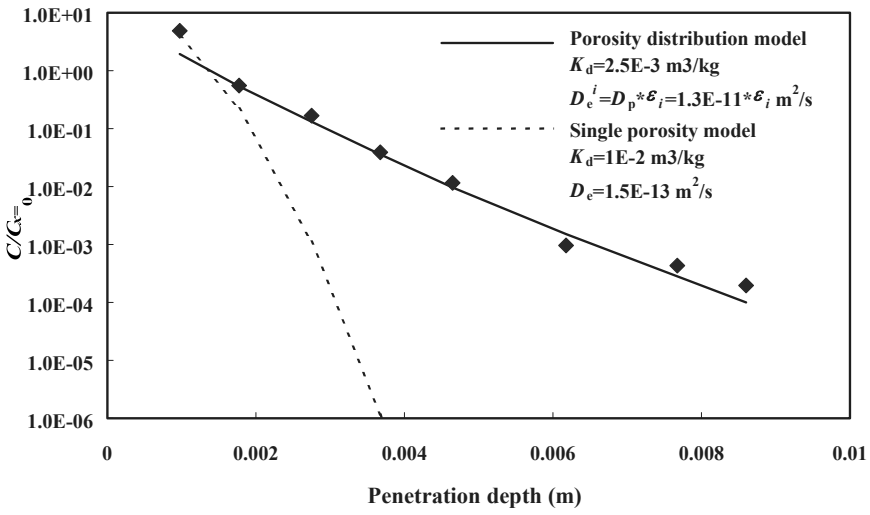

Figure 2-6. *Histogram of porosity as mapped on the surface (top, left) for intact unaltered Äspö diorite, measured from autoradiographs of ^{14}C-PMMA impregnation (middle, right). The line corresponds to a fitted log-normal distribution of the porosity, $\varepsilon = 10^{(-2.75 \pm 0.44)}$. A photograph of the rock sample is also shown (upper, right). An experimentally determined penetration profile for Cs^+ in Äspö diorite, contact time 472 d, is also presented (bottom). In this graph, comparisons are made with a fitted penetration profile using a porosity distribution model (solid line) and to the results of a calculation using a homogeneous single porosity model with the retention parameters recommended in this report (dashed line).*

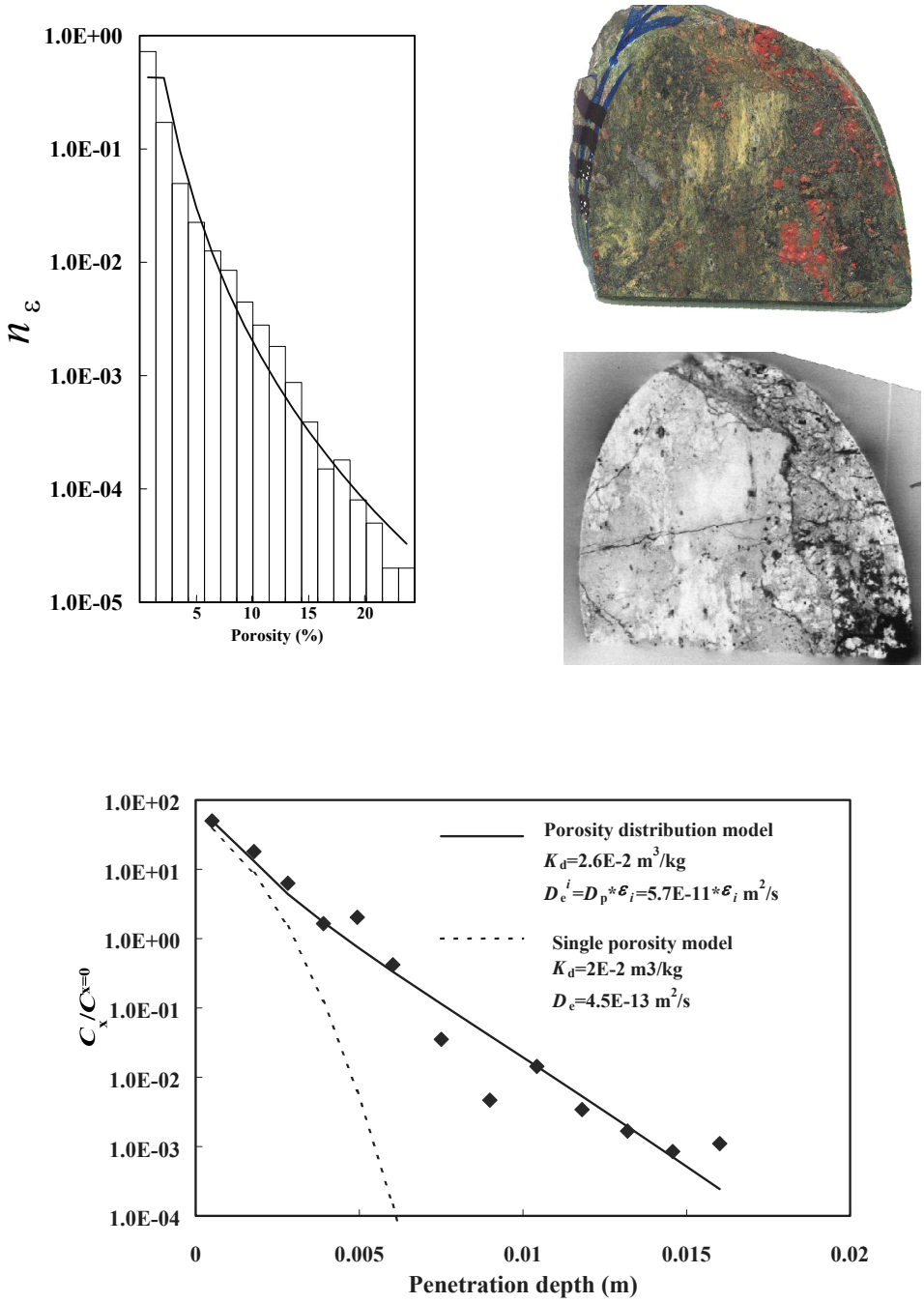

Figure 2-7. *Histogram of porosity as mapped on the surface (top, left) for altered diorite/mylonite, measured from autoradiographs of ^{14}C-PMMA impregnation (middle, right). The line corresponds to a fitted log-normal distribution of the porosity, $\varepsilon=10^{(-2.06\pm0.39)}$. A photograph of the rock sample is also shown (top, right). An experimentally determined penetration profile for Cs^+ in altered diorite/mylonite (contact time 1143 d) is also presented (bottom). In this graph, comparisons are made to a fitted penetration profile using a porosity distribution model (solid line) and the results of a calculation using a homogeneous single porosity model with the retention parameters recommended in this report (dashed line).*

3 Structures and Background Fractures

This section describes the derivation of background fractures, 100 m structures, and 1000 m structures for the hydrostructural models.

3.1 Available database

The Äspö site provides a large database of geologic and hydraulically significant structures at the full range of scales from centimetres to kilometres. In developing the hydrostructural model, emphasis has been placed on data from the TRUE Block Scale, TRUE-1, FCC, Prototype Repository, Task 5, and Alternative Model Project (AMP), cf. references given in Section 1.4.

3.2 Background fractures

Definition : A background fracture is in this context defined as a feature of scale less than approximately 50 m. The feature could either be of Geological Structure Type 1 or 2, and can be made up of one or more discrete features. However, background fractures are generally of Geological Structure Type 2, and are generally made up of one discrete feature, cf. Section 4.4.2.

Analysis of data from the surface characterisation boreholes, Prototype Repository, TBM tunnel, the TRUE Block Scale and TRUE-1 background fracture models indicates two to three fracture sets, with orientations slightly deviation across the site. The analyses of data from the TRUE Block Scale and TRUE-1 rock blocks was carried out in sufficient detail to make it possible to distinguish orientations of conductive and non-conductive structures, respectively. Stereoplots of orientation data from the Prototype

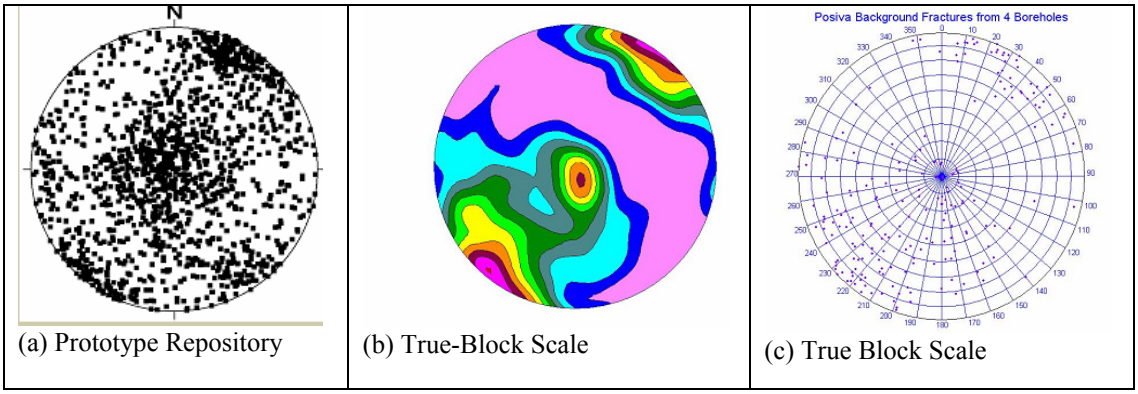

(a) Prototype Repository (b) True-Block Scale (c) True Block Scale

Figure 3-1. *Orientations of background fractures throughout Äspö HRL.*

Repository, TBM tunnel, TRUE Block Scale, and TRUE-1 sites are illustrated in Figure 3-1 Figure 3-1. The variations in orientation visible in Figure 3-1 are considered relatively minor, such that a single population can be used throughout both the 200-m and the 2000-m scale models, using the same statistics.

Hydraulic packer tests, flow logs, and Posiva flow logs were used to identify conductive structures in six boreholes throughout the TRUE Block Scale rock block (Andersson et al., 2002a). After eliminating the flow anomalies corresponding to the interpreted deterministic structures, a statistical analysis was carried out of the remaining flow anomalies and their associated fractures. The results of this analysis in terms of fracture orientation, intensity, spatial pattern, and transmissivity are provided in Table 3-1.

Flow and transport simulations based on the background fracture population presented in Table 3-1 produces a rock mass which is more strongly connected than what in situ hydraulic interference tests indicate (Dershowitz and Klise, 2002). This is probably due to the assumption of fracture size distributions based on the Follin and Hermanson (1996) study in the Äspö HRL TBM tunnel. Considerable data from other areas in the Äspö tunnels supports size distributions for background fractures with average sizes more on the order of 1 to 2m, which would be more consistent with the observed hydraulic connectivity.

Fracture size analyses are summarised in Table 3-2. For the Task 6C model, the current recommendation is to assume a log-normal distribution with a mean of 2m and a standard deviation of 1m, based on data from the adjacent Prototype Repository rock block (Hermanson and Follin, 2000) and the FCC project analyses (Mazurek et al., 1997).

Table 3-1. Parameters of a DFN model of conductive background fractures in the TRUE Block Scale tracer test area (Andersson et al., 2002a).

Parameter	Basis	Set #1	Set #2
Orientation Distribution	Two Fitted Sets (NeurISIS)	Fisher Distribution Mean Pole (Trend, Plunge) =(211,0.6) Fisher Dispersion κ =9.4	Fisher Distribution Mean Pole (Trend, Plunge)=(250,54) Fisher Dispersion κ = 3.8
Intensity P_{32}	Flowing Posiva Log Features 0.29 m^2/m^3 total	0.16 m^2/m^3 (55.2% of fractures)	0.13 (44.8% of fractures)
Size Equivalent Radius	Follin and Hermanson (2001)	Lognormal Distribution mean = 6 m st.dev. = 3 m.	Lognormal Distribution mean = 6 m st.dev. = 3 m.
Transmissivity	Flowing Posiva Log Features, OxFilet Analysis of Packer Tests	Lognormal Distribution mean= -8.95 $\log_{10}$-m^2/s st.dev = 0.93 $\log_{10}$-m^2/s	Lognormal Distribution mean= -8.95 $\log_{10}$-m^2/s st.dev = 0.93 $\log_{10}$-m^2/s
Spatial Pattern	Distribution, Fractal, Geostatistical Analyses	Baecher Model in Structure 20-24 region Fractal (D≈2.6) for larger scale blocks.	Baecher Model in Structure 20-24 region Fractal (D≈2.6) for larger scale blocks.

Table 3-2. Compilation of analyses of size of conductive background fracture population.

Data Studied/ Task Force Application	Mean radius (m)	Std Dev of radius (m)	Reference
Surface Mapping/ ÄMTF Task 1,2	13.7	12.7	Uchida and Geier (1992)
Tunnel Intersections TBM and Blasted Tunnels/ AMTF Task 3,4 TRUE Block Scale	6	2	Hermanson et al. (2001)
Canister-hole Intersections, Prototype Repository/ **Task 6C**	2	2	Stigsson et al. (2001)
Trace Mapping, Prototype Repository	2 to 8 m	2 to 4 m	Hermanson et al. (1999)
FCC Tunnel Mapping/ ÄMTF Task 4	0.1 to 2	0.1 to 2	Bossart et al. (2001)

It is expected that the smaller background size distribution based on Hermanson and Follin (2000) will result in rock mass connectivity more consistent with in situ hydraulic interference test results.

Table 3-3 summarises available information concerning background fracture intensity and transmissivity distributions. For the purposes of Task 6C, the fracture intensity derived for the TRUE Block Scale rock block, including the features down to a cut-off transmissivity of approximately 10^{-9} m^2/s will be considered. Therefore, the intensities and transmissivity distribution from the TRUE Block Scale analysis will be maintained.

In assigning fracture transmissivities to individual fractures, there is some evidence to support a correlation between size and transmissivity (see Section 4.3). This correlation has been used in assigning transmissivities to fractures of the reference background fracture population. The assignment of transmissivity, aperture, and geological structural models to background fractures is described in Chapter 5.

Table 3-3. Transmissivity and intensity of conductive background fracture population.

Study	Log_{10}-mean Transmissivity (m^2/s)	Log_{10} Std Dev Transmissivity (m^2/s)	Intensity P_{32c} (m^2/m^3)	Reference
LPT2 AMTF Task 1	-7.7 ($3.8x10^{-7}$)	0.81 ($7x10^{-6}$)	0.03 (>10^{-8})	Uchida et al., (1994)
Tunnel Drawdown Experiment ÄMTF Task 2	-6.8 ($9x10^{-7}$)	0.81 ($5x10^{-6}$)	.020 (>10^{-8})	Uchida et al., (1996)
TRUE-1 Block ÄMTF Task 4	-9.3	2	2.45	Hermanson et al. (2001)
ÄMTF Task 5	-6.8 ($9x10^{-7}$)	0.81 ($5x10^{-6}$)	.020 (>10^{-8})	Dershowitz et al., (2000)
TRUE Block Scale	-8.95	0.93	0.29 (>10^{-9})	Dershowitz (in Andersson et al. 2002a)
Canister hole Intersections Prototype Repository	-11.50 (set 1) -9.77 (set 2) -11.59 (set 3)	2.30 (set 1) 2.07 (set 2) 1.47 (set 3)	3.41 (>10^{-10})	Stigsson et al. (2001)

Two geological structure types have been defined in Chapter 2: Faults (Geological Structure Type 1), and Non-faults (Geological Structure Type 2). In general, conductive structures of 0.5 m are of Type 2, while structures larger than 100 m are associated with Type 1. However, structures of both Type 1 and Type 2 do occur at all scales. To simplify, the probability of Type 1 structures is defined using an exponential function;

$$P[\text{Type-1}] = 1\text{-}e^{-0.7\ S/R} \qquad (3\text{-}1)$$

where R is the fracture size (radius) at which 50% of structures are Type 1, and 50% are Type 2. Based on a review of TRUE Block Scale structures, the scale R is approximately 20 metres. Geological structure type was assigned to all stochastically generated structures, both background fractures and 100 m scale synthetic structures.

Figure 3-2 and Figure 3-3 provide stereographic projections of background fracture orientations for the two identified fracture sets, cf. Table 3-1. Figure 5-5 and Figure 5-6 provide visualisations of the background fracture realisation, coloured by set, transmissivity, and geological structure type, respectively.

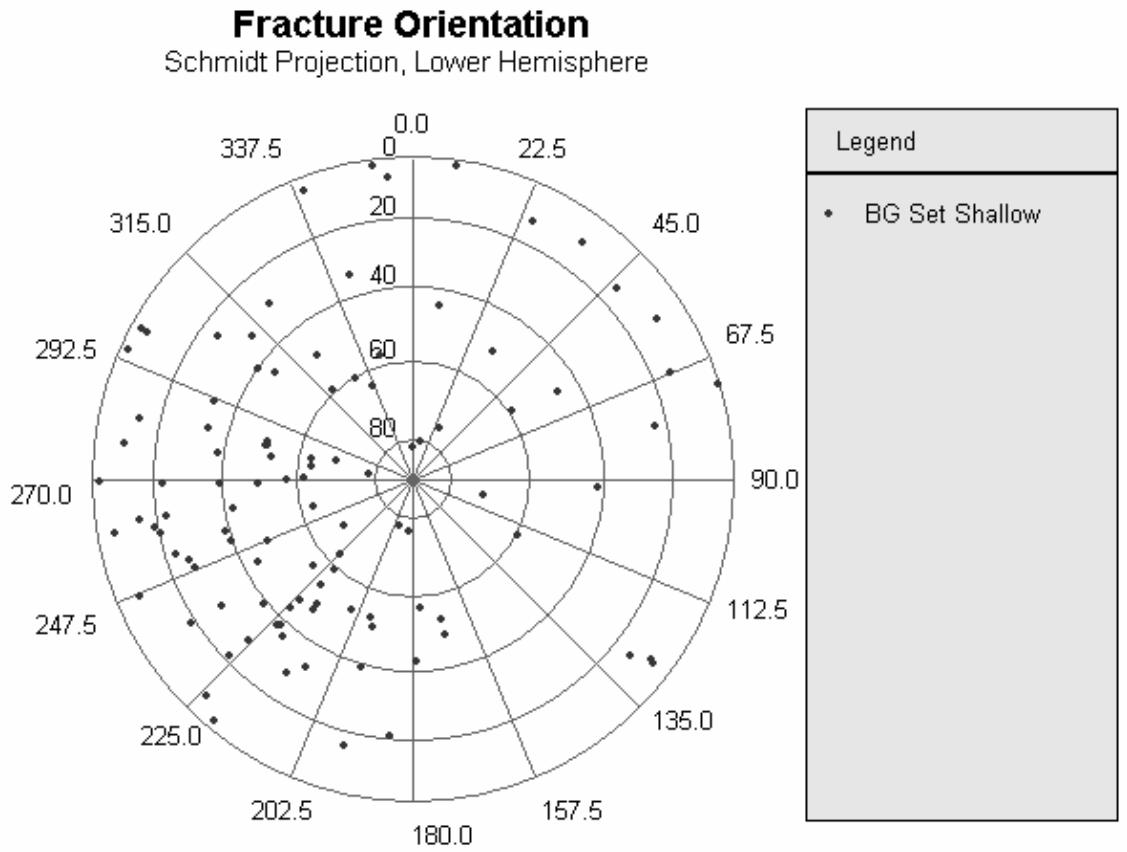

Figure 3-2. *Stereonet of "Background fracture set #2", cf. Table 3-1.*

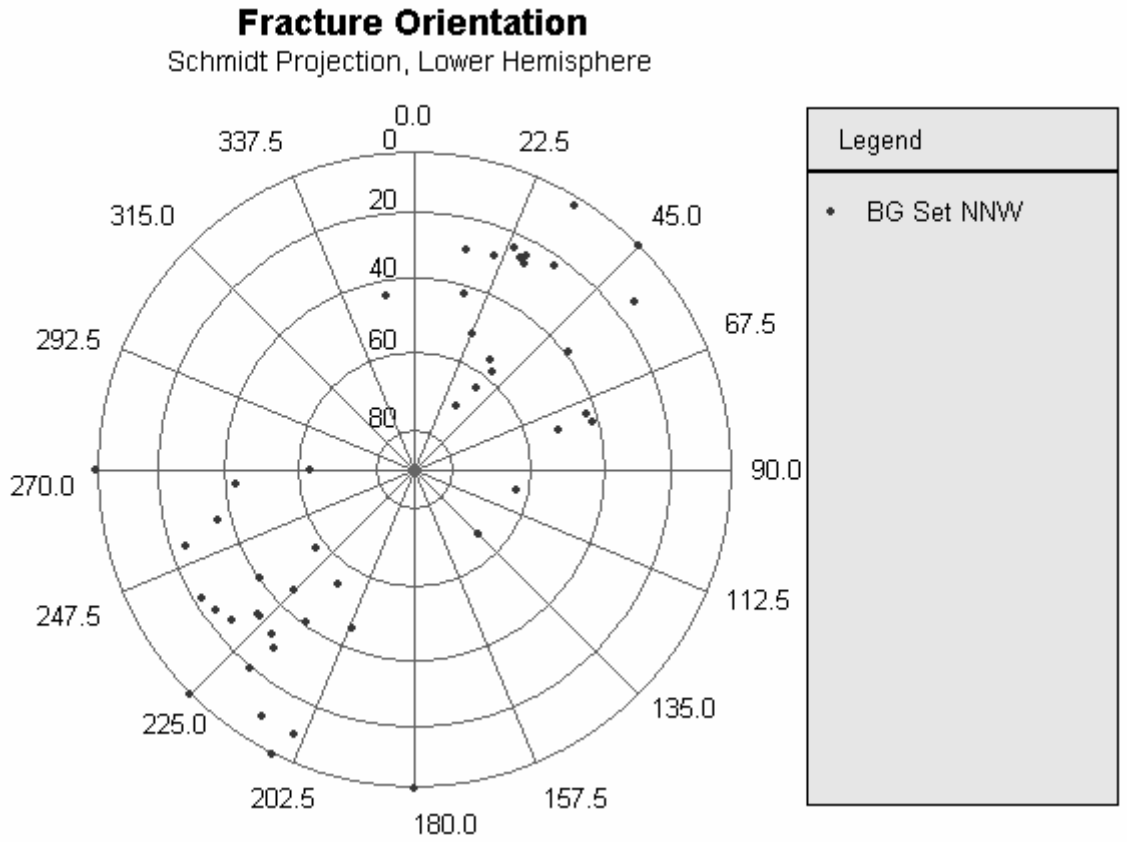

Figure 3-3. *Stereonet of "Background fracture set #1", cf. Table 3-1.*

3.3 100-m Scale Structures

3.3.1 TRUE Block Scale Structures

The primary conductive elements of the 200 m scale Task 6C hydrostructural model are the interpreted deterministic TRUE Block scale structures. Within the 2000 m scale model, and to a lesser extent the 200 m scale model, synthetic 100 m scale structures contribute to flow and transport.

The structural framework of the 200 m scale model is based on the latest version of the TRUE Block Scale structures, including modifications made during 2002. The deterministic structures are specified by four corner points (Table 3-4). Based on an additional analysis of site data for the purpose of Task 6C, the following structures from the TRUE Block Scale hydrostructural model were eliminated:

- Structures 1,2,3 and 4 were eliminated because evidence of their existence was limited to a single borehole (KA2563A) and they were outside the main part of the TRUE Block Scale rock volume
- Structures 8,9,11,12 and 14 were eliminated because hydraulic interference data did not support their existence
- Sub-horizontal structures 15 through 18 were eliminated because they were only postulated based on geological and geophysical data, and there is no borehole, tunnel, or hydrogeologic evidence to support the existence of hydraulically significant sub-horizontal structures.

Structure coordinates are based on the latest TRUE Block Scale analyses. All structures are treated as planar, even through the actual locations of structure intercepts in borehole, when extrapolated, can be off by up to 10 metres. This has been accounted for in the TRUE Block Scale project by using "virtual" packer locations in the developed numerical flow models, rather than the actual locations of structure intersections in the boreholes.

Each of the structures in Table 3-4 has been assigned a single value of transmissivity. Table 3-5 provides structure transmissivity information obtained from packer tests and flow logs, and transmissivity values employed in DFN and Stochastic Continuum modelling of the structures. The data clearly indicates significant variability within the structures. Thus, while the reference model assigns a single transmissivity value, it is anticipated that modelling will also be carried out with more realistic variations within structures. For reference purposes, the geometric mean values are recommended for use in Task 6.

Table 3-4. Corner coordinates of interpreted deterministic structures of the TRUE Block Scale 200-m model (Hermanson and Doe, 2000).

Structure Name	Width (m)	Length (m)	Corner 1 Easting (m)	Northing (m)	Elevation (masl)	Corner 2 Easting (m)	Northing (m)	Elevation (masl)	Corner 3 Easting (m)	Northing (m)	Elevation (masl)	Corner 4 Easting (m)	Northing (m)	Elevation (masl)
5	450.49	500.02	1736.03	7329.37	-200.00	2150.00	7151.68	-200.00	2150.00	7147.35	-700.00	1849.52	7276.33	-700.00
6	77.21	84.91	1894.27	7259.38	-438.46	1898.04	7257.10	-515.54	1943.68	7185.50	-515.54	1942.01	7184.49	-438.46
7	113.55	112.25	1885.40	7237.62	-420.87	1877.60	7222.43	-533.13	1978.11	7172.43	-533.13	1985.91	7187.62	-420.87
10	131.07	124.48	1799.34	7084.83	-414.76	1807.46	7125.05	-539.24	1931.36	7113.05	-539.24	1923.24	7072.83	-414.76
13	145.49	106.66	1844.39	7198.82	-397.01	1890.79	7234.04	-530.33	1955.21	7149.04	-530.33	1908.82	7113.82	-397.01
19	166.41	248.82	1794.96	7316.79	-395.48	1813.76	7289.29	-558.52	1941.28	7075.63	-558.52	1958.78	7042.31	-395.48
20	157.67	120.11	1873.00	7224.29	-380.00	1883.44	7233.52	-537.06	1962.98	7143.52	-537.06	1952.54	7134.29	-380.00
21	91.98	87.08	1908.28	7235.88	-433.46	1881.06	7224.18	-520.54	1915.45	7144.18	-520.54	1942.67	7155.88	-433.46
22	93.34	49.80	1933.48	7211.17	-439.65	1903.29	7196.85	-526.80	1924.62	7151.85	-526.80	1954.81	7166.17	-439.65
23	49.06	24.53	1926.76	7198.00	-452.47	1926.76	7198.00	-501.53	1943.43	7180.00	-501.53	1943.43	7180.00	-452.47
24	34.93	34.06	1931.11	7220.00	-459.97	1923.34	7220.00	-494.03	1949.34	7198.00	-494.03	1957.10	7198.00	-459.97

Table 3-5. Summary of transmissivity established for the interpreted TRUE Block Scale deterministic structures. Example values of transmissivity (m^2/s) and hydraulic conductivity (m/s) are given for reference for the calibrated TRUE Block Scale numerical 3D flow models.

Structure #	Geometric Mean	Arithmetic Mean	Arithmetic StDv	Log10-mean	Log10 St.Dev	Holton (in prep)	Dershowitz et al (2001)	Gómez-Hernández et al (2002) [2]
5	4.02E-07	3.84E-06	7.39E-06	-6.40	0.93		-5.00	-4.62
6	1.91E-07	4.88E-07	8.18E-07	-7.01	1.18		-7.00	-8.29
7	9.76E-08	6.42E-07	1.00E-06	-6.72	0.84		-4.74	-7.37
10	2.98E-08	1.26E-07	1.32E-07	-7.07	0.58		-5.52	-7.41
13	1.38E-08	3.25E-08	2.61E-08	-7.66	0.51		-6.77	-6.59
19	1.02E-07	2.66E-07	3.49E-07	-6.78	0.54		-5.74	-5.52
20	1.43E-07	2.82E-07	4.06E-07	-6.85	0.57	-6.38	-6.02	-6.58
21	6.02E-08	8.88E-08	8.13E-08	-7.22	0.35	-7.33	-6.09	
22	2.19E-08	1.68E-07	1.87E-07	-6.99	0.66	-6.75	-6.43	
23	1.66E-07	2.02E-08	2.09E-08	-7.86	0.57	-6.65	-8.17	
24	8.51E-08	2.98E-08		-7.53	-		-7.53	
Z							-5.30	-7.13
EW-1							-4.92	-6.32
EW-3							-4.77	
NE-1							-3.66	
NE-2							-6.92	
NNW-7							-5.12	

Table 3-6 summarises the geological and structure-geological categorisation attributed to the deterministic 100 m structures interpreted in the TRUE Block Scale rock volume. This assignment is used together with the microstructural assignment to determine transport properties for structures.

Table 3-6 is based on information found in Andersson et al. (2002a).

[2] All elements in the stochastic continuum model of Gómez-Hernández et al are 6.67x6.67x6.67 m, whether classified as intersected by a structure or not. The hydraulic conductivity for the deterministic structures were derived by scaling transmissivity values from short term pump tests, accounting for the distance between packers.

Table 3-6. Attribution of geologic categorisation to 100 m scale deterministic structures (based on information in Andersson et al., (2002a).

Zone	Complexity and Variability	Ductile Precursor Mylonites	Brittle fault rock	Cohesive Cataclasites	Incohesive Faults	Hydro-thermally Altered	Fracture in-fill Mineralogy	Alternation Rim Thickness
5					X		calcite, lithified gouge	
6	x				X		chlorite, calcite, lithified gouge	alteration, oxidation
7					X			altered, oxidised
10	x				X			
13	x	x			25-cm thick fault (0023 and 2563)		calcite	thick alteration
19	x	x			X			10-35cm alteration rim
20	x	x	x	x	X		calcite, gouge	thick alteration
21							calcite, chlorite	
22	x	x	x					
23								
24							open, calcite-coated fracture	

3.3.2 Synthetic 100-m Structures

In addition to the structures introduced by the TRUE Block Scale project, additional structures are included at the periphery of the hydro-structural models based on a single realisation of the stochastic model of 100 m scale structures.

Both 200-m and 2000-m scale models include synthetic structures derived to fill in under-characterised/non-characterised areas to a level of structural detail consistent with the tracer test area of the TRUE Block Scale rock block. These structures are generated based on a statistical analysis of the TRUE Block Scale deterministic structures (Table 3-5). The derived statistical properties for the synthetic 100-m scale structures are summarised in Table 3-7.

Table 3-7. Statistical properties for 100-m scale synthetic structures.

Parameter	Value	Basis
Spatial Model	Baecher (Poisson Process)	Exponential spacing distribution at TRUE Block Scale
Orientation	Single Set Fisher Distribution (κ = 13.6) Mean Pole Trend, Plunge = (45°,1°)	Analysis of TRUE Block Scale conductive deterministic structures (Goodness of Fit Kolmogorov-Smirnov Statistics=99%)
Size	Lognormal Mean=108 m, Stdev=55 m	Statistical analysis of TRUE Block Scale trace lengths (Mean=94.1 m, StDev=44.6 m)
Transmissivity	Correlated to length	See Section 4-3, Figure 4-1
Transport Aperture	Correlated to Transmissivity	See Section 4.3
Intensity	P_{32} = 0.02 m^2/m^3	Statistical analysis of TRUE Block scale deterministic structures

Stochastic 100 m scale structures are generated throughout the full 200 m model region. Within the 200 m model region, stochastic fractures which intersect the TRUE Block Scale boreholes were eliminated since they conflict with the included deterministic structures.

3.4 1000-m Scale Structures

The 1000 m scale structures were assumed to be deterministic, based primarily on the hydrostructural model used for Äspö Task Force Task 5 (Rhén et al., 1997). In addition, the structures were compared with the definitions used in the SKB Alternative Models Project (AMP).

Due to the extensive characterisation of the Äspö HRL site, it is assumed that all the 1000 m scale structures are already characterised, and therefore, no synthetic structures of this scale were generated. For each structure, we provide corner points, thickness, extent, termination, transmissivity, geological structure type, degree of complexity (complexity factor), transmissivity, and aperture. A single generic micro-structural model for all for 1000-m scale structures is defined in Section 4.4.3. This model provides in-fill mineralogy, thickness of alternation rims that can be applied to each 1000-m scale structure.

Tabulation and visualisations of 1000-m scale structures are provided in Sections 4.1 through 4.4.

3.5 Structure heterogeneity

Hydraulic and geologic evidence indicates significant variability in properties across structures. Andersson et al. (2002a) provide BIPS views for each intersection between the TRUE Block Scale structures and the characterisation boreholes. At each location, the structure local aperture, orientation, and microstructure are different. Even the geological structure type of the fracture can be different at local intersections (Figure 3-4).Given the degree of geological variability in structures, it is reasonable to assume a degree of variability in hydraulic and transport properties distributed over the structures. It is anticipated the different approaches to modelling heterogeneity on structures will be a significant focus of Task 6D and 6E modelling activities. Possible approaches include:

- empirical roughness models based on fracture surface profiling (see e.g., Hakami (1995))
- geostatistical variability based on variograms (see e.g., Holton, in prep.)
- fractal variability with conditioning to local measurements
- calibrated heterogeneity based on inverse stochastic continuum modelling (see e.g. Gómez – Hernández et al., (2002))
- conceptual models of geological heterogeneity based on theories of fracture genesis
- channelling approaches based on infill heterogeneity and fracture intersections

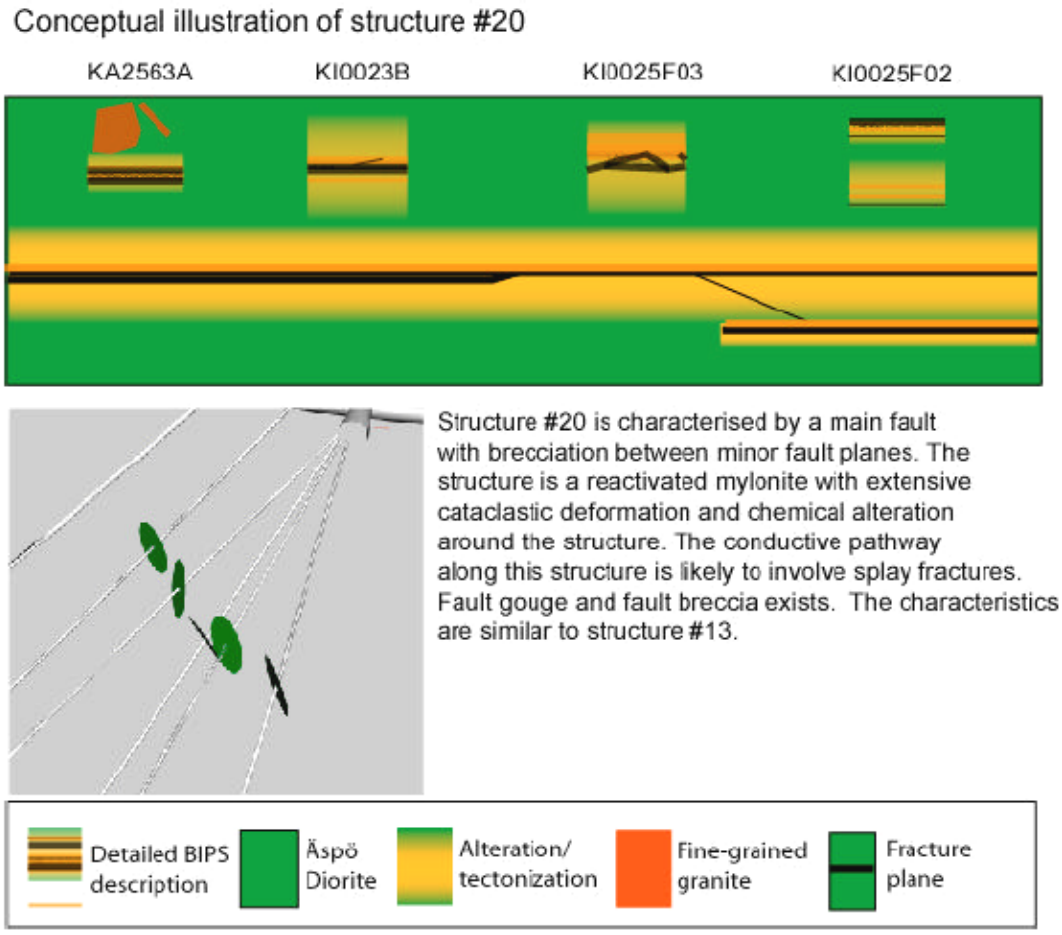

Figure 3-4. *Simplified representation of Structure #20 intersections with TRUE Block Scale boreholes.*

Figure 3-5 and Figure 3-6 illustrate stochastic fields of transmissivity and hydraulic conductivity, respectively, generated on fracture surfaces by Holton, (in prep.) and Gómez –Hernández et al., (2002).

The properties assumed for these fields are summarised in Table 3-8 together with geostatistical data applicable to fracture aperture data reported by Hakami (1995).

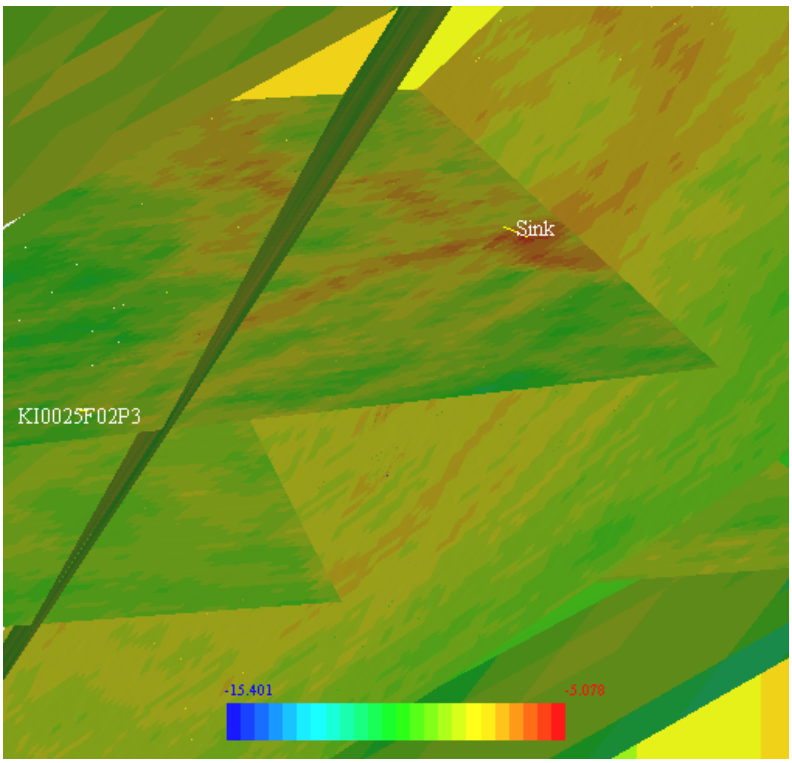

Figure 3-5. *Stochastic transmissivity field on Structure 20 (Holton, in prep.).*

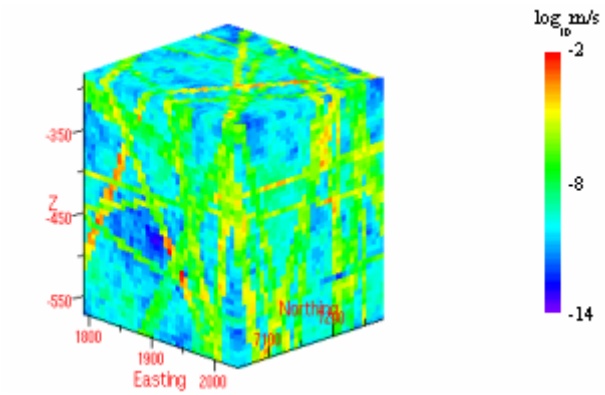

Figure 3-6. *Stochastic field of hydraulic conductivity on structures (Gómez-Hernández et al., 2002).*

Table 3-8. Properties of generated geostatistical stochastic fields of hydraulic material property data

	Gómez – Hernández et al. (2002)	Holton (in prep.)	Hakami (1995)
Variogram type	Spherical	Exponential	Spherical
Correlation length	40-m		7 to 14 cm
Sill			0.20 to 0.25
Coefficient of variation (std.dev/mean)			1.35

One approach for assigning heterogeneity to structures is to start from the hydraulic test results. Posiva flow logs provide the best indicator for local scale transmissivity on individual structures. In summary of the TRUE Block Scale structure transmissivities, cf. Table 3-5, the columns for $\log_{10}$ mean and standard deviation of fracture transmissivity can be used as a basis for defining the level of in plane hydraulic variability. Surprisingly, the $\log_{10}$ standard deviation for the majority of structures is less than 0.7, over distances on the order of 10 to 100 metres. This level of variability indicates that these structures might be treated as hydraulically homogeneous, at least at the inter-borehole scale. The only exceptions are Structures 5, 6, and 7, which show greater than 0.7 orders of magnitude variability, but still show a fairly low variation.

4 Approach for assignment of properties to synthetic structures

4.1 Overview

Synthetic structures in the Task 6C hydrostructural models are specified in terms of a) geometric, b) hydrologic, and c) geologic (transport) properties. These properties are assigned using correlations described in subsequent sections. This chapter summarises the approach for assignment of properties to synthetic structures, using the correlations described in subsequent sections.

For each synthetic structure, the properties of the structure depend on the size of the structure. The generation of synthetic structures is therefore a three-stage process:

1) generate the structure geometry (orientation, location, and size)

2) assign hydrologic properties (transmissivity, storativity, hydraulic aperture) using a correlation to fracture size

3) assign micro-structural model using a correlation to fracture size.

Note that the correlations between size and properties are not one to one, but reflect a degree of variability. This is implemented by assigning properties based on a correlation function, rather than a deterministic relationship. These steps are described below.

4.2 Structure geometry

Structure geometry is specified in terms of intensity, location, orientation, and size (radius).

- **Intensity**: The intensity P_{32} specified for 100-m scale structures is 0.02 m^2/m^3. The intensity P_{32} specified for background structures is 0.29 m^2/m^3. These structures are generated within the model region until this level of intensity is reached.

- **Location**: For both 100-m scale structures and background fractures, the assumed location model is Baecher. Therefore, the locations are specified independently using a Poisson process. Locations are generated as points on the surface of the structure within the model region, such that the structure centres may be outside of the model region.

- **Orientation**: Orientation distributions for 100-m scale structures and background fractures are described in Section 3.3 and 3.4.2. Fracture orientations are generated by the Monte Carlo method following specification of the fracture location.

- **Size**: Fracture size is specified using a lognormal distribution of radius. For 100-m scale structures, the mean is 108 m, and the standard deviation is 55 m. For background fractures the mean is 2 m, and the standard deviation is 2 m. Fracture sizes are generated by the Monte Carlo method. It is noted that a power-law (Pareto) distribution for fracture size can be implemented using parameters shown in Figure A-1, cf. Appendix A.

4.3 Hydraulic properties

Correlations between fracture size and transmissivity have been "postulated" over at least the past 20 years (Long, 1983). Mauldon and Dershowitz (2003) present a generic correlation between feature size and transmissivity based on data from a variety of sites worldwide. For Task 6C, an Äspö HRL specific correlation was developed as shown in Figure 4-1.

The correlation shown in Figure 4-1 is based on the transmissivities of:

- 1000 m Scale Structures in the Task 5 hydrostructural model (Rhén et al., 1997)
- 100 m scale structures in the TRUE Block Scale hydrostructural model Table 3-5 above)
- Stochastically generated background fractures based on the statistics of Table 3-1.

The correlation between fracture size (length-dimension, metres) and transmissivity (m^2/s) can be expressed by:

$$T = a\, L^b \qquad (4\text{-}1)$$

Within each individual scale of features, the correlation between size and transmissivity is unclear. However, when combining data from multiple scales, a power-law correlation emerges, albeit with significant scatter. This correlation can be used to:

- assign transmissivities to structures of all scales in a consistent manner, correlated to fracture size, and
- extrapolate the existence and properties of structures between the well documented scales

The correlation shown in Figure 4-1 is preliminary, and should therefore be used with caution. Nevertheless, it was considered sufficiently reasonable to be used in assigning transmissivities to synthetic background and synthetic 100 m scale structures for both the 2000 m and 200 m scale models.

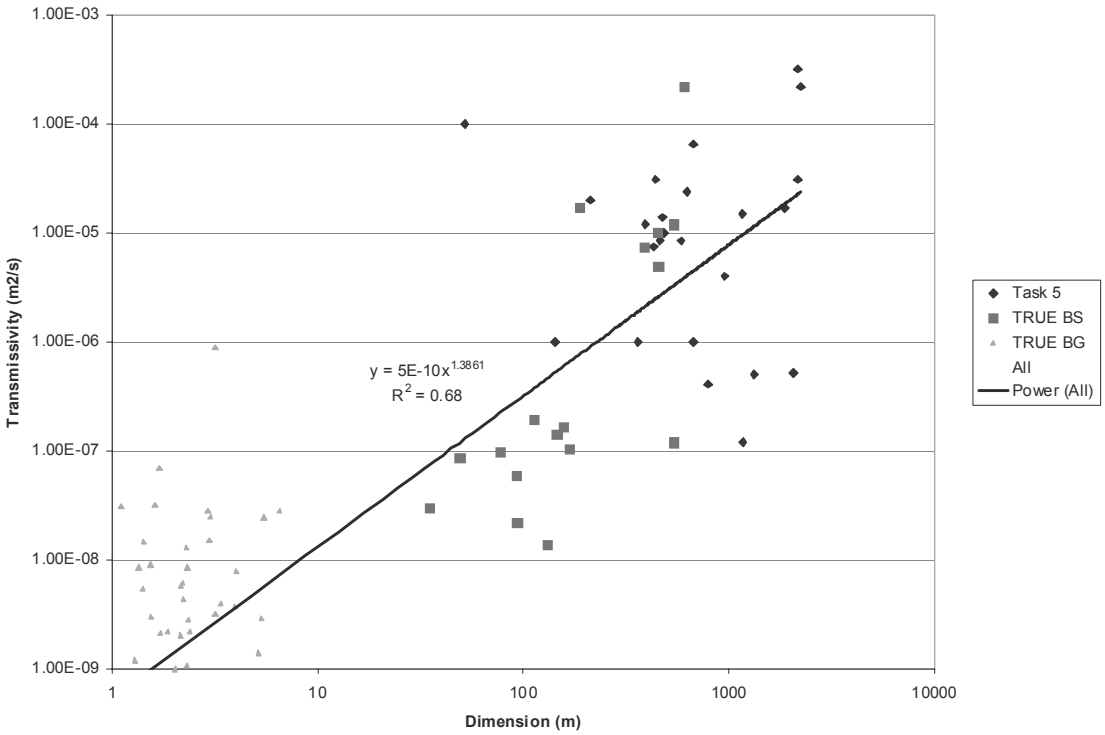

Figure 4-1. *Correlation between structure/fracture size and transmissivity.*

The fracture hydraulic properties are assigned using the correlated to fracture size derived using data from the TRUE Block Scale and Äspö Site Characterisation projects. The transmissivity T (m^2/s) is related to length L (m) as (Figure 4-1)

$$T = 5\ 10^{-10}\ L^{\ 1.386} \tag{4-2}$$

This relationship has a correlation coefficient of 0.68, indicating significant scatter in the relationship between transmissivity and length. Therefore, transmissivity was assigned using Monte Carlo simulation to achieve a similar scatter. For each fracture, the fracture length is calculated as the trace in the horizontal plane. The fracture transmissivity is then assigned stochastically, using the relationship,

$$T(L,r) = 5\ 10^{-10}\ L^{\ (1.386\ +0.3r)} \tag{4-3}$$

where *r* is a uniform (-0.5,0.5) pseudo-random deviate. This relationship produces the same correlation coefficient of 0.68 for a joint analysis of all available data, cf. Figure 4-1.

Fracture storativity S, hydraulic aperture e_h, and transport aperture e_t are assigned directly correlated to fracture transmissivity, using the relationships (cf. Appendix A),

$$S = a_s\ T^{\ b_s} \tag{4-4}$$

$$e_h = a_h\ T^{\ b_h} \tag{4-5}$$

$$e_t = a_t\ e_h \tag{4-6}$$

where a and b are empirical constants. The constants a_s and a_h are 0.46 and 0.5 respectively. The constants b_s and b_h are 0.5 based on the analysis described in Appendix A. The constant a_t is assigned a value of 0.125 based on the results of model calibration to tracer test results (Dershowitz and Klise, 2002).

4.4 Microstructural model

As developed in Chapter 2, the microstructural models has been reduced into two basic types, Geological Structural Type 1 (Fault), and Type 2 (Non-fault). For each type there is a particular specification of the geometry and occurrence of minerals, infillings, and altered zones effecting transport properties within the feature.

This section describes the approach developed for specification of Geological Structural Type, and the distribution of Geological Structural Type among and along the features that make up a given hydraulic structure. The approach for assignment of microstructural models is illustrated in Figure 4-2.

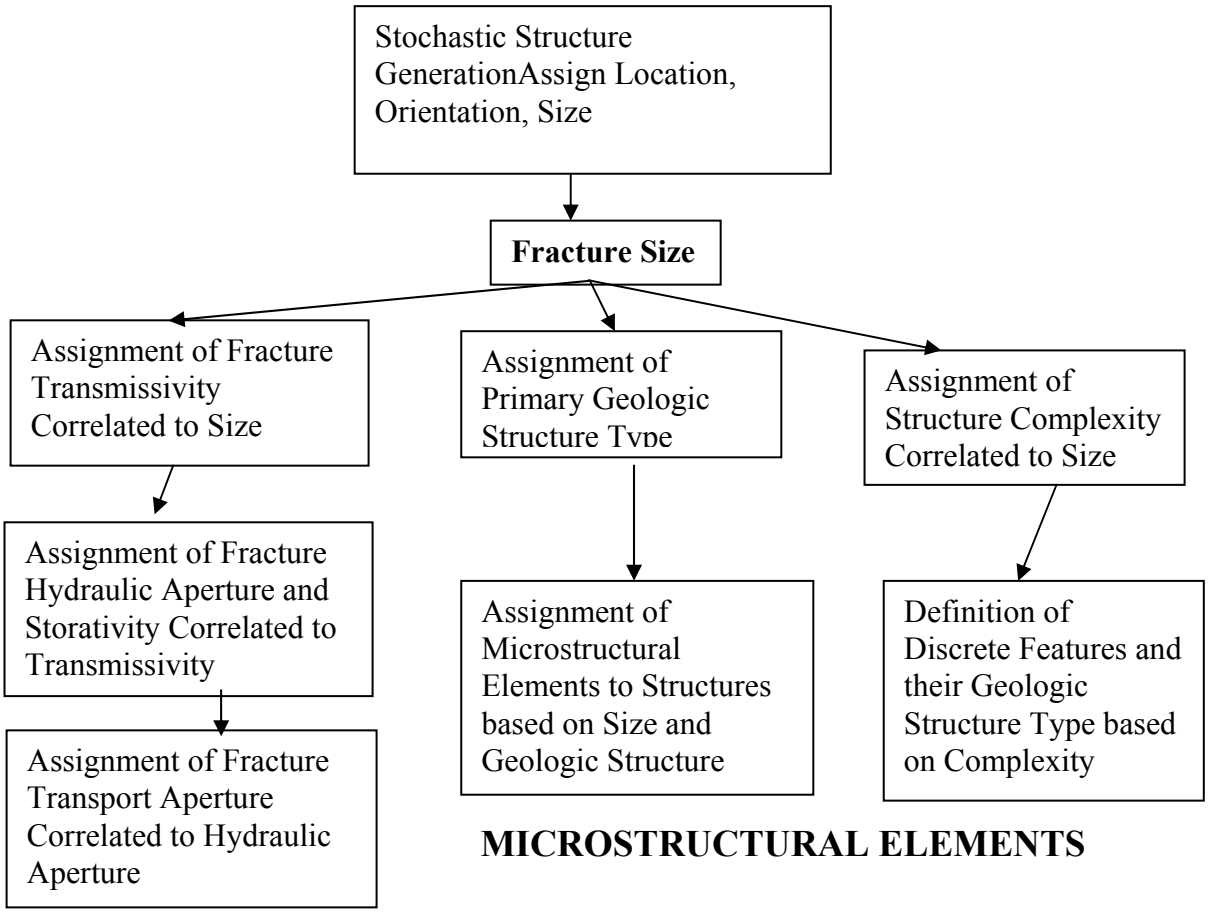

Figure 4-2. *Flow chart showing the basic simplifications used for the micro/macro semi-synthetic structure model.*

The approach to microstructural models defined in Chapter 2 is the key to assignment of transport properties to both deterministic and synthetic structures. This section describes the approach developed to simplify this assignment. The approach consists of two basic components.

First, every conductive structure is assigned a primary "Geological Structure Type", using the terminology of Section 2.2.1, i.e. Geological Structure Type 1 (Fault), and Geological Structure Type 2 (Non-fault).

Secondly, every structure is assigned a "Complexity Factor", cf. definition in Section 4.4.2. This complexity factor reflects three levels of detail:

- the typical number of features (conductive fractures) which make up the structure,
- the variation in the number of features within the structures, where at different locations within the structure it may be composed of a different number of features,
- the variation in the "Geological Structure Type" among the features within the structure, where different features within the structure may have different "Geological Structure Type" at different locations.

The subsequent sections describe the developed approach for assigning microstructural models and properties to structures.

4.4.1 Geological Structure Type

The microstructural model approach depends on the assignment of a geological structure type to each structure. Table 4-1 and Table 4-2 show the assignment of primary geological structure type to each of the deterministic 100 m Scale and 1000 m scale structures. This assignment was made by geologists assigned to Task 6C based on the geological structure type that is most common to the structure. The geological structure type in Table 4-1 is a simplification of the distribution of geological structure types among the fractures that make up structures. More detailed information is contained in Table 4-8 below.

Table 4-1. Geological Structure Type assigned to 100-m Scale deterministic structures

Structure ID	Transmissivity (m^2/s)	Storativity	Transport Aperture (m)	Geological Structure Type
5	4.020E-07	3.170E-04	2.917E-04	1
6	1.910E-07	2.185E-04	2.010E-04	2
7	9.760E-08	1.562E-04	1.437E-04	2
10	2.980E-08	8.631E-05	7.941E-05	1
13	1.380E-08	5.874E-05	5.404E-05	1
19	1.020E-07	1.597E-04	1.469E-04	1
20	1.430E-07	1.891E-04	1.740E-04	1
21	6.020E-08	1.227E-04	1.129E-04	2
22	2.190E-08	7.399E-05	6.807E-05	2
23	1.660E-07	2.037E-04	1.874E-04	2
24	8.510E-08	1.459E-04	1.342E-04	2

Table 4-2. Geological Structure Type assigned to 1000-m Scale deterministic structures

Structure Id	Width (m)	Length (m)	Geological width (m)	Geological Structure Type
EW-1N	2066.13	1002.24	100	1
EW-1S	393.28	654.02	100	1
EW-3 (z=500-200)	1874.09	305.86	25	1
EW-3 (z<200)	1326.33	713.66	25	1
EW-7	1169.95	1013.32	25	1
NE-1	2251.55	1061.15	50	1
NE-2	1174.95	524.04	25	1
NE-3	2168.7	248.67	25	1
NE-4N	2165.43	1067.3	25	1
NE-4S	442.61	799.63	25	1
NW-1	797.52	1773.56	25	1
NNW-1	463.21	1021.32	5	1
NNW-2	626.27	1048.74	5	1
NNW-3	212.61	1000	5	1
NNW-4	671.59	1020.57	5	1
NNW-5	955.22	1000	5	1
NNW-6	475.81	442.5	5	1
NNW-7	430.04	1023.01	5	1
NNW-8	587.04	400	5	1
SFZ11	360.86	1000	200	1
SFZ14a	674.23	1000	200	1
SFZ14b	143.08	1000	200	1

The geologists' assessment of the background fracture population is that they are primary of Geological Structure Type 1. This was implemented with a distribution of 90% Geological Structure Type 1, and 10% Geological Structure Type 2.

To assign geological structure type to synthetic structures, a correlation was derived between structure size and geological structure type. This correlation was derived using the data in Table 4-1 and Table 4-2. The empirical correlation is illustrated in Figure 4-2. As larger structures are considered, the cumulative probability of Type 1 (Fault) structures increases exponentially, converging to 100% for structures of over 1000 m length. This can be approximated by a relationship between fracture size and fracture type as,

$$P[\text{Type 1}] = 1\text{-}e^{-0.7\ S/So}, \qquad (4\text{-}7)$$

where S_0 is 20 metres and S is the structure length/size.

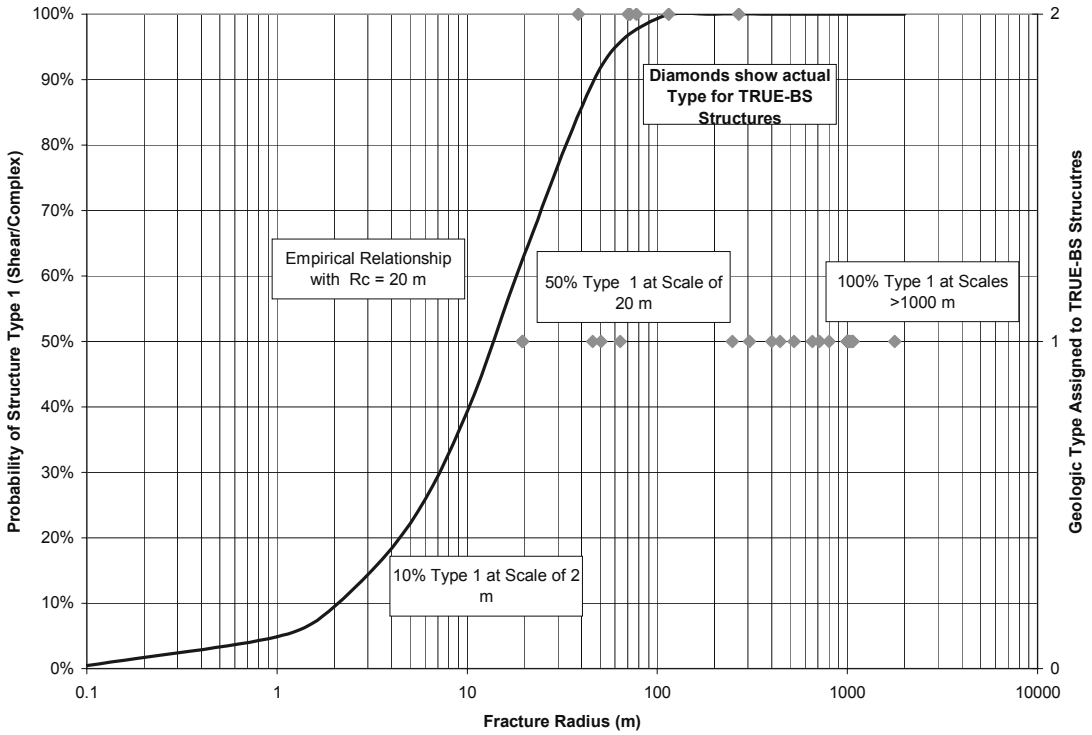

Figure 4-3. *Relationship used for assignment of Geological Structure Type to synthetic 100 m structures and background fractures.*

The relationship of Figure 4-3 was used to assign geological structure type to each of the synthetic 100 m structures, and to all of the background fractures. The result of this assignment is summarised in Table 4-3 and Table 4-4.

Table 4-3. Geological Structure Type assigned to synthetic 100 m structures.

Structure Id.	Width (m)	Length (m)	Geological Structure Type	Complexity Factor
1S	14.11	112.44	1	2
3S	154.39	25.4	2	3
4S	19.12	55.13	2	2
6S	49.78	84.76	1	3
7S	185.43	0.54	2	2
8S	137.11	139.04	1	3
9S	2.73	137.02	1	2
10S	112.02	17.99	1	2
11S	179.49	99.05	1	2
12S	15.45	22.87	1	2
13S	112.2	127.45	1	2
14S	8.31	1.83	2	2
15S	17.45	105.51	1	2
17S	29.19	103.84	1	2
18S	2.35	167.49	1	3
20S	21.05	67.11	1	3
21S	24.18	64.4	1	2
24S	139.91	34.79	1	2
25S	123.71	138.06	1	3

Table 4-4. Geological Structure Type assigned to synthetic background fractures (Sample of N=5648 background fractures in 200 m model)

Fracture Id.	Length (m)	Geologic Structure Type	Complexity Factor
1B	7.34	2	2
2B	3.68	2	1
3B	4.06	2	1
4B	4.96	2	1
5B	8.64	2	1
6B	12.78	2	1
7B	8.22	2	1
8B	8.38	2	1
9B	7.95	2	2
10B	4.91	2	1
11B	18.79	1	1
12B	9.33	2	1
13B	3.65	2	1
14B	3.78	2	1
15B	16.42	1	1
16B	4.51	2	1
17B	3.76	2	1
18B	12.73	2	1
19B	5.85	2	1
20B	6.29	2	1
21B	10.94	2	2
22B	4.17	2	1
23B	8.23	2	1
24B	10.28	2	1
25B	4.48	1	1
26B	4.4	2	1
27B	8.4	2	2
28B	5.52	2	1
29B	4.16	1	1
30B	6.63	2	1
Note: Total of 5648 Background Fractures in 200 m Scale Model. See Task 6C delivery “200 structures ver2.xls ”			

4.4.2 Structure Complexity

Although it is possible to assign a single “representative” geological structure type to each structure, this is a significant simplification. Most structures of 100 m length or longer are made up of several conductive features/fractures, and this number varies over their area. Thus, a given structure may consist of a single fracture of Geological Structure Type 1 at one location, while it consists of two fractures of Geological Structure Type 1 and Type 2, respectively, at another location. This is illustrated schematically in Figure 4-4. The 1000 m scale structures are frequently of thickness greater than 5 m and can contain tens, and possibly even hundreds of hydraulically conductive features/fractures at any given location.

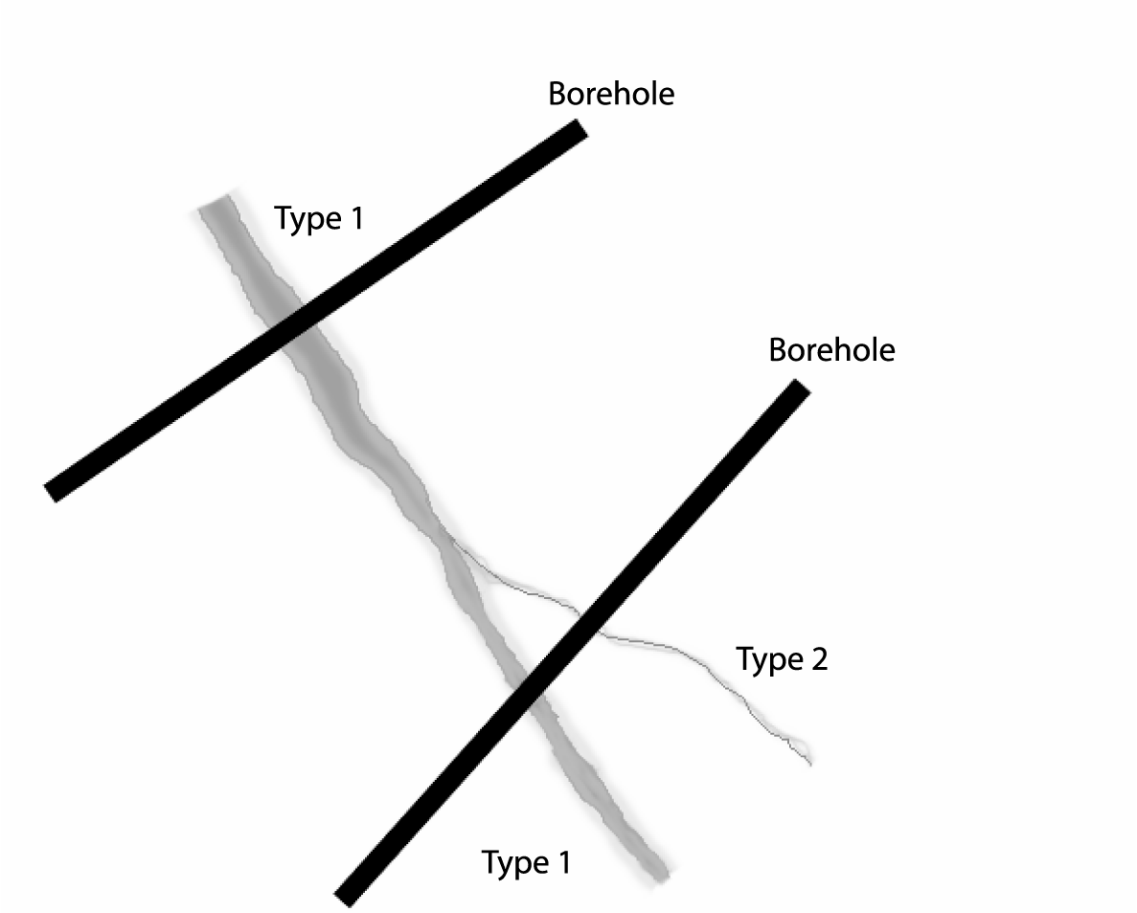

Figure 4-4. *Illustration of the areal coverage of the two different geological structure type concepts. The structures included in the Task 6C reference hydro-structural model contain different areal proportions of geological structure Type 1 and Type 2 along their extent. In the illustration these proportions are roughly 50% geological structure Type 1 and 50% Type 2 + Type 1.*

The variability of geological structure type in a given structure can be specified to varying levels of detail. Ideally, each of the conductive features/fractures that make up the structure should be specified explicitly, complete with its geometric, hydraulic, transport and geologic properties. This level of detail, however, is well beyond the scope of Task 6C, even for the interpreted deterministic structures. Instead, a simplified system has been adopted in which the number of conductive features/fractures, and the combination of primary and secondary geological structure type is specified by a "Complexity Factor". This factor is expressed as a percentage **areal coverage,** as shown in Table 4-5, **related to the outline** (length x depth) of the structure. A complexity factor of 3 implies 1-3 parallel fractures along the extent over which 50-90% of the outline (and associated fracture area) are associated with the primary structure type given in Table 4-5. An example assignment to a synthetic structure is provided in Appendix B.

Table 4-5. Definition of Complexity Factor assigned to modelled synthetic structures (cf. Table 4-3 for application to 100 m scale synthetic structures).

Complexity Factor	Number of (sub-parallel) conductive features/fractures per structure	Percent of primary geological structure type or combination of geological structure types (by area)
1	1	90-100%
2	1 to 2	70 to 100%
3	1 to 3	50 to 90%
4	3 to 10	50 to 90%
5	10+	50 to 90%

In this simplified model, the distance between near parallel features/fractures within a single structure d_N is assumed to be 0.20 m based on available data and observations.

Complexity Factors were assigned to each of the deterministic 100-m scale 1000-m scale structures based on a review of their geology. These assignments are provided in Table 4-6 and Table 4-7. For the deterministic 1000 m structures listed in Table 4-7, structures of geological width greater than 5 metres were assigned a Complexity Factor of 5. The NNW-structures were assigned Complexity Factor of 3 based on their similarity to the TRUE Block Scale deterministic Structures 6, 19, and 20.

Table 4-6. Complexity Factor assigned to 100 m scale deterministic structures.

Structure Id.	Width (m)	Length (m)	Complexity Factor
5	450.49	500.02	2
6	77.21	84.91	3
7	113.55	112.25	3
10	131.07	124.48	2
13	145.49	106.66	2
19	166.41	248.82	3
20	157.67	120.11	3
21	91.98	87.08	2
22	93.34	49.8	2
23	49.06	24.53	2
24	34.93	34.06	2

Table 4-7. Complexity Factor assigned to deterministic 1000-m Scale structures

Structure Id.	Width (m)	Length (m)	Geological width (m)	Complexity Factor
EW-1N	2066.13	1002.24	100	5
EW-1S	393.28	654.02	100	5
EW-3 (z=500-200)	1874.09	305.86	25	5
EW-3 (z<200)	1326.33	713.66	25	5
EW-7	1169.95	1013.32	25	5
NE-1	2251.55	1061.15	50	5
NE-2	1174.95	524.04	25	5
NE-3	2168.7	248.67	25	5
NE-4N	2165.43	1067.3	25	5
NE-4S	442.61	799.63	25	5
NW-1	797.52	1773.56	25	5
NNW-1	463.21	1021.32	5	3
NNW-2	626.27	1048.74	5	3
NNW-3	212.61	1000	5	3
NNW-4	671.59	1020.57	5	3
NNW-5	955.22	1000	5	3
NNW-6	475.81	442.5	5	3
NNW-7	430.04	1023.01	5	3
NNW-8	587.04	400	5	3
SFZ11	360.86	1000	200	5
SFZ14a	674.23	1000	200	5
SFZ14b	143.08	1000	200	5

The use of the complexity factor is illustrated in Figure 4-5. Each deterministic structure is made up of one or more conductive features/fractures at any location. Each of these conductive features/fractures has an assigned geological structure type that defines the appropriate micro-structural retention model, cf. Section 2.2.

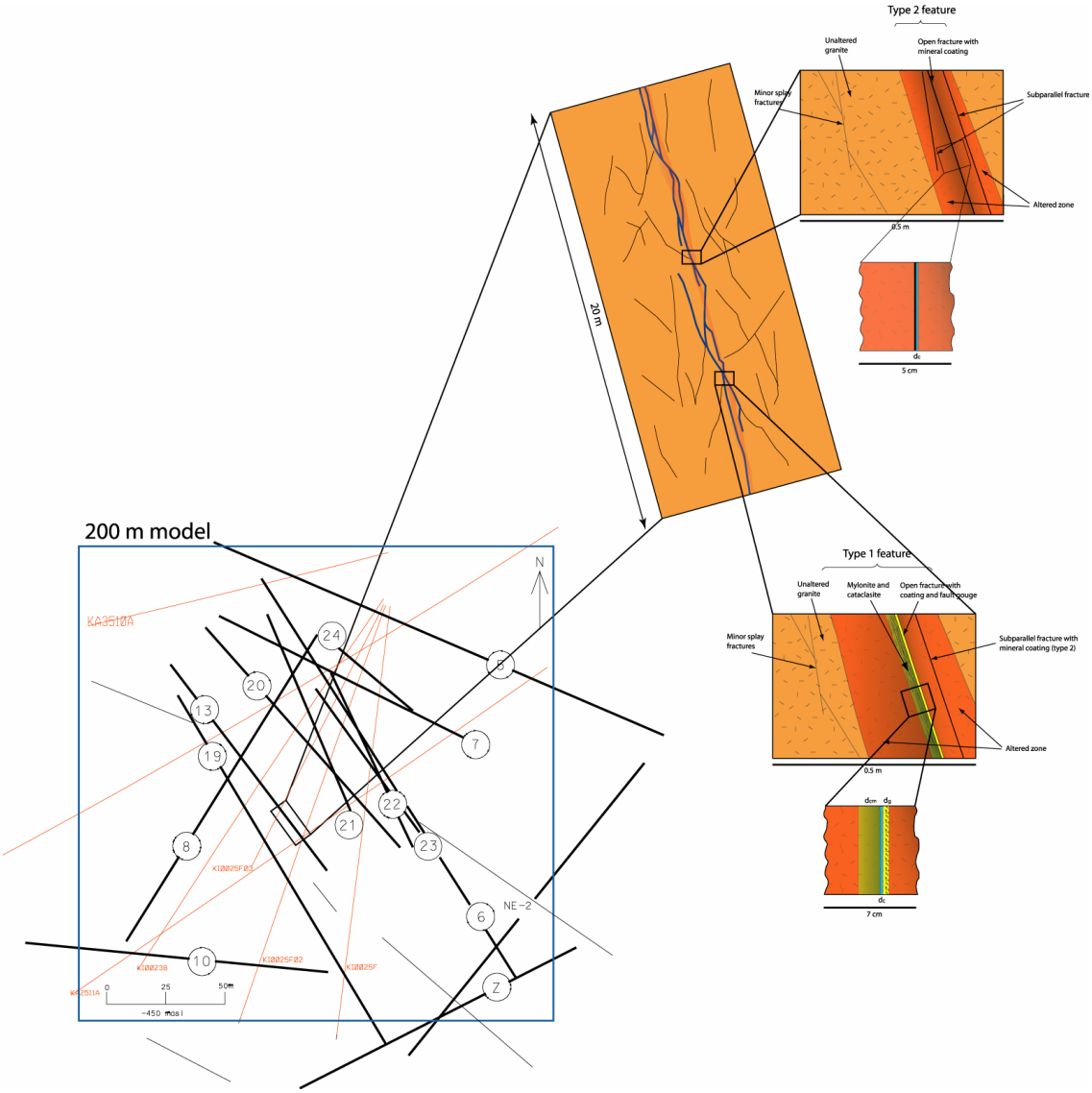

Figure 4-5. *Illustration of geological complexity and the assignment of models of geological structure type over length scales from cm scale to the 200 m reference case Task 6C hydrostructural model.*

The above definition of complexity reflects the fact that for any given structure, the number of features and the Geological Structure Type of features will vary spatially. Consider, for example, Structure 6 in Table 4-6. This structure is assigned a Complexity Factor of 3. From Table 4-5, it can be seen that structures of Complexity Factor 3 vary between 1 and 3 conductive fractures over their extent, and that 50-90% of these structures are comprised of features/fractures of the primary Geological Structure Type. For Structure 6, the primary Structure is Type 1, as specified in Table 4-1. According to the Complexity Factor 3 specification, at some locations, Structure 6 is composed of one feature of Geological Structure Type 1; at other locations of two features, one of which is Geological Structure Type 1; and the other Geological

Structure Type 2; and at still other locations of three features, of both Geological Structure Types 1 and 2. This level of complexity reflects the geologic reality as observed at borehole intercepts during the TRUE Block Scale Project (Andersson et al., 2002a).

The above illustration of the use of complexity factor is extended to all of the deterministic 100-m Scale Structures in Table 4-8 for the TRUE Block Scale deterministic 100 m structures. For each structure and complexity factor, Table 4-8 provides an explicit specification of the number of features/fractures, the Geological Structure Type, and the areal coverage of any given combination of structure types.

For each structure, the complexity factor accounts only for the range in number of conductive features/fractures that make up the structure. Thus, in Figure 4-7, Structure 6 is assigned a Complexity Factor of 3, implying 1-3 features/fractures, with the primary Geological Structure Type (1) covering Table 4-8 shows how this variability manifested itself in the TRUE Block Scale deterministic structures, as observed in the characterisation boreholes. Using these characterisation boreholes, Table 4-8 specifies the percentage areal coverage of the primary combination of geological structure types with the interpreted percentage coverage of secondary combinations of geological structure types. For synthetic structures, the variability in the number of conductive fractures/features and associated Geological Structure Type along the structure area is specified as an interval in the complexity factor. The percentage values provided in Table 4-8 can be used by analogy to extend this variability to the synthetic structures. A higher complexity factor corresponds to a greater variability in the number of fractures and combinations of Geological Structure types.

Table 4-8 provides an explicit assessment/assignment of the spatial pattern of multiple conductive fractures/features and geological structure types for the TRUE Block Scale 100-m scale structures. This table can be used as a guide in building patterns of complexity also for the synthetic 100-m scale structures. Table 4-8 was developed by examining the geology of each of the intercepts of the interpreted deterministic 100-m structures in the TRUE Block Scale characterisation boreholes. Generally, the structures with a Complexity Factor of 2 or 3, and are made up of 2 to 3 conductive fractures/features. However, all the structures exhibit a considerable variability.

Table 4-8. Detailed Assignment of "Overall Complexity" to the deterministic TRUE Block Scale100-m Scale Structures

Structure Id.	Complexity Factor	Percentage areal coverage of combinations of geological structure types	Feature 1	Feature 2	Feature 3
5	2	50%	Type 1	Type 2	
		20%	Type 1	Type 1	
		30%	Type 1	-	
6	3	50%	Type 1	Type 2	-
		30%	Type 2	Type 2	Type 2
		20%	Type 1	Type 2	Type 2
7	3	50%	Type 1	Type 2	-
		30%	Type 2	Type 2	Type 2
		20%	Type 1	Type 2	Type 2
10	2	50%	Type 1	Type 2	
		35%	Type 1		
		15%	Type 2	-	
13	2	50%	Type 1	Type 2	-
		35%	Type 1		-
		15%	Type 2	-	-
19	3	50%	Type 1	Type 2	-
		20%	Type 1	Type 1	-
		30%	Type 1	-	-
20	3	50%	Type 1	Type 2	
		20%	Type 1	Type 1	
		30%	Type 1	-	
21	2	50%	Type 2	Type 2	-
		35%	Type 2	-	-
		15%	Type 1	-	-
22	2	50%	Type 2	Type 2	-
		35%	Type 2	-	-
		15%	Type 1	-	-
23	2	50%	Type 2	Type 2	-
		35%	Type 2	-	-
		15%	Type 1	-	-
24	2	50%	Type 2	Type 2	-
		35%	Type 2	-	-
		15%	Type 1	-	-

For the TRUE Block Scale deterministic structures, (Table 4-6) 64% are of Complexity Factor 2 and 36% are of Complexity Factor 3. The 1000 m scale deterministic structures generally are of Complexity Factor 3 to 5, cf. Table 4-7, although no detailed assignment has been made here in accordance of Table 4-8. This indicates some correlation between complexity factor and fracture size, although the correlation is definitely not one-to-one.

Complexity factor is assigned to synthetic structures at various scales using a correlation between size and complexity factor. This relationship was derived based

Table 4-9. Probability of a given complexity factor for typical scales of synthetic structures.

↓Complexity Factor	Size →	5 m	20 m	100 m	500 m
1		90%	80%	10%	0%
2		10%	20%	30%	0%
3		0%	0%	60%	0%
4		0%	0%	0%	10%
5		0%	0%	0%	90%

on the information in Table 4-6. The correlation between size and complexity factor is summarised in Table 4-9.

An analytical expression will be developed to facilitate interpolation between scales. For smaller structures of 20 m and less, the Complexity Factor is either 1 or 2, see above.

Figure 4-5 illustrates the relationship between complexity and size for the TRUE Block Scale deterministic structures. For lengths less than 50 m, all of the structures are of Complexity Factor 2, such that the probability of Complexity Factor 3 is zero. As the size increases, more Complexity Factor 3 structures are encountered, until the overall population percentage of Complexity 3 (36%) is reached. The assuagement of complexity as a function of structure size is illustrated in Figure 4-6. The right hand y-axis shows the complexity values for deterministic structures, as a function of their size. For example, in Figure 4-6, all the structures of size less than 50 m are either of Complexity Factor 1 or 2, while the structures or around 100 m are about 70% Complexity Factor 2, and 30% Complexity Factor 3.

The left hand y-axis of Figure 4-6 shows the fit of an exponential relationship between complexity factors of 2 and 3 vs. size. As size increases, the probability of Complexity Factor 3 increases, and the probability of Complexity Factor less than 3 decreases.

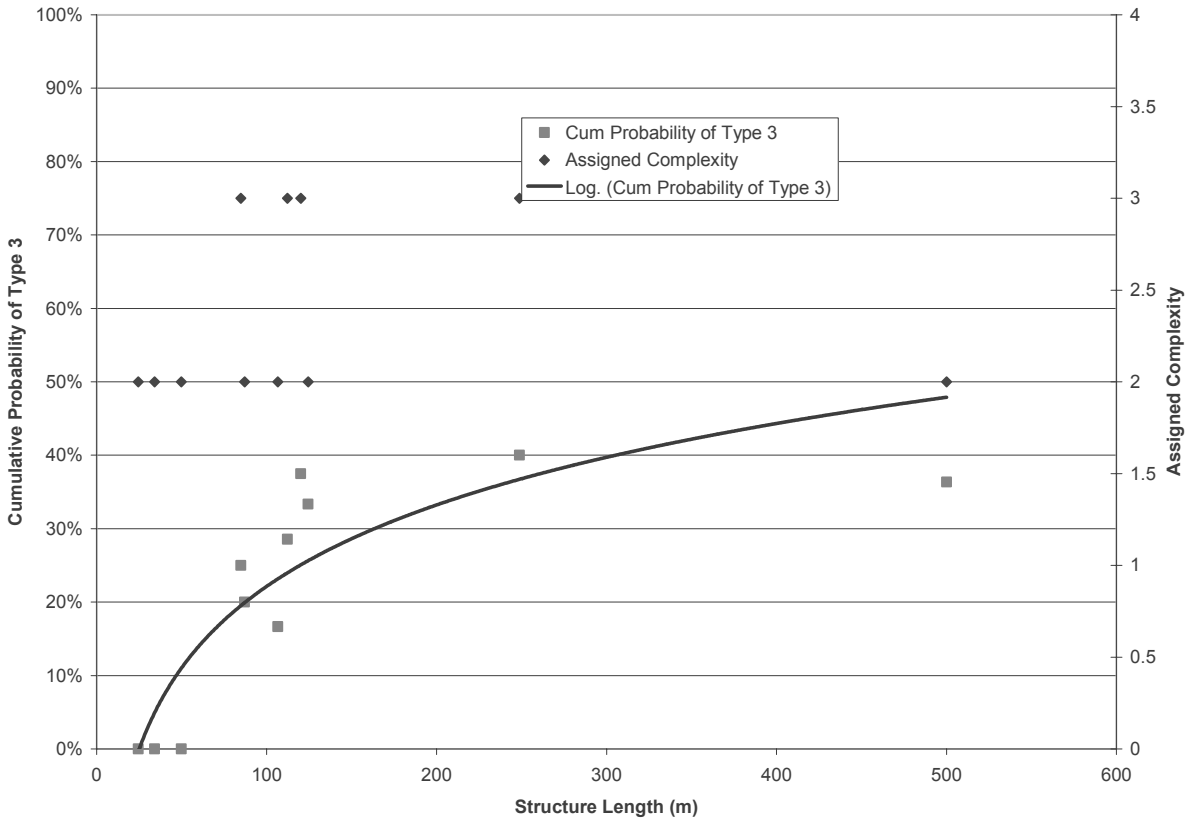

Figure 4-6. *Relationship between Complexity Factor and structure size for TRUE Block Scale deterministic 100 m scale structures.*

To assign complexity factors to background fractures, a simple relationship of 80% Complexity Factor 1, and 20% Complexity Factor 2 was used. For the synthetic 100 m scale structures, the complexity factor was assigned correlated to length according to the relationship

$$P[\text{Complexity Factor 3}] = 1\text{-}e^{-S/So}, \quad (4\text{-}8)$$

where S_0 is 200 metres and S is the structure length/size.

Table 4-3 and Table 4-4 include the complexity factors applied to the synthetic 100m based on this relationship and those of the background fractures, respectively. The complexity factor is assigned to synthetic structures using the exponential relation above.

4.4.3 Scaling of parameters of Microstructural models

For geological structure types Type 1 and Type 2, there is some scale dependence in the geometrical parameters included in the microstructural models. This scale dependence is a result of the difference in geological and geochemical history/evolution and conditions affecting fractures of different sizes. Table 4-10 and Table 4-11 shows how the parameters of the microstructural models vary with the size of the structure involved. The properties provided in Table 4-10 and Table 4-11 are per-discrete feature within the structure. The complexity factor is used to determine the number of discrete features, cf. Section 4.4.2.

100 m scale structures: The microstructural model parameters for 100 m scale structures are based on examination of the TRUE-Block Scale deterministic structures as observed in borehole intersections. The intact wall rock thickness is effectively the distance between the discrete features, past the altered zone. A value of 2 m was specified, since beyond 2 m at least background fractures would generally be encountered based on available statistics. However, a larger value can be used depending on how the model is implemented.

1000 m scale structures: The microstructural model parameters for 1000 m scale structures are generally similar to those for 100 m scale structures. However, since the thickness of these structures is on the range of 5 to 100 m, most of the discrete features making up the structures are completely surrounded by altered wall rock, and no intact wall rock is available except for the outermost discrete features. The altered zone per structure is found by dividing the total thickness of the structure by twice the number of features within the structure at any location. Cataclasite and Fault Gouge thickness are assessed as slightly greater than those for 100 m scale structures due to the increased shear displacement on these structures. However, for simplicity and unified assignment, the geometrical parameter values given in table 4-10 and 4-11 are postulated for all 1000 m structures and conductive features contained in them, irrespective of width and complexity.

***Background fractures*:** The altered zone around background fractures is approximately one order of magnitude less than that for 100 m scale structures due to the smaller amount of geothermal fluid circulation. The thickness of intact wall rock is approximately equal to the half spacing of background fractures. Cataclasite and Fault Gouge thicknesses are slightly less than those for 100 m scale structures due to the decreased shear displacement on these structures.

Table 4-10. Scaled geometrical properties of the microstructural model related to Geological Structure Type 1 attributed to their occurrence at different length scales, ranging in length. Geometrical properties are specified per discrete feature within the structure.

	100 m scale structures			1000-m scale structures			Background fractures (>0.5m)		
Rock type	Thick-ness (cm)	Porosity (%)	Formation factor (−)	Thick-ness (cm)	Porosity (%)	Formation factor (−)	Extent Thick-ness (cm)	Porosity (%)	Formation factor (−)
Intact wall rock	200	0.3	$7 \cdot 10^{-4}$	0	0.3	$7 \cdot 10^{-4}$	200	0.3	$7 \cdot 10^{-4}$
Altered zone	20	0.6	$2 \cdot 10^{-4}$	500	0.6	$2 \cdot 10^{-4}$	2	0.6	$2 \cdot 10^{-4}$
Cataclasite D_{cat}	2	1	$5 \cdot 10^{-4}$	50	1	$5 \cdot 10^{-4}$	0.2	1	$5 \cdot 10^{-4}$
Fault gouge D_g	0.5	20	$5 \cdot 10^{-2}$	1.5	20	$5 \cdot 10^{-2}$	0.05	20	$5 \cdot 10^{-2}$
Fracture coating D_c	0.05	5	$6 \cdot 10^{-3}$	0.05	5	$6 \cdot 10^{-3}$	0.05	5	$6 \cdot 10^{-3}$

Table 4-11. Scaled geometrical properties of the microstructural model related to Geological Structure Type 2 attributed to their occurrence at different length scales, ranging in length from 0.5 m fractures to >1000 m fracture zones. Geometrical properties are specified per discrete feature within the structure.

	100 m scale structures			1000 m scale structures			Background fractures (> 0.5 m)		
Rock type	Thick-ness (cm)	Porosity (%)	Formation factor (−)	Thick-ness (cm)	Porosity (%)	Formation factor (−)	Thick-ness (cm)	Porosity (%)	Formation factor (−)
Intact wall rock	200	0.3	$7 \cdot 10^{-4}$	0	0.3	$7 \cdot 10^{-4}$	200	0.3	$7 \cdot 10^{-4}$
Altered zone	20	0.6	$2 \cdot 10^{-4}$	500	0.6	$2 \cdot 10^{-4}$	2	0.6	$2 \cdot 10^{-4}$
Fracture coating D_c	0.05	5	$6 \cdot 10^{-3}$	0.05	5	$6 \cdot 10^{-3}$	0.05	5	$6 \cdot 10^{-3}$

5 Semi-synthetic hydrostructural models

This chapter describes the implementation of the Task 6C 200-m and 2000-m Scale Semi-Synthetic Hydrostructural models. These models were developed by combining the deterministic and stochastic elements described in Chapters 2 and 3 and the methodology to account for variability and complexity outlined in Chapter 4.

5.1 Block scale (200-m) Semi-Synthetic Hydrostructural Model

The 200-m scale hydrostructural model is based primarily on the TRUE Block Scale hydrostructural model (Andersson et al., 2002a). In addition, the model considers the context of both larger, site scale structures, and the smaller scale, background fractures.

The centre for the 200-m Block Scale model box is at the following Äspö co-ordinates:

- Easting: 1900 m
- Northing: 7170 m
- Elevation: -450 masl

The box is aligned North-South in Äspö coordinates, ±100 m in each horizontal direction, and ±100 metres in each vertical direction.

Deterministic 100 m scale structures are described in Table 5-1. Synthetic 100 m scale structures are described in Table 5-2.[3]

[3] Synthetic structures 2S, 5S, 16S, 19S, 22S, and 23S were removed in the 200-m scale hydrostructural model in the Task 6C electronic data distribution because they conflict with deterministic structures identified in boreholes.

Table 5-1. Deterministic structures of the Task 6C reference case 200 m semi-synthetic hydrostructural model (based on Hermanson and Doe, 2000).

Structure Name	Width (m)	Length (m)	Corner 1 Easting (m)	Northing (m)	Elevation (masl)	Corner 2 Easting (m)	Northing (m)	Elevation (masl)	Corner 3 Easting (m)	Northing (m)	Elevation (masl)	Corner 4 Easting (m)	Northing (m)	Elevation (masl)
5	450.49	500.02	1736.03	7329.37	-200.00	2150.00	7151.68	-200.00	2150.00	7147.35	-700.00	1849.52	7276.33	-700.00
6	77.21	84.91	1894.27	7259.38	-438.46	1898.04	7257.10	-515.54	1943.68	7185.50	-515.54	1942.01	7184.49	-438.46
7	113.55	112.25	1885.40	7237.62	-420.87	1877.60	7222.43	-533.13	1978.11	7172.43	-533.13	1985.91	7187.62	-420.87
10	131.07	124.48	1799.34	7084.83	-414.76	1807.46	7125.05	-539.24	1931.36	7113.05	-539.24	1923.24	7072.83	-414.76
13	145.49	106.66	1844.39	7198.82	-397.01	1890.79	7234.04	-530.33	1955.21	7149.04	-530.33	1908.82	7113.82	-397.01
19	166.41	248.82	1794.96	7316.79	-395.48	1813.76	7289.29	-558.52	1941.28	7075.63	-558.52	1958.78	7042.31	-395.48
20	157.67	120.11	1873.00	7224.29	-380.00	1883.44	7233.52	-537.06	1962.98	7143.52	-537.06	1952.54	7134.29	-380.00
21	91.98	87.08	1908.28	7235.88	-433.46	1881.06	7224.18	-520.54	1915.45	7144.18	-520.54	1942.67	7155.88	-433.46
22	93.34	49.80	1933.48	7211.17	-439.65	1903.29	7196.85	-526.80	1924.62	7151.85	-526.80	1954.81	7166.17	-439.65
23	49.06	24.53	1926.76	7198.00	-452.47	1926.76	7198.00	-501.53	1943.43	7180.00	-501.53	1943.43	7180.00	-452.47
24	34.93	34.06	1931.11	7220.00	-459.97	1923.34	7220.00	-494.03	1949.34	7198.00	-494.03	1957.10	7198.00	-459.97

Table 5-2. Stochastic 100m scale structures in the Task 6C reference case 200 m scale semi-synthetic hydrostructural model.

Structure Name	Width (m)	Length (m)	Geol. Struct. Type	Complexity Factor	Corner 1 Easting (m)	Northing (m)	Elevation (masl)	Corner 2 Easting (m)	Northing (m)	Elevation (m)	Corner 3 Easting (m)	Northing (m)	Elevation (masl)	Corner 4 Easting (m)	Northing (m)	Elevation (masl)	Easting (m)	Northing (m)	Elevation (masl)
1S	14.11	112.44	1	2	2000.00	7144.09	-518.82	1988.50	7152.26	-518.73	1998.41	7164.92	-407.44	2000.00	7163.79	-407.46			
3S	154.39	25.4	2	3	1967.54	7167.72	-550.00	1851.89	7270.00	-550.00	1846.00	7270.00	-525.30	1966.04	7165.00	-530.80			
4S	19.12	55.13	2	2	1800.00	7270.00	-490.05	1800.00	7264.18	-471.84	1849.24	7245.23	-487.83	1838.78	7270.00	-549.39			
6S	49.78	84.76	1	3	1928.78	7270.00	-350.00	1968.34	7239.78	-350.00	2000.00	7207.97	-421.90	2000.00	7207.23	-428.90	1908.37	7270.00	-497.02
7S	185.43	0.54	2	2	1969.48	7088.66	-550.00	1929.53	7269.74	-550.00	1929.55	7270.00	-549.53	1936.92	7270.00	-503.11	1973.86	7148.75	-438.96
8S	137.11	139.04	1	3	1913.12	7070.00	-550.00	1800.00	7147.47	-550.00	1800.00	7148.98	-410.96	1913.75	7070.00	-510.78			
9S	2.73	137.02	1	2	1800.00	7220.75	-350.00	1802.23	7219.19	-350.00	1829.53	7220.51	-484.26	1800.00	7242.03	-490.06			
10S	112.02	17.99	1	2	1878.97	7170.65	-350.00	1928.15	7070.00	-350.00	1931.88	7070.00	-367.60	1901.94	7149.02	-408.54			
11S	179.49	99.05	1	2	1879.46	7270.00	-405.10	1954.11	7194.85	-550.00	1889.59	7270.00	-550.00						
12S	15.45	22.87	1	2	1878.81	7070.00	-515.33	1876.14	7078.44	-502.67	1895.09	7070.00	-493.05						
13S	112.2	127.45	1	2	2000.00	7098.52	-350.00	2000.00	7093.43	-462.08	1886.75	7140.90	-427.98	1908.09	7135.79	-350.00			
14S	8.31	1.83	2	2	1943.25	7070.00	-426.75	1940.37	7070.63	-418.98	1941.97	7070.00	-418.34						
15S	17.45	105.51	1	2	1984.20	7270.00	-350.00	2000.00	7262.59	-350.00	2000.00	7265.99	-455.46	1991.53	7270.00	-456.66			
17S	29.19	103.84	1	2	1800.00	7249.89	-350.00	1829.13	7248.04	-350.00	1900.37	7238.94	-425.00	1800.00	7239.55	-520.41			
18S	2.35	167.49	1	3	1913.80	7270.00	-350.00	1915.76	7268.70	-350.00	1969.83	7224.69	-502.29	1898.19	7270.00	-540.82			
20S	21.05	67.11	1	3	1890.40	7070.00	-350.00	1904.07	7070.00	-366.00	1884.90	7126.63	-396.50	1837.86	7135.75	-350.00			
21S	24.18	64.4	1	2	1800.00	7253.47	-550.00	1800.00	7249.86	-526.09	1840.89	7206.24	-550.00						
24S	139.91	34.79	1	2	1800.00	7196.89	-533.05	1856.41	7070.00	-515.95	1849.30	7070.00	-550.00	1800.00	7188.38	-550.00			
25S	123.71	138.06	1	3	1800.00	7257.32	-350.00	1876.56	7160.15	-350.00	1800.00	7231.02	-440.42						

Figure 5-1 provides a visualisation for the deterministic 100 m scale structures in the 200 m scale model region. Figure 5-2 presents a visualisation of synthetic 100-m scale structures in the 200-m scale model.

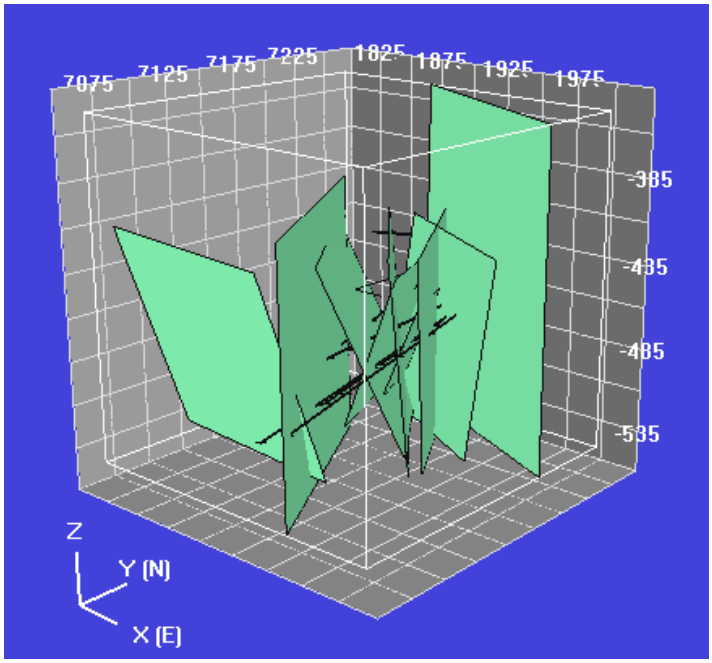

Figure 5-1 *Deterministic 100 m scale structures in the 200-m scale model region.*

In Figure 5-3, the structures are coloured according to transmissivity. Figure 5-4 presents a horizontal slice through the model at the –450 masl.

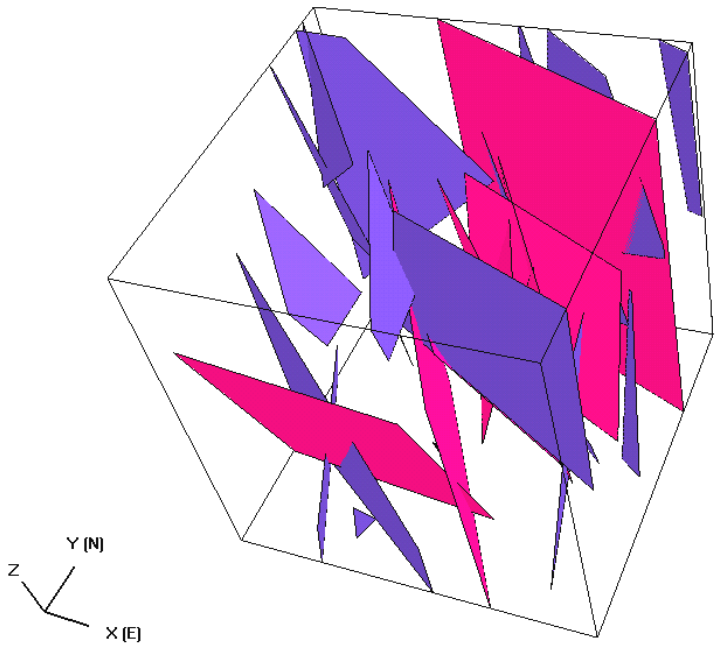

Figure 5-2. *Synthetic 100-m Structures (Blue) with Deterministic 100-m Structures (Red) in 200-m Scale Model.*

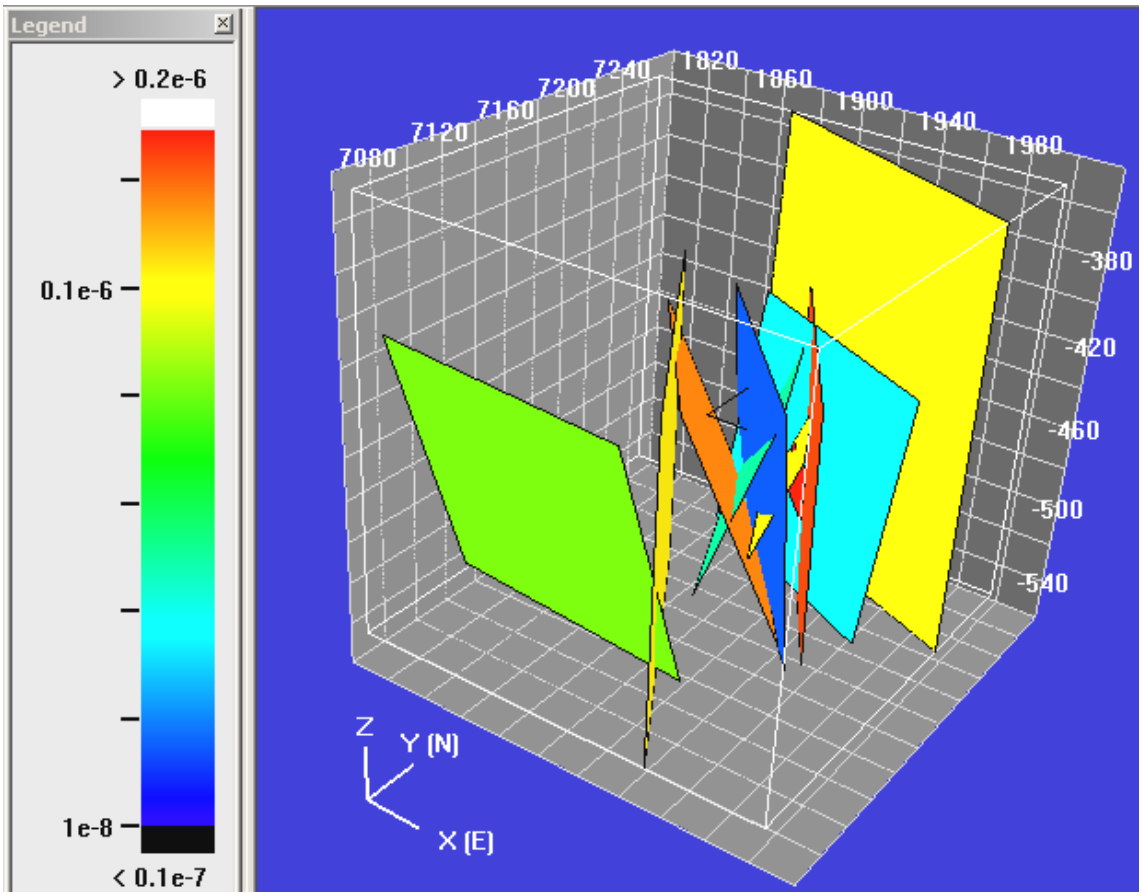

Figure 5-3. *Deterministic 100 m scale structures coloured according to transmissivity.*

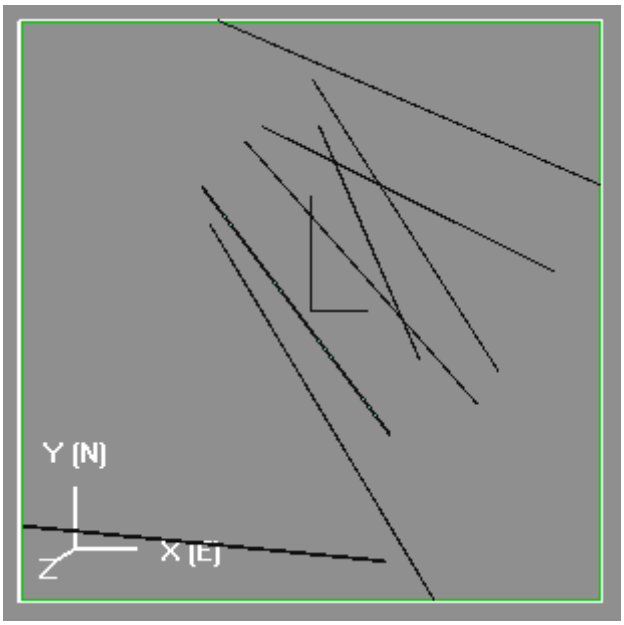

Figure 5-4. *Horizontal section (trace map) through the deterministic 100 m structures of the 200 m model at Z= –450 masl.*

An example sample of 20 synthetic background fractures and their properties are tabulated in Table 5-3. For the complete list of synthetic background fractures in the 200 m scale block model, c.f. Task 6C delivery "200 structures ver2.xls" in the accompanying data distribution. A total of 5660 synthetic background fractures are included the 200 m scale block model. This represents background fracture intensity P_{32} of 0.050 m^2/m^3, obtained by adjusting the fracture intensity according to truncated distributions for radius and transmissivity. The model intensity P_{32} of 0.29 m^2/m^3 was first reduced to 0.092 m^2/m^3 to reflect the removal of background fractures of radius less than 2 m, according to a truncated lognormal distribution. The model intensity P_{32} was then reduced to 0.05 m^2/m^3 to reflect a truncated lognormal distribution of transmissivity, with a minimum of 10^{-9} m^2/s. Note that the background fractures provided in "200 structures ver2.xls" do include fractures less than 10^{-9} m^2/s, because the fracture transmissivities are assigned correlated to radius, rather than directly from the transmissivity distribution. A more complete fracture population reflecting fractures of radius down to 0.5 m, with intensity P_{32} of 0.29 m^2/m^3 was also generated, and is available to the modeling groups as "bg fracs BigPop.zip".

Table 5-3. Example sample (20 Fractures) from background fracture realisation used in Task 6C reference case semi-synthetic hydrostructural models

Fracture #	Length (m)	Geological Structure Type	Complexity Factor	Transmissivity (m^2/s)	Aperture (m)	Corner 1 Easting (m)	Northing (m)	Elevation (masl)	Corner 2 Easting (m)	Northing (m)	Elevation (masl)	Corner 3 Easting (m)	Northing (m)	Elevation (masl)	Corner 4 Easting (m)	Northing (m)	Elevation (masl)
1B	7.34	2	2	2.40E-09	2.25E-05	1980.31	7149.57	-521.95	1977.14	7154.36	-517.39	1970.81	7153.63	-521.03	1973.98	7148.84	-525.59
2B	3.68	2	1	1.23E-08	5.09E-05	1817.78	7189.33	-480.97	1818.90	7186.71	-483.30	1818.90	7184.27	-480.55	1817.79	7186.89	-478.22
3B	4.06	2	1	4.38E-09	3.04E-05	1874.42	7111.45	-463.94	1874.40	7109.39	-460.43	1871.53	7111.88	-458.99	1871.55	7113.94	-462.49
4B	4.96	2	1	5.13E-09	3.29E-05	1955.17	7261.75	-511.20	1952.77	7262.35	-515.50	1956.46	7260.05	-517.88	1958.86	7259.45	-513.58
5B	8.64	2	1	4.82E-09	3.19E-05	1923.86	7077.57	-446.83	1926.53	7074.74	-454.54	1933.75	7071.67	-450.92	1931.08	7074.50	-443.20
6B	12.78	2	1	1.17E-08	4.99E-05	1803.56	7260.66	-418.66	1802.11	7263.52	-431.03	1805.67	7251.66	-434.19	1807.13	7248.80	-421.82
7B	8.22	2	1	6.44E-09	3.69E-05	1953.51	7240.68	-363.59	1959.88	7239.15	-358.64	1956.45	7243.79	-352.79	1950.08	7245.32	-357.75
8B	8.38	2	1	2.31E-08	6.99E-05	1847.12	7114.79	-460.27	1850.99	7114.61	-467.71	1855.18	7107.74	-465.36	1851.30	7107.91	-457.93
9B	7.95	2	2	7.12E-09	3.88E-05	1898.88	7186.97	-531.39	1905.86	7184.40	-534.21	1907.78	7181.68	-527.00	1900.81	7184.24	-524.17
10B	4.91	2	1	7.55E-09	4.00E-05	1925.40	7256.23	-510.77	1926.35	7256.63	-505.96	1921.76	7258.22	-505.19	1920.81	7257.82	-509.99
11B	18.79	1	1	2.67E-08	7.52E-05	1921.68	7123.03	-433.05	1908.32	7130.46	-422.14	1900.40	7138.37	-437.23	1913.76	7130.93	-448.14
12B	9.33	2	1	7.25E-09	3.92E-05	1832.94	7132.08	-460.00	1832.16	7131.79	-469.29	1838.58	7125.02	-469.61	1839.36	7125.32	-460.32
13B	3.65	2	1	1.72E-09	1.91E-05	1906.00	7102.92	-403.50	1909.10	7101.00	-403.66	1908.11	7099.14	-400.68	1905.00	7101.06	-400.52
14B	3.78	2	1	2.37E-09	2.24E-05	1941.53	7075.17	-418.16	1943.15	7074.61	-414.80	1939.74	7074.20	-413.22	1938.12	7074.76	-416.59
15B	16.42	1	1	1.12E-08	4.87E-05	1892.86	7189.28	-367.68	1877.40	7189.02	-373.18	1882.20	7180.39	-386.29	1897.66	7180.64	-380.79
16B	4.51	2	1	1.75E-09	1.92E-05	1972.08	7255.84	-362.41	1973.60	7251.61	-362.74	1972.08	7250.74	-358.58	1970.57	7254.98	-358.25
17B	3.76	2	1	1.89E-09	2.00E-05	1845.85	7267.05	-451.85	1846.30	7266.72	-448.14	1845.16	7270.27	-447.69	1844.71	7270.60	-451.40
18B	12.73	2	2	3.21E-08	8.24E-05	1903.37	7270.86	-392.66	1907.00	7264.72	-403.20	1918.71	7263.37	-398.37	1915.07	7269.52	-387.83
19B	5.85	2	1	1.73E-08	6.06E-05	1829.84	7134.57	-447.21	1832.66	7132.49	-442.53	1828.29	7134.31	-439.10	1825.47	7136.39	-443.78
20B	6.29	2	1	1.81E-08	6.20E-05	1799.37	7221.09	-481.49	1803.49	7216.34	-481.83	1801.41	7214.13	-476.32	1797.29	7218.88	-475.98

Figure 5-5 and Figure 5-6 provide visualisations of the background fracture realisation, coloured by set, transmissivity, and geological structure type, respectively.

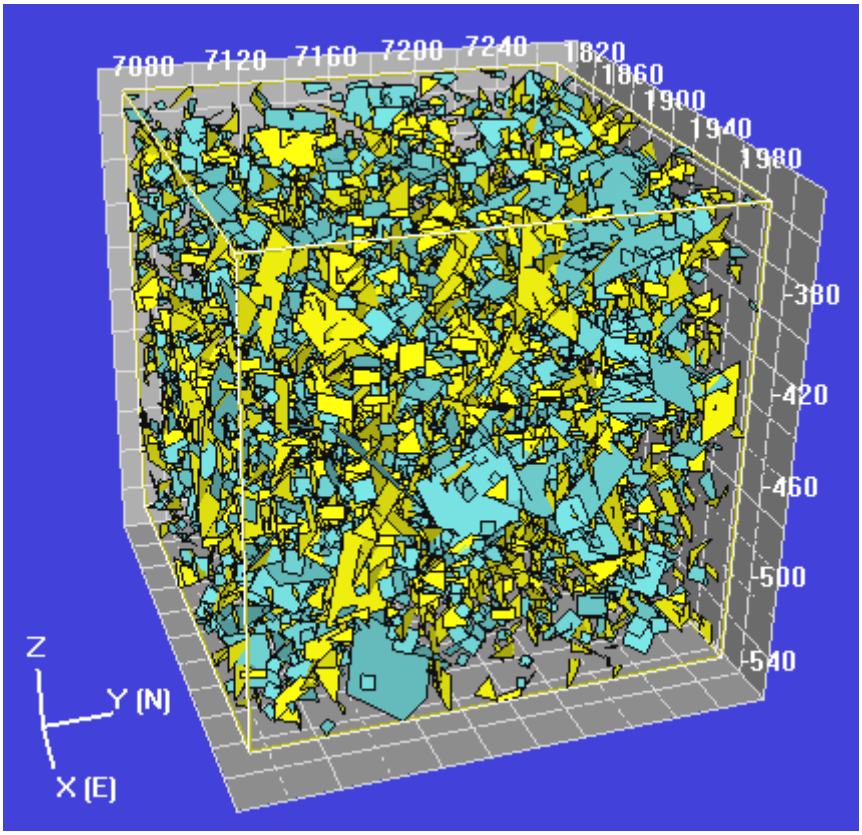

Figure 5-5. *Background fractures coloured by set, Shallow set (blue), NNW (yellow).*

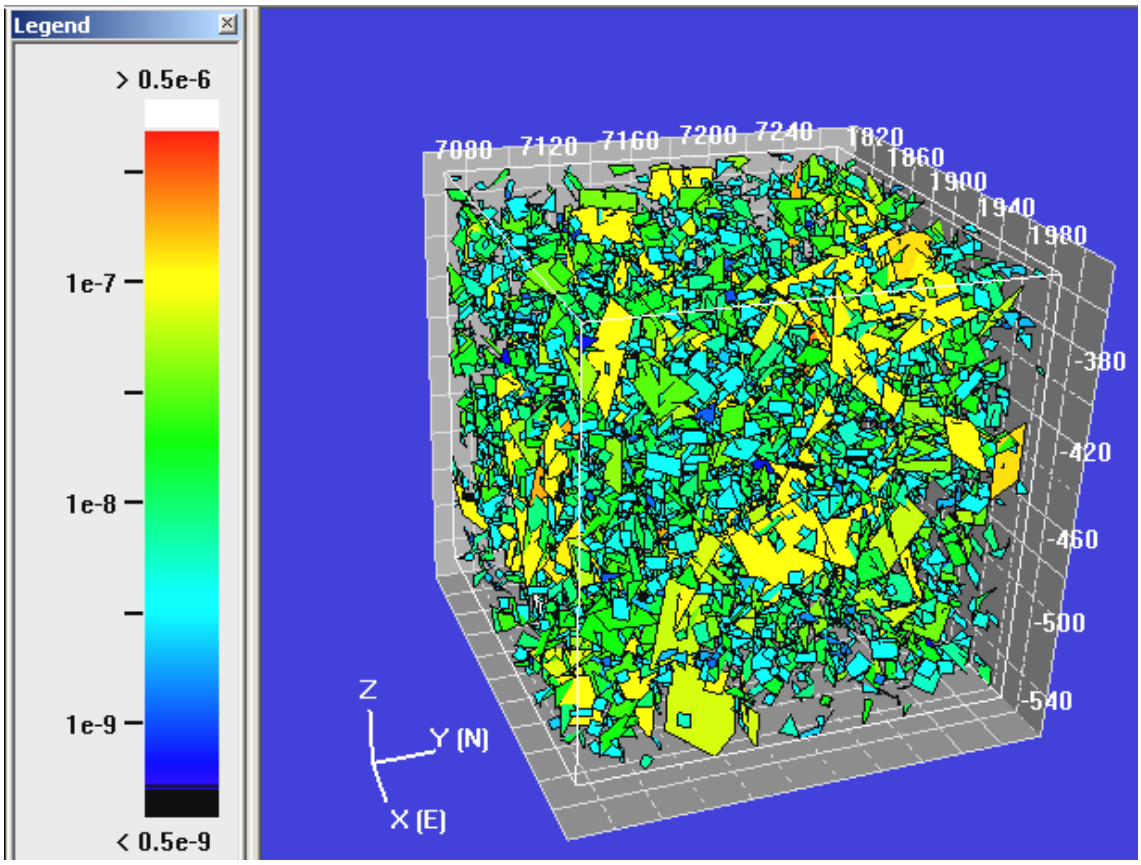

Figure 5-6. *Background fractures coloured by transmissivity (log scale).*

5.2 Site scale (2000-m) Semi Synthetic Hydrostructural Model

The site-scale hydrostructural model is based primarily on the Task 5 Site Scale-Model (Rhén et al., 1997). This model was also the source for the Alternative Models Project hydrostructural model (Selroos et al., 2002). In addition, the model provides the context for the smaller scale rock volume models developed for the TRUE-1 and TRUE Block Scale sites/rock volumes.

The centre for the 2000-m Block Scale model box is at the following Äspö HRL local co-ordinates:

- Easting: 2000 m
- Northing: 7000 m
- Elevation: -450 masl

The box is aligned North-South in Äspö local coordinates, ±1000-m in each horizontal direction, and ±500-meters in each vertical direction.

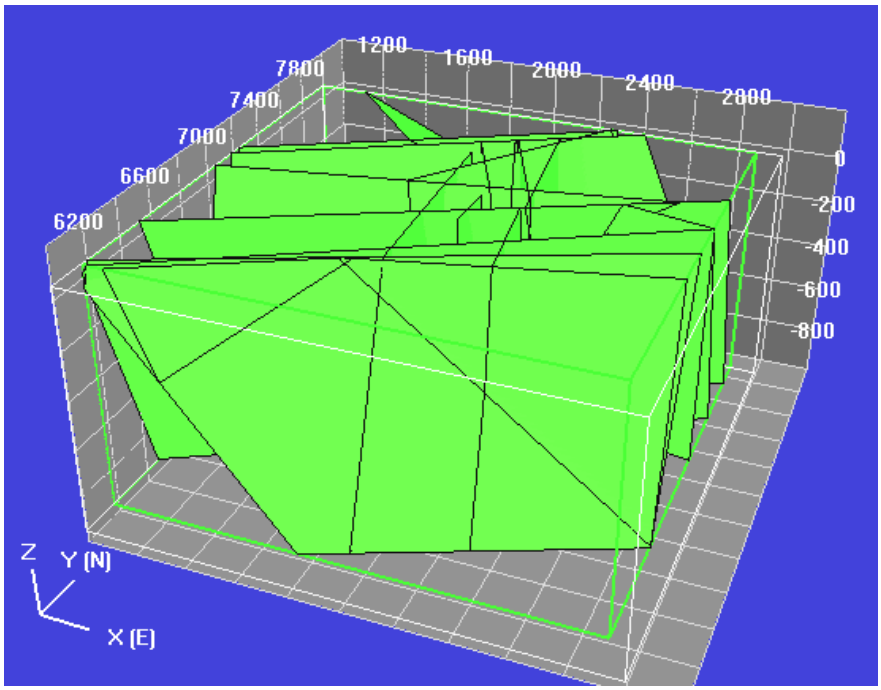

Figure 5-7. *1000-m Scale Structures.*

The 2000-m scale model contains both the deterministic, TRUE-Block scale 100-m scale structures, and synthetic 100-m scale structures generated as described in Section 3.4.2 above.

Due to the extensive characterisation of the Äspö HRL site, it is assumed that all the 1000 m scale structures are already fully characterised, and therefore, no synthetic structures of this scale were generated. Visualisations of 1000-m scale structures are provided in Figure 5-7 and Figure 5-8. The 1000 m scale structures are summarised in Table 5-6 and Table 5-7. For each structure, we provide corner points, thickness, extent, termination, transmissivity, and hydraulic aperture. Geological structure type and complexity factors are as listed in Table 4-2 and Table 4-7. In-fill mineralogy and thickness of alternation rims are based on geological structure type, as provided in Table 4-10 and Table 4-11.

Synthetic 100-m scale structures in the 2000-m scale model are illustrated in Figure 5-9 and Figure 5-10 and are listed in Table 5-5.

Background structures within the 2000-m scale model were generated using the statistics provided in Table 3-1. For each of the background fractures, hydraulic, transport, and geologic properties are assigned using the procedure described in Section 4.1. Background fractures were generated throughout the 2000 m model region. Synthetic background fractures of >10m are illustrated in Figure 5-11. Example synthetic background fractures are listed in Table 5-4.

Table 5-4. Example sample of synthetic background fractures in Task 6C reference case semi-synthetic 2000 m hydrostructural models.

Fracture #	Length (m)	Geo-logical Structure Type	Complexity Factor	Transmissivity (m^2/s)	Aperture (m)	Corner 1 Easting (m)	Northing (m)	Elevation (masl)	Corner 2 Easting (m)	Northing (m)	Elevation (masl)	Corner 3 Easting (m)	Northing (m)	Elevation (masl)	Corner 4 Easting (m)	Northing (m)	Elevation (masl)
55B	6.42	2	1	4.92E-09	3.23E-05	1915.14	7201.93	-384.01	1917.94	7202.95	-378.33	1913.21	7206.97	-376.72	1910.41	7205.96	-382.40
56B	10.15	2	2	1.37E-08	5.37E-05	1837.52	7210.77	-483.36	1844.20	7205.90	-477.48	1839.04	7208.78	-469.23	1832.36	7213.66	-475.12
57B	3.95	1	1	4.38E-10	9.63E-06	1826.14	7120.06	-453.14	1824.51	7122.01	-456.16	1827.34	7120.67	-458.56	1828.98	7118.72	-455.54
58B	4.54	2	1	3.29E-09	2.64E-05	1959.13	7221.48	-407.32	1960.86	7219.56	-403.59	1957.78	7221.72	-401.05	1956.05	7223.64	-404.78
59B	7.75	1	1	7.78E-09	4.06E-05	1993.51	7160.63	-487.12	1990.74	7154.61	-483.10	1989.87	7159.16	-476.89	1992.64	7165.18	-480.91
60B	3.87	1	2	3.43E-09	2.70E-05	1908.82	7249.77	-360.70	1906.93	7252.51	-362.68	1907.96	7250.81	-366.00	1909.86	7248.08	-364.02
61B	4.73	2	1	3.47E-09	2.71E-05	1810.12	7261.77	-517.17	1813.20	7258.24	-516.52	1814.01	7259.76	-512.12	1810.93	7263.29	-512.77
62B	4.93	2	1	1.10E-08	4.82E-05	1841.05	7197.68	-477.95	1836.19	7197.94	-477.17	1835.48	7198.94	-481.95	1840.34	7198.67	-482.73
63B	5.58	2	1	7.43E-09	3.97E-05	1821.72	7254.56	-496.57	1817.21	7255.07	-499.82	1819.83	7252.31	-503.90	1824.34	7251.80	-500.66
64B	4.35	2	1	2.18E-09	2.15E-05	1954.89	7084.77	-362.90	1956.17	7083.33	-366.80	1959.44	7081.15	-364.91	1958.15	7082.59	-361.01
65B	5.61	1	2	8.86E-10	1.37E-05	1935.00	7178.48	-420.41	1930.63	7176.61	-423.40	1934.14	7174.73	-427.35	1938.51	7176.60	-424.37
66B	4.29	2	1	4.70E-09	3.15E-05	1887.82	7236.75	-442.62	1884.23	7238.97	-441.84	1882.44	7237.31	-445.37	1886.03	7235.09	-446.16
67B	4.29	2	1	7.64E-10	1.27E-05	1957.51	7173.34	-361.99	1959.41	7170.46	-364.53	1961.64	7168.98	-361.18	1959.73	7171.86	-358.64
68B	8.53	2	1	1.42E-08	5.49E-05	1801.64	7118.68	-521.51	1795.97	7121.07	-527.42	1799.01	7115.14	-532.74	1804.67	7112.75	-526.83
69B	5.07	2	1	3.48E-09	2.71E-05	1949.10	7072.54	-540.92	1944.94	7075.43	-540.78	1942.61	7072.22	-543.94	1946.77	7069.33	-544.08
70B	4.95	2	1	1.25E-08	5.14E-05	1905.90	7231.46	-414.70	1910.83	7231.43	-414.24	1910.46	7228.19	-410.51	1905.53	7228.22	-410.97
71B	5.87	2	1	4.76E-09	3.17E-05	1915.69	7177.50	-530.26	1912.66	7175.36	-525.70	1908.19	7178.93	-526.99	1911.21	7181.08	-531.55
72B	13.75	1	2	2.62E-08	7.44E-05	1815.05	7112.10	-414.45	1827.82	7109.73	-418.96	1832.70	7112.00	-406.30	1819.93	7114.37	-401.80
73B	14.4	2	1	8.12E-09	4.15E-05	1833.58	7195.61	-407.12	1830.72	7198.05	-393.22	1818.36	7204.47	-396.89	1821.22	7202.03	-410.79
74B	3.8	2	1	2.93E-09	2.49E-05	1829.35	7156.53	-484.90	1832.03	7157.03	-482.24	1830.52	7160.40	-481.35	1827.84	7159.91	-484.01
75B	7.4	2	1	1.14E-08	4.92E-05	1985.09	7188.76	-529.98	1989.66	7188.72	-524.16	1984.85	7192.86	-520.36	1980.27	7192.90	-526.18
76B	3.93	2	1	5.42E-09	3.39E-05	1829.41	7126.53	-538.44	1825.98	7127.00	-540.31	1827.48	7125.26	-543.50	1830.91	7124.79	-541.63

Table 5-5. Synthetic 100 m scale structures the Task 6C reference case semi-synthetic 2000 m hydrostructural model.

Fracture #	Length (m)	Geologic Structure type	Complexity Factor	Trans-missivity (m^2/s)	Aperture (m)	Corner 1 Easting (m)	Northing (m)	Elevation (masl)	Corner 2 Easting (m)	Northing (m)	Elevation (masl)	Corner 3 Easting (m)	Northing (m)	Elevation (masl)	Corner 4 Easting (m)	Northing (m)	Elevation (masl)	Corner 5 Easting (m)	Northing (m)	Elevation (masl)
1S	76.61	1	2	1.394E-07	1.717E-04	2770.45	6335.90	-930.78	2693.15	6352.55	-950.00	2618.21	6368.46	-950.00	2586.05	6373.58	-816.18	2734.07	6341.70	-779.38
2S	275.71	1	2	1.199E-06	5.037E-04	2705.13	7010.17	-678.22	2638.28	7267.24	-604.32	2526.27	7171.16	-371.42	2593.13	6914.09	-445.33			
3S	330.73	1	2	9.213E-07	4.415E-04	1298.62	6227.38	50.00	1582.49	6116.99	50.00	1633.49	6117.64	-276.77	1289.37	6254.81	-330.20	1231.65	6254.07	39.60
4S	263.53	1	2	9.179E-07	4.407E-04	1624.93	7208.48	30.19	1781.31	7064.14	-125.24	1715.85	7214.99	-331.17	1559.47	7359.32	-175.74			
5S	140.09	1	2	8.418E-07	4.220E-04	2621.96	6697.90	-311.00	2724.44	6618.82	-364.56	2684.36	6654.52	-493.96	2581.88	6733.60	-440.40			
6S	107.5	1	3	3.243E-07	2.620E-04	1382.48	7840.77	-205.60	1329.47	7860.44	-114.18	1398.60	7797.91	-60.64	1451.61	7778.24	-152.06			
7S	177.87	1	3	4.616E-07	3.125E-04	1417.95	7142.35	-562.43	1294.73	7151.35	-690.38	1176.23	7211.29	-572.05	1299.45	7202.28	-444.10			
8S	147.84	1	2	1.101E-06	4.827E-04	1679.96	6992.61	-336.96	1800.32	6933.38	-274.80	1831.90	6864.37	-401.68	1711.54	6923.60	-463.84			
9S	150.31	1	2	6.945E-07	3.833E-04	2280.99	6628.73	-50.46	2416.81	6623.45	13.70	2470.56	6550.27	-106.09	2334.73	6555.55	-170.25			
10S	109.13	1	2	6.724E-07	3.772E-04	1428.05	7872.00	-8.14	1439.33	7840.80	50.00	1518.94	7766.15	50.00	1531.53	7756.96	42.62	1512.12	7810.63	-57.39
11S	188.84	1	2	1.183E-06	5.003E-04	1740.34	6416.93	-348.22	1625.22	6412.02	-497.83	1513.48	6540.42	-416.06	1628.60	6545.34	-266.45			
12S	87.43	1	2	2.705E-07	2.393E-04	1709.35	6489.96	-187.70	1684.33	6543.90	-123.60	1741.77	6506.25	-69.49	1766.79	6452.30	-133.59			
13S	213.98	1	3	9.741E-07	4.540E-04	2628.04	7770.19	-950.00	2615.44	7784.45	-944.32	2639.19	7724.20	-740.38	2775.02	7570.60	-801.57	2757.73	7614.45	-950.00
14S	241.43	2	2	1.769E-06	6.117E-04	1817.49	6545.99	-750.44	1964.19	6516.93	-560.90	2073.67	6333.70	-673.73	1926.98	6362.76	-863.27			
15S	327.24	1	3	2.643E-06	7.478E-04	1210.36	7697.38	50.00	1235.23	7680.03	50.00	1496.96	7515.93	-57.96	1426.62	7622.30	-390.16	1142.02	7800.73	-272.76
16S	124.97	1	2	2.978E-07	2.510E-04	2548.84	7412.05	-725.56	2454.45	7483.45	-685.43	2477.45	7447.78	-567.89	2571.84	7376.38	-608.02			
17S	227.77	1	3	5.931E-07	3.543E-04	1762.79	6843.82	-950.00	1794.72	6839.93	-790.40	1873.17	6627.12	-811.28	1845.42	6630.50	-950.00			
18S	565.51	1	3	3.963E-06	9.158E-04	1749.80	7437.38	50.00	1903.93	7134.81	-317.68	1590.32	7425.12	-688.04	1416.17	7766.99	-272.60	1689.33	7514.12	50.00
19S	353.43	1	3	1.344E-06	5.333E-04	1300.35	7960.23	-796.56	1226.03	7885.03	-459.32	1266.05	7540.52	-527.32	1340.37	7615.73	-864.56			
20S	109.42	1	3	5.450E-07	3.396E-04	2298.12	7503.47	-726.19	2263.46	7574.96	-801.43	2200.31	7623.38	-726.33	2234.97	7551.89	-651.09			
21S	136.96	2	2	9.676E-07	4.525E-04	1620.51	6380.67	-793.68	1557.24	6438.33	-686.77	1622.35	6352.66	-602.04	1685.62	6295.00	-708.94			
22S	342.44	1	3	2.086E-06	6.644E-04	1009.03	6301.19	-788.38	1000.00	6325.19	-760.18	1000.00	6421.41	-431.54	1083.59	6311.04	-310.83	1164.58	6095.78	-563.73
23S	155.23	1	2	3.408E-07	2.685E-04	1054.79	6625.65	-212.41	1007.12	6667.65	-70.78	1089.50	6551.68	-8.66	1137.18	6509.68	-150.29			
24S	208.88	1	3	1.090E-06	4.802E-04	2915.41	6172.05	-527.29	2982.81	6109.70	-714.91	2820.68	6205.71	-805.06	2753.28	6268.06	-617.44			
25S	200.68	1	2	6.632E-07	3.746E-04	2668.28	7430.34	-335.19	2758.52	7319.37	-475.95	2616.47	7371.23	-607.89	2526.24	7482.19	-467.12			
26S	115.13	1	3	3.737E-07	2.812E-04	3000.00	6957.34	50.00	3000.00	6962.39	-59.69	2901.68	7008.78	-21.80	2922.89	6995.09	50.00			
27S	346.19	1	3	1.437E-06	5.515E-04	1318.06	6540.21	-950.00	1257.51	6581.62	-762.89	1563.35	6475.27	-640.39	1663.53	6406.76	-950.00			
28S	340.37	1	3	1.342E-06	5.329E-04	1951.81	6521.47	-83.87	2000.03	6482.60	50.00	2195.29	6203.81	50.00	2102.19	6278.86	-208.48			
29S	174.69	2	3	1.105E-06	4.836E-04	3000.00	7795.78	-372.74	3000.00	7822.35	-651.78	2863.18	7920.70	-697.86	2793.81	7944.00	-442.20			
30S	222.72	2	3	1.322E-06	5.289E-04	2907.49	7851.31	-476.57	3000.00	7800.16	-566.21	3000.00	7867.10	-778.63	2976.83	7900.53	-821.62	2809.11	7993.27	-659.09
31S	492.54	1	3	2.033E-06	6.559E-04	1699.93	6765.98	-950.00	1866.51	6635.56	-533.95	2101.45	6258.31	-746.27	2019.88	6322.17	-950.00			
32S	112.64	1	3	4.287E-07	3.012E-04	2383.26	7646.76	-160.54	2474.12	7593.49	-200.49	2441.94	7617.52	-305.73	2351.08	7670.79	-265.79			
33S	287.15	1	3	1.612E-06	5.841E-04	1715.79	6713.30	26.27	1955.30	6586.71	-68.95	1826.26	6530.90	-319.33	1586.75	6657.49	-224.11			
34S	159.15	1	3	8.399E-07	4.216E-04	2710.66	7364.56	-720.55	2794.18	7243.14	-780.62	2779.72	7305.31	-926.41	2696.19	7426.73	-866.33			
35S	134.47	1	3	3.907E-07	2.875E-04	1366.28	7164.00	-310.18	1329.93	7166.07	-439.62	1244.08	7266.32	-413.91	1280.43	7264.24	-284.46			
36S	329.11	1	3	1.074E-06	4.766E-04	1562.38	6851.17	50.00	1588.11	6876.25	-145.19	1370.72	7123.32	-142.11	1345.40	7098.64	50.00			
37S	166.54	1	3	3.908E-07	2.876E-04	1497.73	6562.54	-781.02	1449.54	6629.32	-950.00	1329.60	6744.87	-950.00	1255.61	6810.49	-902.97	1322.21	6718.20	-669.44
38S	83.98	1	2	1.109E-07	1.532E-04	1522.88	6158.11	-950.00	1444.30	6198.95	-950.00	1400.34	6208.79	-879.13	1493.91	6147.97	-812.65	1561.90	6132.75	-922.28
39S	188.09	1	2	6.532E-07	3.718E-04	2655.74	6784.07	-317.53	2781.61	6647.46	-347.04	2691.99	6599.05	-505.17	2566.13	6735.67	-475.65			
40S	98.59	1	2	2.338E-07	2.224E-04	2038.80	7310.07	-102.78	1978.25	7387.57	-109.62	1972.66	7391.88	-11.28	2033.22	7314.38	-4.44			
41S	166.32	1	2	5.121E-07	3.292E-04	1376.34	7221.23	-799.89	1480.85	7165.96	-682.90	1566.02	7082.13	-798.58	1461.51	7137.40	-915.57			
42S	125.06	1	2	4.451E-07	3.069E-04	1798.13	7775.56	-342.15	1663.30	7955.57	-431.79	1645.77	8000.00	-316.21	1660.51	8000.00	-187.32	1764.19	7861.57	-118.38
43S	222.46	1	2	1.244E-06	5.130E-04	2603.65	7490.32	13.33	2628.31	7452.03	50.00	2810.06	7323.76	50.00	2858.41	7313.98	7.27	2765.99	7457.48	-130.14
44S	294.94	1	3	1.731E-06	6.052E-04	2634.41	6903.32	-950.00	2628.00	6918.48	-944.56	2610.21	6812.44	-669.91	2719.27	6554.50	-762.45	2731.41	6626.91	-950.00
45S	51.08	1	2	8.793E-08	1.364E-04	3000.00	7823.27	-876.00	3000.00	7844.88	-950.00	2960.34	7877.08	-950.00	2933.03	7885.50	-902.96	2990.22	7826.28	-859.15
46S	85.31	2	2	1.261E-07	1.633E-04	1817.67	6513.50	-29.83	1879.94	6475.20	-73.79	1845.99	6503.66	-146.69	1783.71	6541.96	-102.73			

Table 5-6. Geometric properties of 1000 m scale structures employed in Task 6C reference case semi-synthetic hydrostructural models (data from Rhén et al., 1997)

			Corner 1			Corner 2			Corner 3			Corner 4			Corner 5		
Structure Name	Width (m)	Length (m)	Easting (m)	Northing (m)	Elevation (masl)	Easting (m)	Northing (m)	Elevation (masl)	Easting (m)	Northing (m)	Elevation (m)	Easting (m)	Northing (m)	Elevation (masl)	Easting (m)	Northing (m)	Elevation (masl)
EW-1N	2066.13	1002.24	900.00	7159.11	-950.00	2701.94	8170.00	-950.00	2634.96	8170.00	50.00	900.00	7196.69	50.00			
EW-1S	393.28	654.02	2748.90	8170.00	50.00	2900.00	8170.00	-313.09	2900.00	8021.38	-950.00	900.00	6900.02	-950.00	900.00	7133.36	50.00
EW-3 (z=500-200)	1874.09	305.86	2735.02	7426.33	50.00	900.00	7045.65	50.00	900.00	6986.09	-250.00	2198.68	7255.51	-250.00			
EW-3 (z<200)	1326.33	713.66	2198.68	7255.51	-250.00	900.00	6986.09	-250.00	900.00	6847.12	-950.00	947.21	6856.91	-950.00			
EW-7	1169.95	1013.32	1769.94	6547.69	50.00	2900.00	6850.59	50.00	2900.00	6686.85	-950.00						
NE-1	2251.55	1061.15	2900.00	7511.64	50.00	900.00	6477.48	50.00	900.00	6832.50	-950.00	2900.00	7866.66	-950.00			
NE-2	1174.95	524.04	2428.53	8170.00	50.00	1737.87	7219.47	50.00	1822.69	7135.75	-460.31	2248.91	7529.99	-950.00	2713.94	8170.00	-950.00
NE-3	2168.70	248.67	2900.00	7254.39	50.00	1021.88	6170.00	50.00	900.00	6170.00	-166.76	900.00	6424.27	-950.00	2900.00	7579.03	-950.00
NE-4N	2165.43	1067.30	921.87	6170.00	50.00	2900.00	7050.95	50.00	2900.00	6677.94	-950.00	1759.44	6170.00	-950.00			
NE-4S	442.61	799.63	1083.61	6170.00	50.00	1261.37	6170.00	-355.34	1822.08	6570.90	50.00						
NW-1	797.52	1773.56	1589.24	7583.42	50.00	1048.90	8170.00	50.00	2681.39	8170.00	-643.18						
NNW-1	463.21	1021.32	2125.71	7299.93	50.00	1983.13	7740.65	50.00	2047.03	7543.14	-950.00	2185.90	7113.88	-950.00			
NNW-2	626.27	1048.74	1994.01	7746.75	50.00	2245.32	7173.12	50.00	2118.51	7462.57	-950.00	2076.08	7559.42	-950.00			
NNW-3	212.61	1000.00	2043.60	7195.40	50.00	2036.90	6982.90	50.00	2036.90	6982.90	-950.00	2043.60	7195.40	-950.00			
NNW-4	671.59	1020.57	2225.95	7163.10	50.00	2141.31	7829.34	50.00	2251.36	7657.70	-950.00	2266.44	7539.05	-950.00			
NNW-5	955.22	1000.00	1909.97	6610.05	50.00	1862.80	7564.10	50.00	1862.80	7564.10	-950.00	1928.02	6245.08	-950.00			
NNW-6	475.81	442.50	2209.15	7154.41	50.00	2275.94	6683.31	50.00	2285.71	6614.38	-386.98	2313.72	6416.84	-950.00	2162.25	7485.18	-950.00
NNW-7	430.04	1023.01	2043.28	7282.83	50.00	1862.57	7673.05	50.00	2024.61	7530.57	-950.00	2214.80	7119.88	-950.00			
NNW-8	587.04	400.00	1915.10	7754.90	-250.00	1500.00	8170.00	-250.00	1500.00	8170.00	-650.00	1924.76	7745.25	-650.00			
SFZ11	360.86	1000.00	2546.27	7328.73	50.00	2900.00	7257.34	50.00	2900.00	7257.34	-950.00	2052.44	7428.40	-950.00			
SFZ14a	674.23	1000.00	995.00	8030.00	50.00	900.00	7362.50	50.00	900.00	7362.50	-950.00	995.00	8030.00	-950.00			
SFZ14b	143.08	1000.00	995.00	8030.00	50.00	1024.53	8170.00	50.00	1024.53	8170.00	-950.00	995.00	8030.00	-950.00			

Table 5-7. Hydrogeological properties 1000 m scale structures included in Task 6C reference case semi-synthetic hydrostructural models - (data from Rhén et al., 1997).

Task 6C Structure number	Structure Name	Transmissivity (m^2/s)	Hydraulic Aperture (m)
1T	EW-1N	5.20E-07	1.44E-03
2T	EW-1S	1.20E-05	6.93E-03
3T	EW-3 (z=500-200)	1.70E-05	8.25E-03
4T	EW-3 (z<200)	5.00E-07	1.41E-03
5T	EW-7	1.50E-05	7.75E-03
6T	NE-1	2.20E-04	2.97E-02
7T	NE-2	1.20E-07	6.93E-04
8T	NE-3	3.20E-04	3.58E-02
9T	NE-4N	3.10E-05	1.11E-02
10T	NE-4S	3.10E-05	1.11E-02
11T	NW-1	4.10E-07	1.28E-03
12T	NNW-1	8.60E-06	5.87E-03
13T	NNW-2	2.40E-05	9.80E-03
14T	NNW-3	2.00E-05	8.94E-03
15T	NNW-4	6.50E-05	1.61E-02
16T	NNW-5	4.00E-06	4.00E-03
17T	NNW-6	1.40E-05	7.48E-03
18T	NNW-7	7.50E-06	5.48E-03
19T	NNW-8	8.40E-06	5.80E-03
20T	SFZ11	1.00E-06	2.00E-03
21T	SFZ14a	1.00E-06	2.00E-03
22T	SFZ14b	1.00E-06	2.00E-03

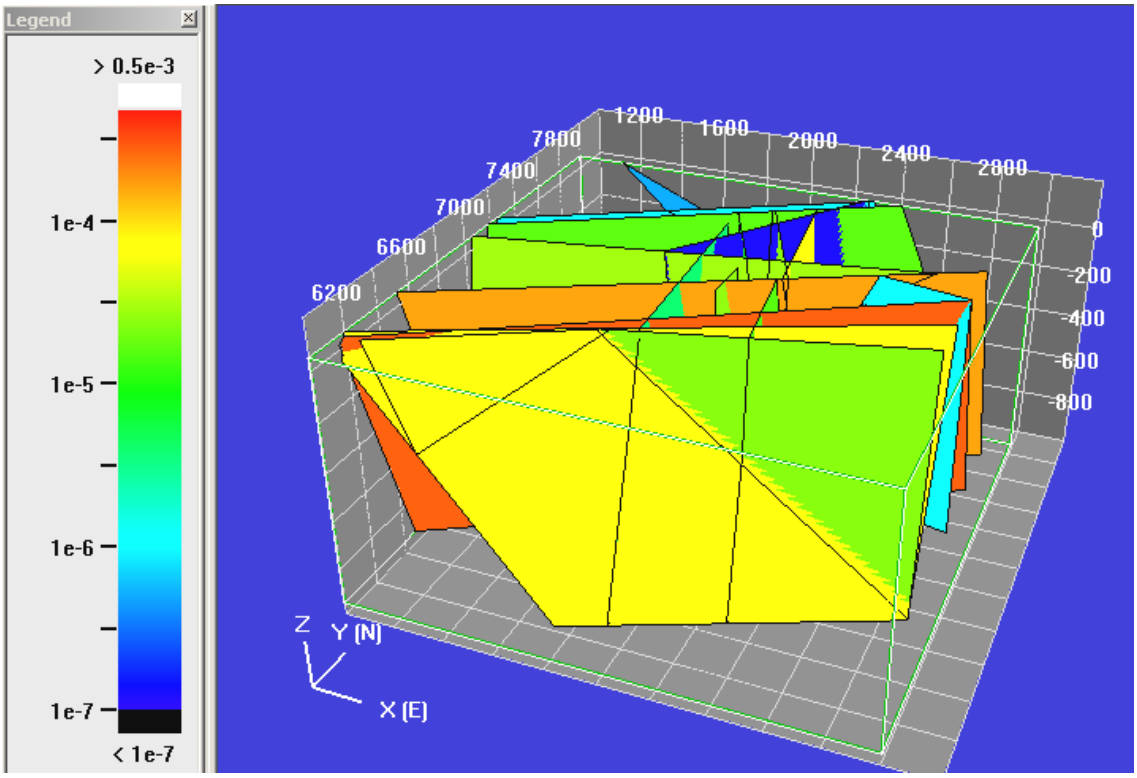

Figure 5-8. *1000 m scale structures in the 2000 m scale model coloured according to their transmissivity.*

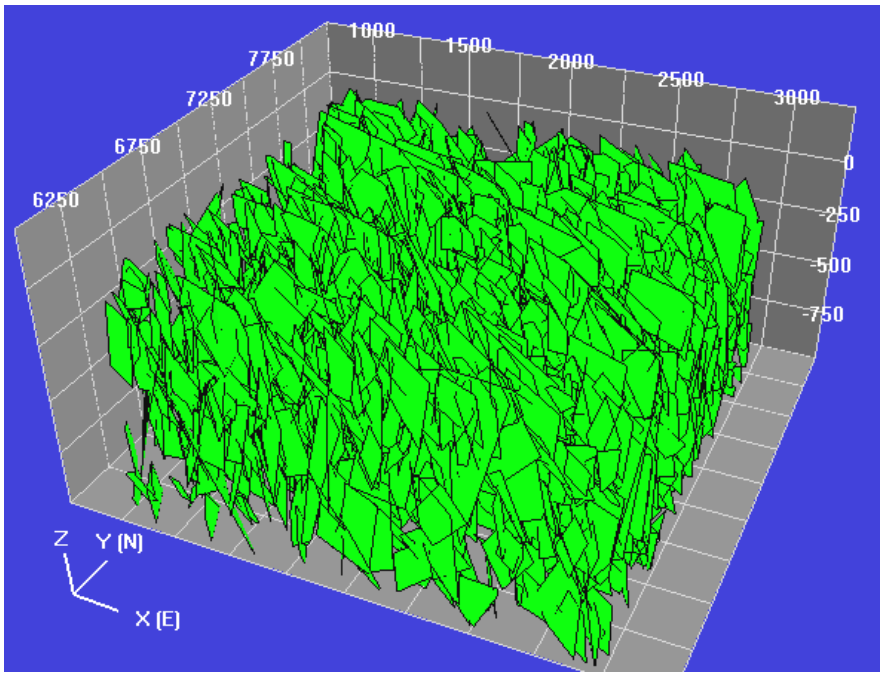

Figure 5-9. *Synthetic 100 m scale structures in the 2000 m scale model.*

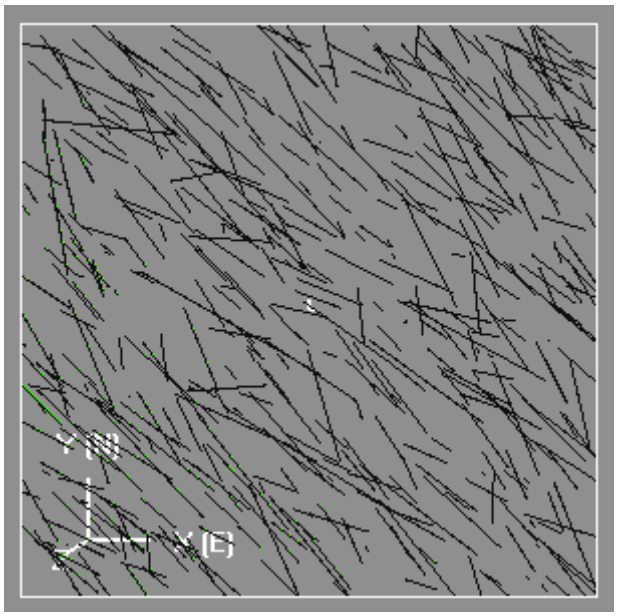

Figure 5-10. *Plan view trace map of synthetic 100 m scale structures in the 2000 m scale model at Z= –450-masl.*

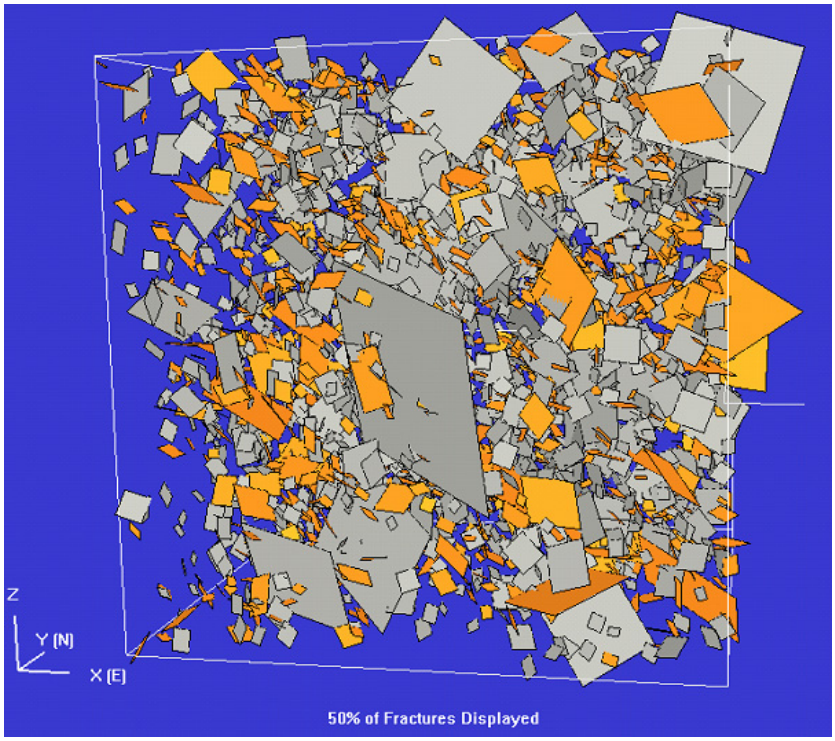

Figure 5-11. *Visualisation of background fractures in the 2000 m model. Size cut-off employed : L>10m.*

6 Boundary Conditions

6.1 Block Scale (200-m)

Boundary conditions for the Block Scale model were obtained by interpolation from head measurements in the TRUE Block Scale rock block. These head data are summarised on 10 m scale panels for each of the faces of the TRUE Block Scale rock block in Table 6-1 of the data distribution (200 Structures Ver2.xls). A visualisation for the head field is provided in Figure 6-1. These head values have to be adjusted further to condition to measured head in boreholes transecting the rock block. The coordinates for the panels in Table 6-1 are given in values relative to the centre of the TRUE Block Scale volume at Äspö HRL (Northing=7170 m, Easting=1900 m, Z=-450 m masl).

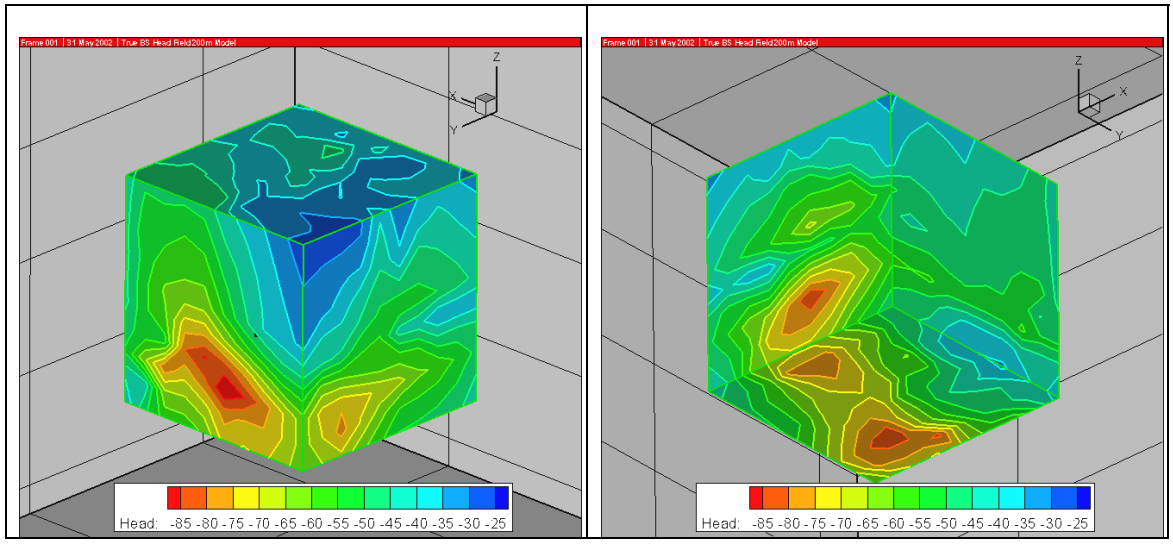

Figure 6-1. *Boundary Conditions on 200-m model block (NB not conditioned to measure hydraulic head in boreholes).*

Table 6-1. Hydraulic head boundary conditions on the 200 m model rock block faces (Example).

X (m)	Y (m)	Z (masl)	Head (masl)
1888.89	7270.00	-505.56	-89.75
1933.33	7270.00	-483.33	-80.06
1888.89	7270.00	-527.78	-76.73
1866.67	7070.00	-527.78	-72.78
1911.11	7136.67	-550.00	-69.42
1911.11	7270.00	-527.78	-67.85
1866.67	7070.00	-505.56	-65.75
1800.00	7270.00	-550.00	-60.74
1800.00	7158.89	-483.33	-57.34
1911.11	7070.00	-416.67	-56.34
2000.00	7114.44	-505.56	-55.79
1822.22	7270.00	-461.11	-44.41
2000.00	7181.11	-372.22	-43.47
1800.00	7136.67	-461.11	-41.86
2000.00	7114.44	-394.44	-40.20
1800.00	7225.56	-416.67	-36.46
1822.22	7158.89	-350.00	-34.27
1822.22	7181.11	-350.00	-32.94
1800.00	7270.00	-372.22	-28.80
1822.22	7225.56	-350.00	-28.39
1800.00	7247.78	-350.00	-27.88
1800.00	7270.00	-350.00	-27.11
1800.00	7225.56	-350.00	-26.37

6.2 Site scale (2000-m)

The site scale model for Task 6C has the same coordinates as those used for Task 5 and the SKB Alternative Models Project. For this boundary condition, interpolated fresh water heads are available based on Svensson (1997). These head data were calculated from pressures and salinities in Svensson's modelling.

Figure 6-2 illustrates the fresh-water head data at the top surface of the model, at elevation Z=0-masl. The estimated fluxes for each of the six faces of the model region are summarised in Table 6-2.

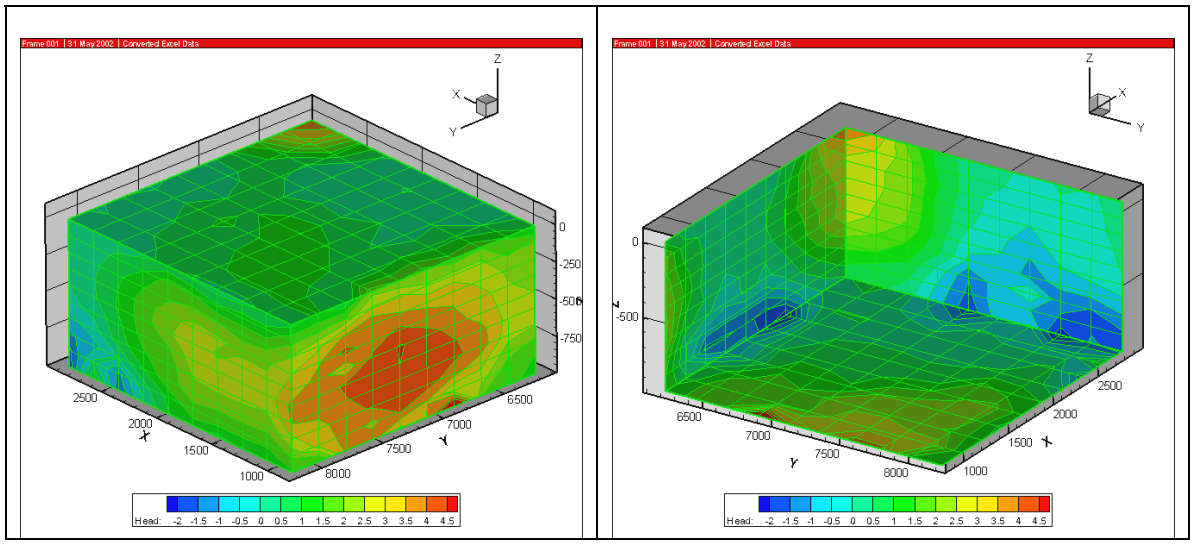

Figure 6-2. *Fresh-water hydraulic head (m) at the top of the 2000-m model.*

Table 6-2. Net fluxes on the faces of 2000 m scale model rock block.

Face	Flux (l/	Direction
Bottom	1.2	into model
Top	10.6	out of model
West	10.3	into model
North	1.0	out of model
East	0.3	out of model
South	0.4	into model

The Svensson (1997) head distributions are available from the Äspö Task Force web site as “Data Distribution #10” related to Task 5.

6.3 Block Scale tracer tests

Tracer tests performed at the TRUE Block Scale site are summarised by Andersson et al. (2002b). The tracer Test Stage was made up of three phases. The last of these phases (Phase C) included injections of radioactive sorbing tracers in three different source locations (Andersson et al, 2001).

Tracer tests C2 involves transport from KI0025F03:P7 to KI0023B:P6 along a pathway through Structures 23, 22, 20, and 21 (Andersson et al., 2002b). Table 6-3 details the boundary conditions for tracer test C2. Figure 6-3 and Table 6-4 contain the injection function information used to run the tracer tests.

Table 6-3. Experimental specifics for TRUE Block Scale Phase C tracer injection C2 (primarily based on Andersson et al., 2002b).

Parameter	Test C2
Source section	KI00F03:P7
Sink section	KI0023B:P6
Cartesian distance	17 m
Distance along deterministic structures of the TRUE Block Scale hydrostructural model	97 m
DFN Path Length	66 m
Structures involved	23, 22, 20, 21
Injection rate (Forced injection, based on tracer dilution measurement)	1.5 x 10^{-7} m^3/s (9 ml/min)
Pumping rate	3.27 x 10^{-5} m^3/s (1.96 l/min)

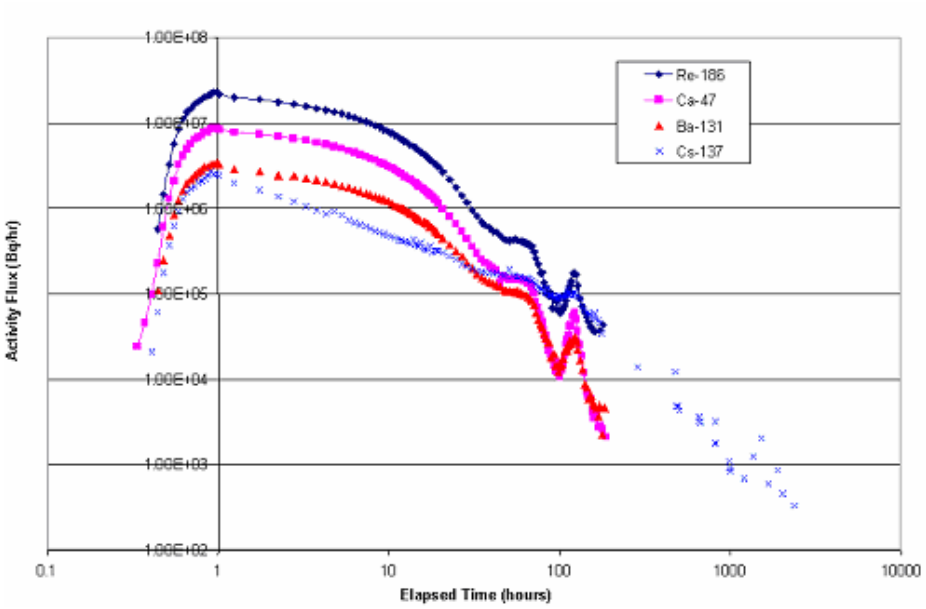

Figure 6-3. *Test C2 injection functions for Re-186, Ca-47, Ba-131, and Cs-137.*

Table 6-4. Measured and estimated Test C2 injection activity.

Tracer	Injection activity (Bq) - Measured	Injection activity (Bq) - Estimated
Re-186	$1.71 \cdot 10^8$	$2.29 \cdot 10^8$
Ca-47	$5.64 \cdot 10^7$	$8.69 \cdot 10^7$
Ba-131	$2.57 \cdot 10^7$	$3.69 \cdot 10^7$
Cs-137	$2.35 \cdot 10^7$	$4.07 \cdot 10^7$

7 Discussion and recommendations

Task 6C is intended to provide semi-synthetic hydrostructural models for radionuclide migration at block and site scales. The bases for these models are existing descriptive models and databases applicable to the Äspö HRL.

In the case of Task 6C, the textural patterns observed in TRUE Block Scale rock volume have been duplicated on larger scales in terms of synthetic structures fitted within the network of deterministic structures (fracture zones), 100-m to1000-m in length, which are present on a site scale. When assigning material properties to the synthetic structures, developed relationships between average transmissivity and size have been employed.

Two conceptual geological structure types with associated retention characteristics have been defined; Type 1 (Fault) and Type 2 (Non-fault). These types are applicable to all of the modelled structures. Type 1 includes cataclasite and fault gouge material, while Type 2 features only include fracture coating. Both types, however, are characterised by altered wall rock of slightly variable extent. Geometrical extents are given for the various geological entities at various scales. It should be pointed out that the two defined structure types basically define two end-members of a possible spectrum of alternative structure types (compositions).

Retention properties for sorption (K_d) have been estimated for the various geological entities based on defined mineralogy, water composition and literature values of cation exchange capacities of the minerals in question. Likewise, formation factors have been defined for the geological entities based on corresponding porosities established in the laboratory.

In order to allow for a possible description of chemistry-dependent distribution coefficients, K_d values are provided for fresh water and brine. These data facilitate a possibility to include a description of chemistry dependent retention. Such variability over time may ia. be induced by the advance and retreat of an inland ice mass

The set of parameters defined for the retention models of the two geological structure types have been extrapolated to a smaller scale (background fractures) and larger scale structures (100-m and 1000-m). In this process the first approximation regarding the retention properties is that they are assumed constant, irrespective of scale/structure size. It is only assumed that the geometrical extents of the cataclasite and fault gouge zones are affected by the structure size.

Simulations of solute/radionuclide transport are to be undertaken both at experimental conditions (Task 6 D) and at performance assessment (PA) conditions. The former situation needs to take into account the underground openings of Äspö HRL. In order to avoid construction of complex 3D models, boundary conditions that embed the underground openings, without including them explicitly in the models, are proposed. Boundary conditions for PA time scales are provided on the basis of existing site-scale and regional scale models.

Task 6C to a very high degree mimics the process of constructing site-descriptive models at various scales for a conceived geological repository site. The similarity lies in the need to integrate information at different scales to meet the demands of constructing mutually consistent (geometry and boundary conditions) models at two consecutive and coupled scales, in the case of Task 6C the 200-m and 2000-m length scales.

A similarity also lies in the need to make plausible and yet well-sustained simplifications of a complex and heterogeneous subground system on the basis of a small number of borehole intercepts, and on a limited number of laboratory data.

Task 6C from this perspective constitutes an important training ground for testing out methodologies for integrating large geoscientific data sets for performance assessment purposes.

Task 6C presents a possible methodology for abstraction of information from Äspö HRL studies at different scales and attribution of properties to generated synthetic structures of variable sizes. The generated numerical values of various properties are intended for use primarily in the context of Task 6. The data should not be used in a safety and/or performance assessment context without properly reviewing the underlying data, underlying uncertainties and assumptions made.

8 References

Allard, B., Karlsson, M., Tullborg, E-L. and S-Å. Larsson, 1983. Ion exchange capacity and surface areas of some major component sand common fracture filling materials of igneous rock. Swedish Nuclear Fuel and Waste Management Company. SKB Technical Report TR 83-64.

Andersson P, Ludvigsson J-E, Wass E and Holmqvist M, 2000a. Interference tests, dilution tests and tracer tests, Phase A, Swedish Nuclear Fuel and Waste Management Company, International Progress Report IPR-00-28.

Andersson P, Wass E, Holmqvist M and Fierz T, 2000b. Tracer tests, Phase B. Swedish Nuclear Fuel and Waste Management Company, Äspö Hard Rock Laboratory, International Progress Report IPR-00-29.

Andersson P., Byegård J., Holmqvist M., Skålberg M., Wass E., Widestrand H., 2001c. TRUE Block Scale Tracer Test Stage. Tracer test, Phase C. Swedish Nuclear Fuel and Waste Management Company. Äspö Hard Rock Laboratory. International Progress Report IPR-01-33.

Andersson, P., Byegård, J., Doe, T., Hermanson, J., Meier, P., Tullborg, E-L., and Winberg, A. 2002a. "TRUE Block Scale Project Final Report – 1. Characterisation and model development", Swedish Nuclear Fuel and Waste Management Company (SKB), Technical Report TR-02-13.

Andersson, P., Byegård, and Winberg, A. 2002b. "TRUE Block Scale Project Final Report – 2. Tracer tests in the block scale", Swedish Nuclear Fuel and Waste Management Company (SKB), Technical Report TR-02-14.

Bath, A. and Jackson, C.P. 2003 . Task Force on modlling of groundwater flow and transport of solutes - Review report of Task 5. Swedish Nuclear Fuel and Waste Management Company (SKB), Äspö Hard Rock Laboratory, International Cooperation Report IPR-03-10.

Benabderrahmane, H., Dershowitz, W.S., Selroos, J-O., Uchida, M. and A. Winberg 2000 . Task 6 proposal - Performance Assessment Modelling Using Site Characterisation Data (PASC). Unpublished proposal to the Äspö Task Force, November 2000.

Bossart, P., Hermanson, J. and Mazurek, M. 2001 . Analysis of fracture networks based on the integration of structural and hydrogeological observations on different scales. Swedish Nuclear Fuel and Waste Management Company (SKB), Technical Report TR-01-21.

Byegård J, Skarnemark G and Skålberg M, 1995 . The use of some ion-exchange sorbing tracer in in situ experiments in high saline groundwaters, Mat. Res. Soc. Symp. Proc. 353, 1077–1084.

Byegård, B., Johansson, H., Skålberg, M. and E-L. Tullborg. 1998. "The interaction of sorbing and non-sorbing tracers with different Äspö rock types – Sorption and diffusion experiments in the laboratory scale", Swedish Nuclear Fuel and Waste Management Company (SKB), Technical Report TR-98-18.

Byegård, J., Widestrand, H., Skålberg, M., Tullborg, E-L.., and Siitari-Kauppi, M. 2001. : First TRUE Stage – Complementary investigation of diffusivity, porosity and sorptivity of Feature A site-specific geological material. Swedish Nuclear Fuel and Waste Management Company (SKB), Äspö Hard Rock Laboratory, International Cooperation Report ICR-01-04.

Byegård, J., Widestrand, H. 2003 . Scoping calculations for the use of diffusion experiment in order to determine the sorption and diffusion characteristics for technetium under reducing conditions. Ontario Power Gerenation Technical Report, in press.

Carbol, P., Engkvist, I., (1997). Compilation of radionuclide sorption coefficients for performance assessment, SKB report R-97-13, Swedish Nuclear Fuel and Waste Management Company, Stockholm.

Comans, R.N.J, Haller, M. and P. DePreter 1991 . Sorption of Cesium on illite - non-equillibrium behaviour and reversibility, Geochimica and Cosmochimica Acta, 55(2): 433-440.

Cvetkovic, V., Cheng, H. and J-O. Selroos. 2000. "Evaluation of Tracer Retention Understanding Experiments (first stage) at Äspö", Swedish Nuclear Fuel and Waste Management Company, International Cooperation Report ICR-00-01.

Cvetkovic, V. And H. Cheng (in press). Evaluation of the TRUE Block Scale Phase C Experiments using the LaSAR approach. Swedish Nuclear Fuel and Waste Management Company, Äspö HRL International Progress Report IPR-02-34.

Dershowitz, W., Eiben, T., Follin, S., and J. Andersson 1999. SR 97 – Alternative models project. Discrete fracture network modelling for performance assessment of Aberg. Swedish Nuclear Fuel and Waste Management Company (SKB), Technical Report R-99-42. ISSN 1402-3091.

Dershowitz, B.,Shuttle, D., Klise, K., Uchida, M., Metcalfe, R. and M. Cave 2002. FracMan Modeling of Geochemical End-Member Transport Pathways, Aspo HRL, Aspo Sweden: Task 5. Swedish Nuclear Fuel and Waste Management Company, Äspö HRL International Progress Report IPR-02-37.

Dershowitz, B. and K. Klise, 2002. Evaluation of fracture network transport pathways and processes using the Channel Network approach. Swedish Nuclear Fuel and Waste Management Company. Äspö Hard Rock Laboratory. International Progress Report IPR-02-34.

Elert, M. 1999. "Evaluation of modelling of the TRUE-1 radially converging tests with conservative tracers, The Äspö Task Force on Modelling of Groundwater Flow and Transport of Solutes., Tasks 4C and 4D", Swedish Nuclear Fuel and Waste Management Company (SKB), Technical Report TR-99-04.

Elert, M. and H. Svensson. in press. "Evaluation of modelling of the TRUE-1 radially converging tests with conservative tracers, The Äspö Task Force on Modelling of Groundwater Flow and Transport of Solutes., Tasks 4E and 4F". Swedish Nuclear Fuel and Waste Management Company (SKB), Technical Report TR-01-12.

Eliasson, T., 1993. Mineralogy, geochemistry and petrophysics of red coloured granite adjacent to fractures. SKB Technical Report, TR 93-06, ISSN 0284-3757.

Follin, S. and J. Hermanson 2001. A discrete fracture network model of the Äspö TBM tunnel rock mass. Swedish Nuclear Fuel and Waste Management Company (SKB), Äspö Hard Rock Laboratory, International Progress Report IPR-01-71. December 1996.

Gómez-Hernández, J-J., Franssen, H-J., Medina Sierra, A. and J. Carrera Ramirez, 2002. Stochastic continuum modelling of flow and transport. . Swedish Nuclear Fuel and Waste Management Company. Äspö Hard Rock Laboratory. International Progress Report IPR-02-31 (in press).

Gylling, B. Moreno, L. and I. Neretnieks 1999. SR 97 - Alternative models project. Channel network modelling of Aberg. Performance assessment using CHAN3D. Swedish Nuclear Fuel and Waste Management Company (SKB), Technical Report R-99-44. ISSN 1402-3091.

Hakami, E. 1995. Aperture distribution of rock fractures. Doctoral Thesis. Royal Institute of Technology, Stockholm, Sweden. ISBN 91-7170-835-9.

Hermanson, J. and T. Doe, 2000. TRUE Block Scale Project Tracer test stage. March'00 structural and hydraulic model based on borehole data from KI0025F03. Swedish Nuclear Fuel and Waste Management Company, Äspö HRL International Progress Report IPR-00-34.

Hermanson, J., Stigsson, M. and A. Pringle 1999. Äspö HRL – Prototype repository DFN Model No. 1. Swedish Nuclear Fuel and Waste Management Company, Äspö HRL International Progress Report IPR-99-09.

Hermanson, Follin, S. and LingLi Wei 2001. TRUE Block Scale Experiment. Input data for discrete feature network modelling of the TRUE Block Scale site. Part1 – Structural analysis of fracture tracers in boreholes KA2563A and KA3510A and in the TBM tunnel. Swedish Nuclear Fuel and Waste Management Company, Äspö Hard Rock Laboratory, International Progress Report IPR-01-70.

Holton, D. (in prep). Evaluation of the Phase C tracer tests using the discrete fracture network approach. Swedish Nuclear Fuel and Waste Management Company. Äspö Hard Rock Laboratory. International Progress Report IPR-02-30.

Jakob, A., Mazurek, M. and W. Heer 2002. Solute transport in crystalline rocks at Äspö – II: Blind predictions, inverse modelling and lessons learnt from test STT1. , J. of Cont. Hydrology (61), pp.175-190.

Johansson, H. 2000. Retardation of tracers in crystalline rocks. Thesis at Chalmers University of Technology, Ny serie 1582, ISSN0346-718x.

Kelokaski, M., Oila, E. and Siitari-Kauppi, M. 2001. TRUE Block Scale Project - Investigation of porosity and micro-fracturing in granitic fracture wall rock and fault breccia specimens using the PMMA technique. Swedish Nuclear Fuel and Waste Management Company, Äspö HRL International Progress Report IPR-01-27.

Kulmala, S., Hakanen, M. 1995. Sorption of alkaline-earth elements Sr, Ba and Ra from groundwater on rocks from two investigation areas, Report YJT-95-03, Nuclear Waste Commission of Finnish Power Companies.

Kumplulainen and Uusheimo (1989). Diffusivity and electrical resistivity measurements in rock matrix around fractures Report YJT-89-19, Nuclear waste Commission of Finnish Power Companies, Helsinki

Landström, O., Tullborg, E-L., Eriksson, G., Sandell, Y.2001. Studies of matrix diffusion and redox conditions at the surface and in a fracture at 170-m - Results from drill core studies in porphyritic quartz monzodiorite from Äspö, SE Sweden. SKB Report R-01-37.

Long, J.C.S 1983. Investigations of Equivalent Porous Medum Permeability in Networks of Discontiniuous Fractures. PhD Dissertation, Earth Science Division, Lawerence Berkeley Laboratory, University of California, Berkeley.

Mauldon, M. and W. Dershowitz 2003. Fracture Abundance Measures: Density, Intensity, and Porosity. International Journal of Rock Mechanics and Mining Sciences (in press).

Mazurek, M., Bossart, P. and T. Eliasson. 1997. "Classification and characterisation of water-conducting features at Äspö : Results of investigations on the outcrop scale", Swedish Nuclear Fuel and Waste Management Company (SKB), Äspö Hard Rock Laboratory, International Cooperation Report ICR-97-01.

Mazurek, M., Jakob A. and P. Bossart 2002. Solute transport in crystalline rocks at Äspö — I: Geological basis and model calibration, J. of Cont. Hydrology (61), pp.157-174.

Mills, R. and V.M.M Lobo 1989. Self-diffusion in electrolute solution - a critical examination of data compiled from the literature. Elsevier, Amsterdam.

Munier, R. and Hermanson, J. 1994. Updating of the geological structural model. Swedish Nuclear Fuel and Waste Management Company (SKB), Äspö Hard Rock Laboratory, Progress Report 25-94-05.

Neretnieks, I. 2002. A stochastic multi-channel model for solute transport - analysis of tracer tests in fractured rock." Journal of Contaminant Hydrology 55(3-4): 175-211, 2002.

Ohlsson Y, 2000. Studies of Ionic Diffusion in Crystalline Rock. Doctoral thesis. Royal Institute of Technology, Stockholm, Sweden. ISBN 91-7283-025-5.

Ohlsson, Y. and I. Neretnieks 1997. Diffusion data in granite, Recommended values. Swedish Nuclear Fuel and Waste Management Company. SKB Technical Report TR-97-20.

Outters, N. and Shuttle, D. 2000. Sensitivity analysis of a discrete fracture network model for performance assessment of Aberg. Swedish Nuclear Fuel and Waste Management Company (SKB), Technical Report R-99-42. ISSN 1402-3091.

Patel, S. and L-O. Dahlström, in prep. Äspö HRL Prototype Repository, Geology - Summary report of investigations before the operation phase (tentative title). Äspö HRL IPR report in prep.

Poteri. A., Billaux, D., Cvetkovic, V., Dershowitz, B., Gómez-Hernández, J-J., Hautojärvi, A., Holton, D., Medina, A. and A. Winberg 2002. TRUE Block Scale Project. Final Report – 3. Modelling of flow and transport. Swedish Nuclear Fuel and Waste Management Company. Technical Report TR-02-15. (in prep).

Puigdomenech, I., Ambrosi, J-P., Banwart, S.A. Bateman, K., Eisenlohr, L., Griffoult, L., Gustafsson, E., Hama, K., Kotelnikova, S., Lartige, J-E. Michaud, V., Milodowski, A.E. Pedersen, K., Rivas Perez, J., Trotignon, L., Tullborg, E-L., West, J.M. Yoshida, H. 1999. O_2 depletion in granitic media: The REX project. SKB Technical Report, TR 01-05 ISSN 0284-3757.

Puigdomenech, I. (Ed): 2001. Hydrochemical stability of groundwaters surrounding a spent nuclear fuel repository in 100 000 year perspective. SKB Technical Report TR_01-28. ISSN 0284-3757.

Rhén, I., Gustafsson, G., Stanfors, R., Wikberg, P., 1997. Äspö HRL-Geoscientific evaluation 1997/5. Models based on site characterisation 1986-1995. Swedish Nuclear Fuel and Waste Management Company. SKB Technical Report TR 97-06.
Rhén I and T. Forsmark 2001. Äspö HRL - Prototype Repository. Hydrogeology - Summary report of investigations before the operation phase. Swedish Nuclear Fuel and Waste Management Company, Äspö Hard Rock Laboratory, International Progress Report IPR-01-65.

Rhén, I. and Smellie, J. 2003. Task Force on modelling of groundwater flow and transport of solutes, Task 5 summary report. Swedish Nuclear Fuel and Waste Management Company. SKB Technical Report TR 03-01.

Selroos, J-O. , Walker, D.D., Ström, A., Gylling, B. and S. Follin 2002. Comparison of alternative modelling approaches for groundwater flow in fractured rock. Journal of Hydrology 257 (2002): pp.174-188.

Skagius (1986). Diffusion of dissolved species in the matrix of some Swedish crystalline rocks. Ph. D Thesis, Royal Institute of Technology, Stockholm.

Stigsson, M., Outters, N. and Hermanson, J. 2001. Prototype Repository – Hydraulic DFN model No:2. Swedish Nuclear Fuel and Waste Management Company, Äspö Hard Rock Laboratory, International Progress Report IPR-01-39.

Svensson, U. 1997. A site scale analysis of groundwater flow and salinity distribution in the Äspö area. Swedish Nuclear Fuel and Waste Management Company. SKB Technical Report TR 97-17.

Svensson, U. 1999. A laboratory scale analysis of groundwater flow and salinity in the Äspö area. Swedish Nuclear Fuel and Waste Management Company. SKB Technical Report TR 99-24.

Svensson U, 2001. Groundwater Flow, Pressure and Salinity around the Prototype Repository, Continuum model No 1. Swedish Nuclear Fuel and Waste Management Company, Äspö Hard Rock Laboratory, International Progress Report IPR-01-40.

Tullborg, E-L. 2002. Personal communication

Uchida, M. and J. Geier, 1992. Fracture Mapping on Äspo Island. SKB Geotab Database, Aspo HRL. Unpublished work. SKB, Stockhom.

Uchida, M., Doe, T., Dershowitz, W., Thomas, A., Wallmann, P. and A. Sawada, 1994. Discrete-fracture Modeling of the Äspo LPT-2, Large-Scale Pumping and Tracer Test. Swedish Nuclear Fuel and Waste Management Company, Äspö Hard Rock Laboratory, International Cooperation Report ICR 94-09.

Uchida, M., T. Doe, A. Sawada, W. Dershowitz, and P. Wallmann, 1997. FracMan Discrete Fracture Modeling for the Aspo Tunnel Drawdown Experiment. Swedish Nuclear Fuel and Waste Management Company, Äspö Hard Rock Laboratory, International Cooperation Report ICR 97-03.

Widén, H. and Walker, D. 1999. SR 97 – Alternative models project. Stochastic Continuum modelling of Aberg. Swedish Nuclear Fuel and Waste Management Company (SKB), Technical Report R-99-42. ISSN 1402-3091.

Winberg, A. 1997. "Test plan for the TRUE Block Scale Experiment", Swedish Nuclear Fuel and Waste Management Co, Äspö Hard Rock Laboratory. International Cooperation report ICR 97-02.

Winberg, A., Andersson, P., Hermanson, J., Byegård, J., Cvetkovic, V. and L. Birgersson. 2000. "Final report of the first stage of the Tracer Retention Understanding Experiments", Swedish Nuclear Fuel and Waste Management Company (SKB), Technical Report TR-00-07. ISSN 1404-0344.

Winberg, A., Andersson, P., Byegård, J., Poteri, A., Cvetkovic, V., Dershowitz, B., Doe, T., Hermanson, J., Gómez-Hernández, J-J., Hautojärvi, A., Billaux, D., Tullborg, E-L., Meier, P. and A. Medina 2002. TRUE Block Scale Project. Final Report – 4. Synthesis of flow, transport and retention in the block scale. Swedish Nuclear Fuel and Waste Management Company. Technical Report TR-02-16.

Appendices

Appencix A – Scaling rules

Much of the work related to the development of scaling rules and correlations to apply properties to defined structures, and to generate synthetic structures and assign properties to them. These derivations are distributed throughout the preceding report text where they are first used. This section attempts to provide a more systematic treatment of the scaling rules and correlations.

A.1 Size

The sizes of structures has been recorded at three scales: the borehole/canister hole/tunnel) scale (0.1 to 5 m), the 200-m block-scale, and the 2000-m site scale. In between these scales, there are gaps in data, which reflect discontinuities in the scales of measurement rather than discontinuity in the occurrences of fractures, features and structures at those scales.

The fractal approach is very popular for integrating data at a variety of scales. Figure A-1 illustrates the three scales of data (Background fractures, TRUE Block-Scale, and Task 5) normalised by area and plotted on a single log-log plot. Although the re-normalisation process provides for considerable artifice (LaPointe, 2000), we do obtain a reasonable straight line with a fractal dimension of 1.6.

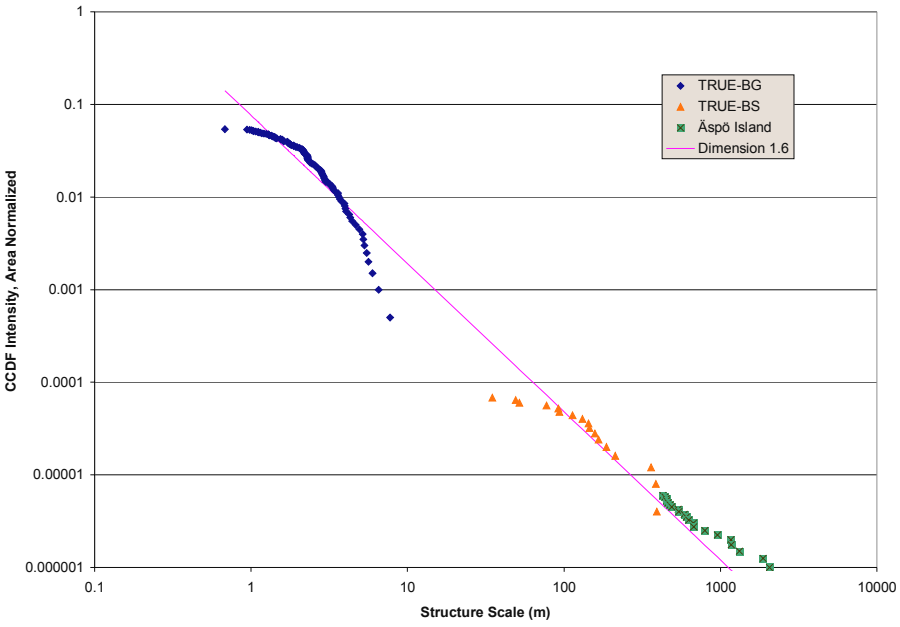

Figure A-1. *The three scales of data (Background, TRUE Block Scale, and Task 5) normalised by area and plotted on a single log-log plot.*

This is exactly the same dimension obtained by LaPointe (1999) in his evaluation of lineaments in the Simpevarp area. The total intensity of structures with transmissivity greater than 10^{-9} m^2/s can be found by adding together each of the intensities found at the different scales (Table A-1). In Table A-1, the total intensity is adjusted to account for under-sampling of the missing scales. This is estimated at 30% by a visual inspection of Figure A-1.

Table A-1. Fracture intensity.

Set	P_{32}	Scale
Background fractures	0.29	1 to 20-m
100-m scale	0.02	20 to 200-m
1000-m	0.0043	200 to 2000-m
Total	0.3143	1 to 2000-m
30%	0.09429	missing
Total	0.40859	

Figure A-2 illustrates synthetic fractures of scales 10 to 500-m generated in the 2000-m model using the fractal size distribution, with the 200-m scale conductive fracture orientation distribution. Figure A-3 presents the size distribution for these synthetic fractures.

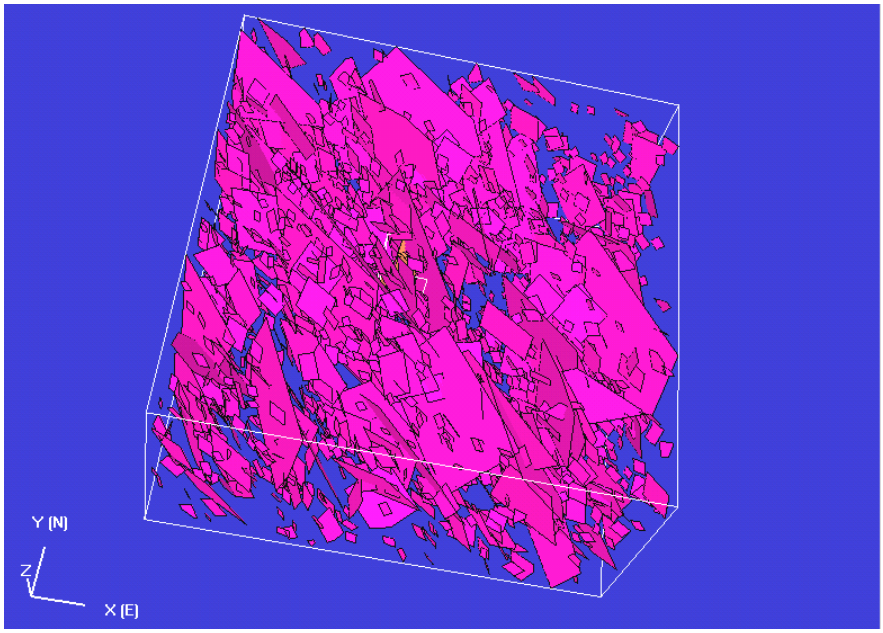

Figure A-2. *Power law (D=1.6) Fracture Model, 10% intensity shown, 20m to 500-m Structures, 2000-m Scale.*

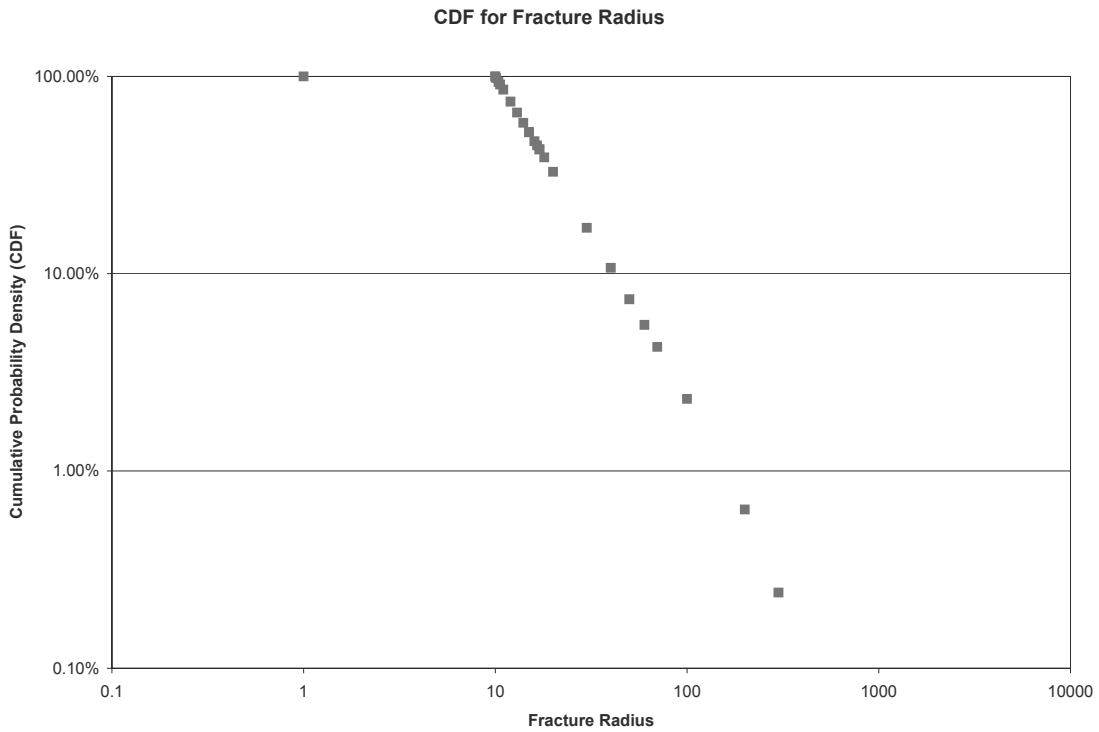

Figure A-3. *Power Law Fractures in the 200-m Scale Model*

A.2 Geological Width

Larger structures such as fracture zones at Äspö have thicknesses on the order of meters to tens of meters. Within these thicknesses, the flow and transport pathways are generally made up of just a few individual fractures. However, it is possible that there is a correlation between the structure geological thickness and the structure size and between the geological thickness and the number of transport pathways. Such relationships would support development of scaling rules for the larger structures.

Figure A-4 illustrates the relationship between structure size and geological thickness, as estimated from tunnel intersections. Figure A-5 illustrates the relationship between geological thickness and effective hydraulic transmissivity. No clear correlation is visible for either of these cases. Consequently, the concept of geological width does not seem to be useful for scaling of synthetic fractures. This implies that even for the largest structures, the transmissivity of a few individual flow paths determines the hydraulic behaviour of the entire zone.

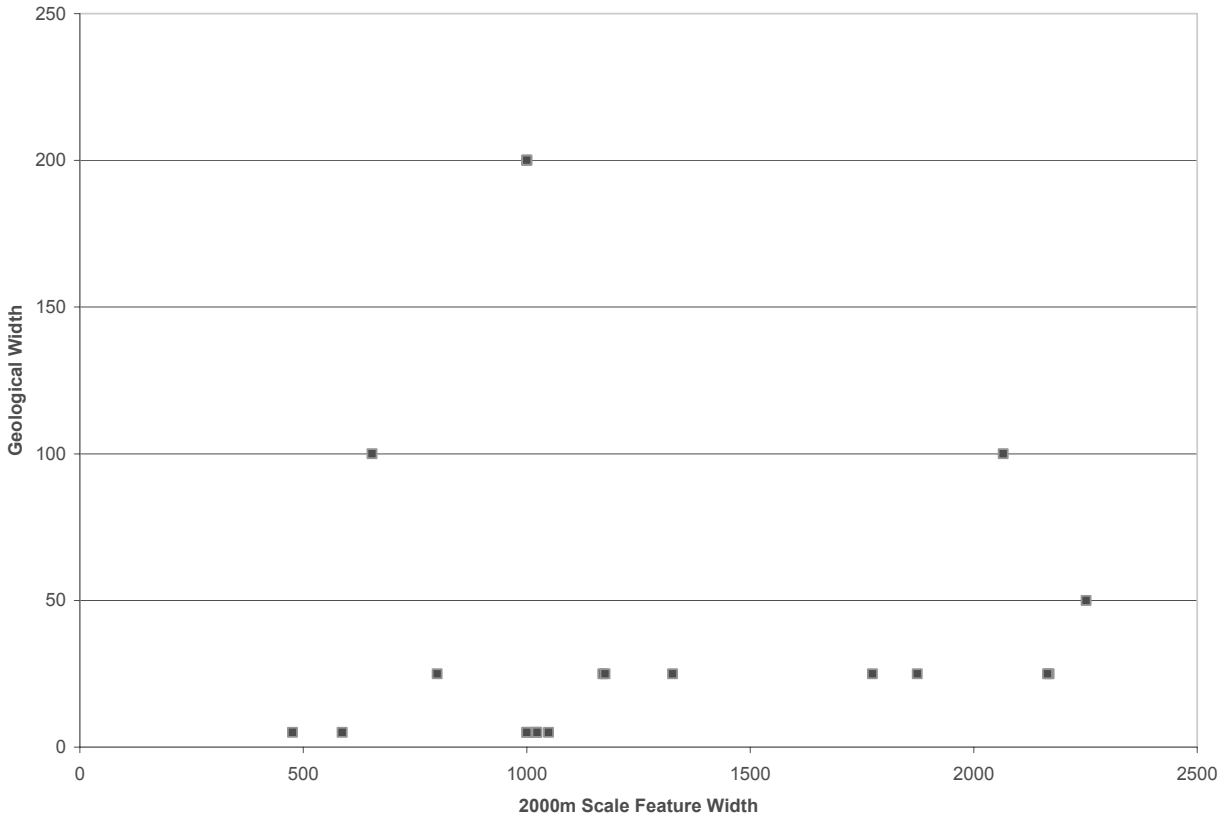

Figure A-4. *Correlation between structure size (Length) and Geologic width, 1000-m scale Äspö structures.*

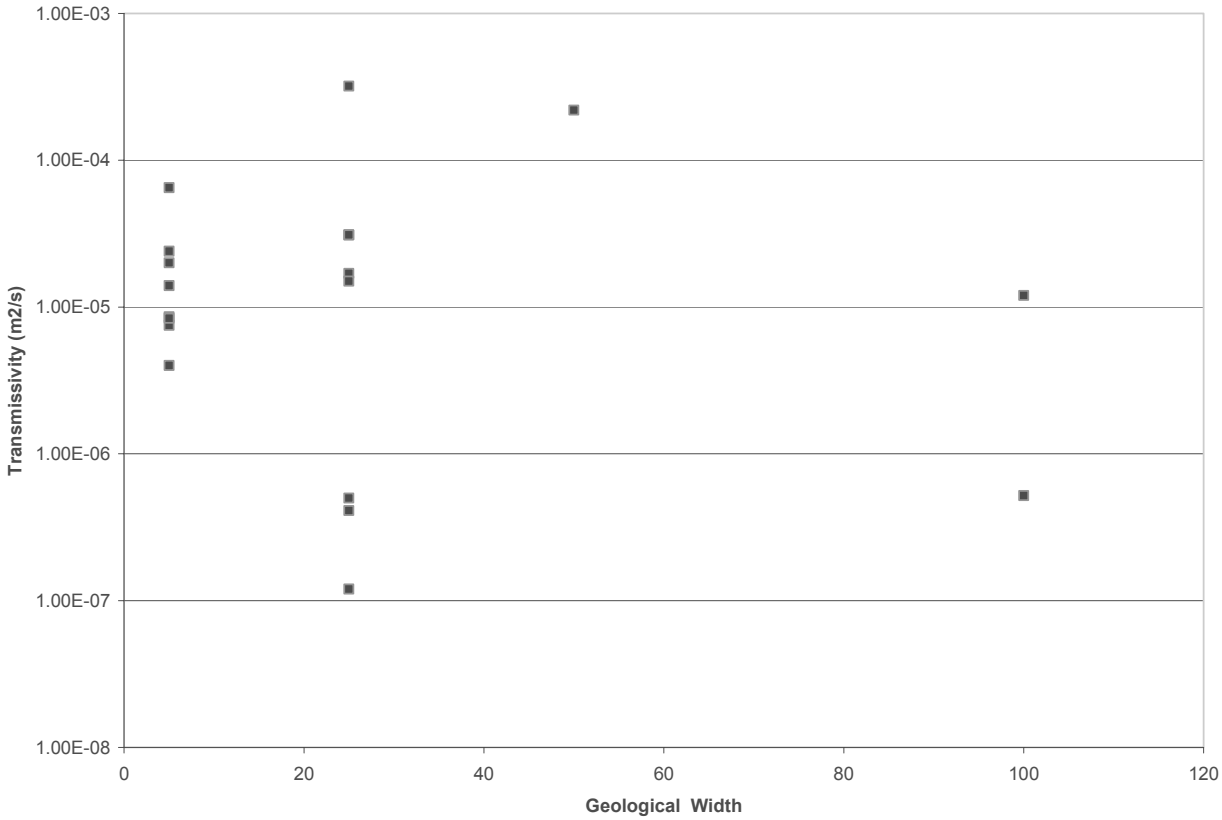

Figure A-5. *Correlation between Geologic Width and Transmissivity, 1000-m scale Äspö structures.*

A.3 Size and Transmissivity

While no clear correlation was found between geological width and transmissivity for 1000-m scale deterministic structures, there is a clear relationship between fracture size and transmissivity. Figure A-6 was generated by combining fracture transmissivities from the TRUE-Block Scale background fractures, deterministic 100-m scale structures from TRUE Block Scale and deterministic 1000-m scale structures from the Task 5 model. For the background fractures, transmissivities were assigned to fractures directly from Posiva flow logging. The sizes of the background fractures are not known, however, and were therefore assigned from the fracture-size distribution without assuming any correlation. For the 100-m scale and 1000-m scale deterministic structures, the transmissivities used to derive Figure A-6 are larger-scale effective transmissivities based on packer testing, and confirmed by DFN modelling. These transmissivities are assigned to individual structures, and each of these structures has an estimated trace length based on a combination of geophysical, geological, and hydrologic evidence.

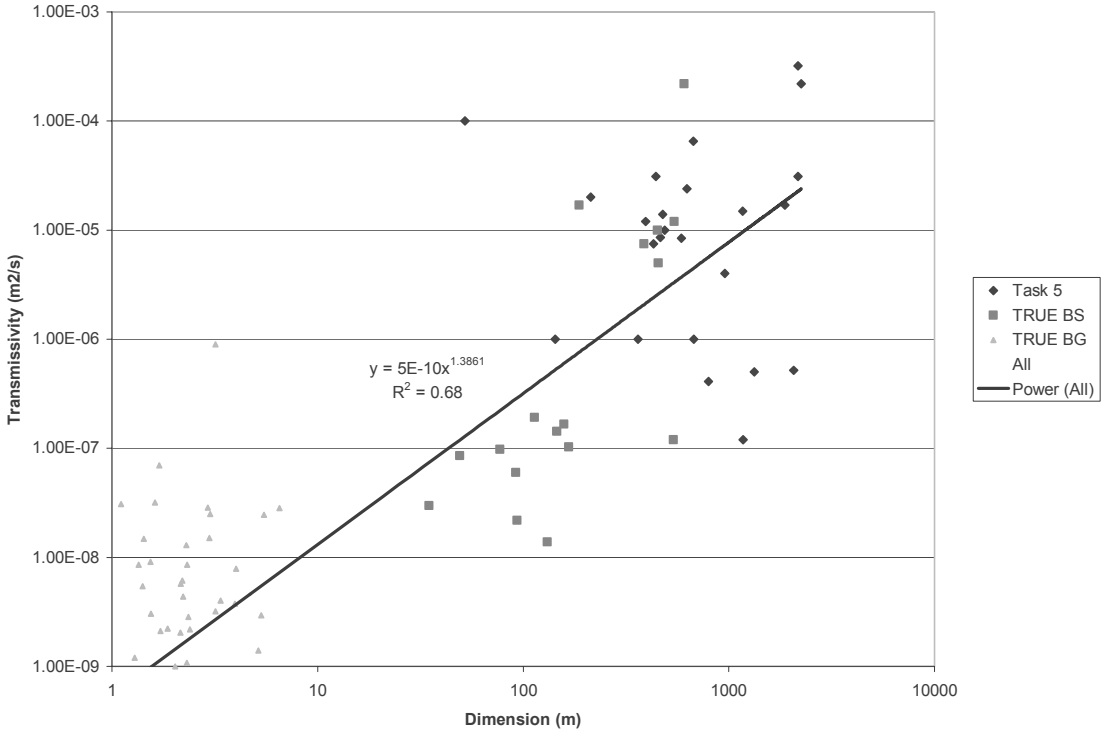

Figure A-6. *Relationship between structure size and transmissivity.*

At any given scale, there is no clear correlation between size and transmissivity. This is to be expected for the background fractures, which had their size assigned uncorrelated to transmissivity. However, for the 100-m and 1000-m structures, no correlation would be seen if this data were plotted by itself. However, by plotting the data together from all three scales, a pattern of a transmissivity-dimension correlation emerges. We have used this relationship to assign transmissivity to all synthetic structures. The correlation between transmissivity and structure size for synthetic structures preserves the same correlation coefficient ($R^2 = 0.7$) found from the Figure A-6.

A.4 Transport Properties

The aperture of structures is described in Chapter 4.3. Aperture can be related to the flow and transport properties. Commonly, the cubic law, $e_h = \sqrt[3]{(12\mu T)/\rho g)}$ relates transmissivity to an idealised, perfect parallel-plate aperture, which can be denoted the hydraulic aperture, e_h. This aperture will be less than the actual physical fracture wall separation, often by a considerable amount, as the fracture walls have a roughness and portion that do not participate directly in the flow streams.

For a completely filled fracture, the hydraulic aperture e_h is related to transmissivity according to $e_h = T/K$ where K is the hydraulic conductivity (m/s). The relationship between hydraulic aperture and transmissivity is therefore between 1/3 and 1.
The hydraulic aperture e_t can be correlated to transmissivity in a general form as (Uchida et al., 1994):

$e_h = \text{a } T^{\text{b}}$

According to this relationship and hydraulic experiments in the TRUE Block Scale block, a=0.46 (0.25 to 0.60), and b=1/2.

The storage aperture, e_S, is can be determined from storativity by $e_S = S/(\rho g C)$, where C is fluid compressibility and fracture normal stiffness is neglected. This aperture is influenced by all connected pore spaces in the fracture, and may be considered a maximum value for aperture. Storativity is unlikely to be a concern in the semi-synthetic model, as all the calculations will be made assuming steady state.

The transport aperture e_t is used to relate water particle velocity v (m/s) to flux q (m^2/s),

$v = q/e_t$

Transport aperture e_t can be related to hydraulic aperture e_h as,

$e_t = \text{c } e_h$

The value of c ranges from 0.135 to 0.300 in calibrations to TRUE Block Scale tracer experiments (Dershowitz et al., in prep).

The thickness of the alteration zone of deterministic structures is assumed to vary from 0.2 m (Type 1) to 0.1 m (Type 2) for 100 m structures. Scaled geometrical entities applicable to background fractures and 1000 m structures are discussed in Section 4.3

A.5 Geological Structure Type and Complexity Factor

Geological Structure Type is clearly correlated to fracture size. Geological structure type was assigned to each of the TRUE Block Scale deterministic 100 m structures and Task 5 structures (Tables 5-2 through 5-5). Based on these tables, the cumulative probability that structures will be of Type 1 can be calculated as illustrated in Figure A-7. As larger structures are considered, the cumulative probability of complex structures (Type 1) increases exponentially, converging to 100% for the largest structures. This can be approximated by a relationship between fracture size and fracture type as, $P[\text{Type-1}] = 1\text{-}e^{-0.7\ S/So}$, where S_0 is 20-metress and S is the structure length.

This equation was used to assign primary geological structure type to each of the synthetic fractures at the 200-m scale, as shown in Figure A-8, and to the background fracture population.

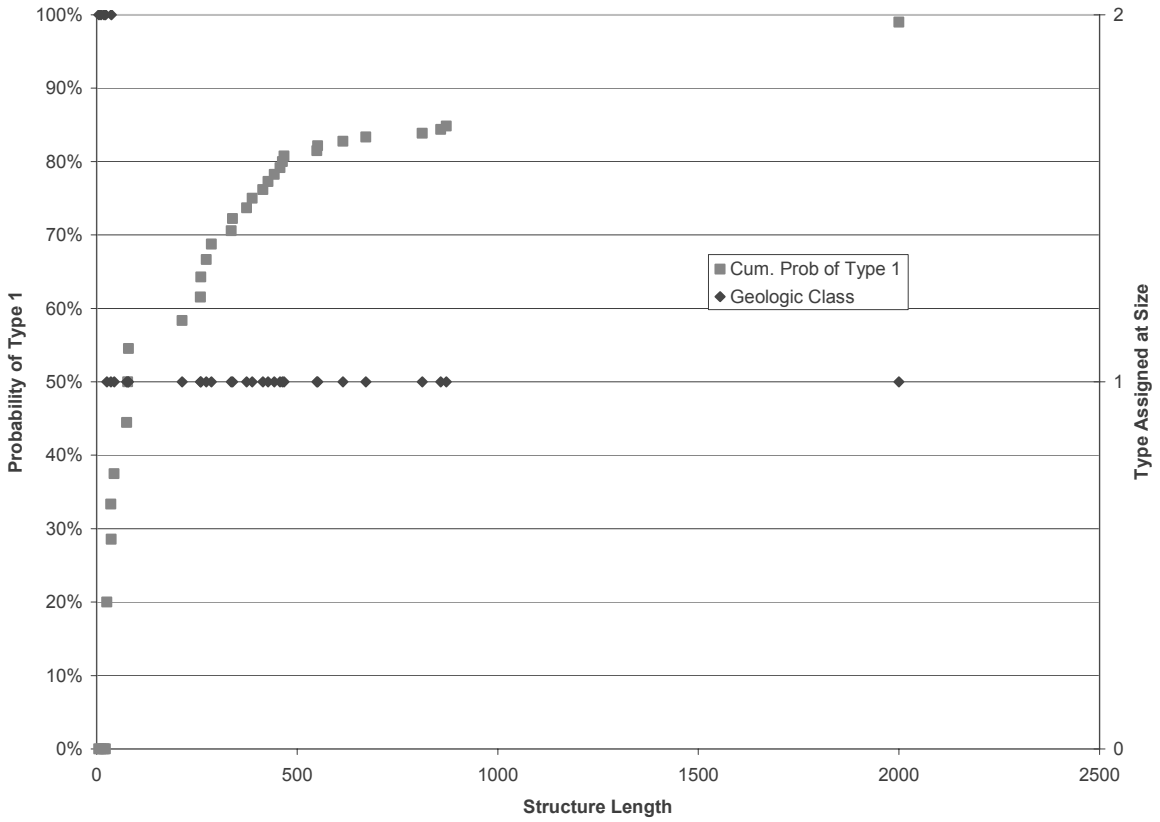

Figure A-7. *Geological Structure Type for 100-m and 1000-m structures.*

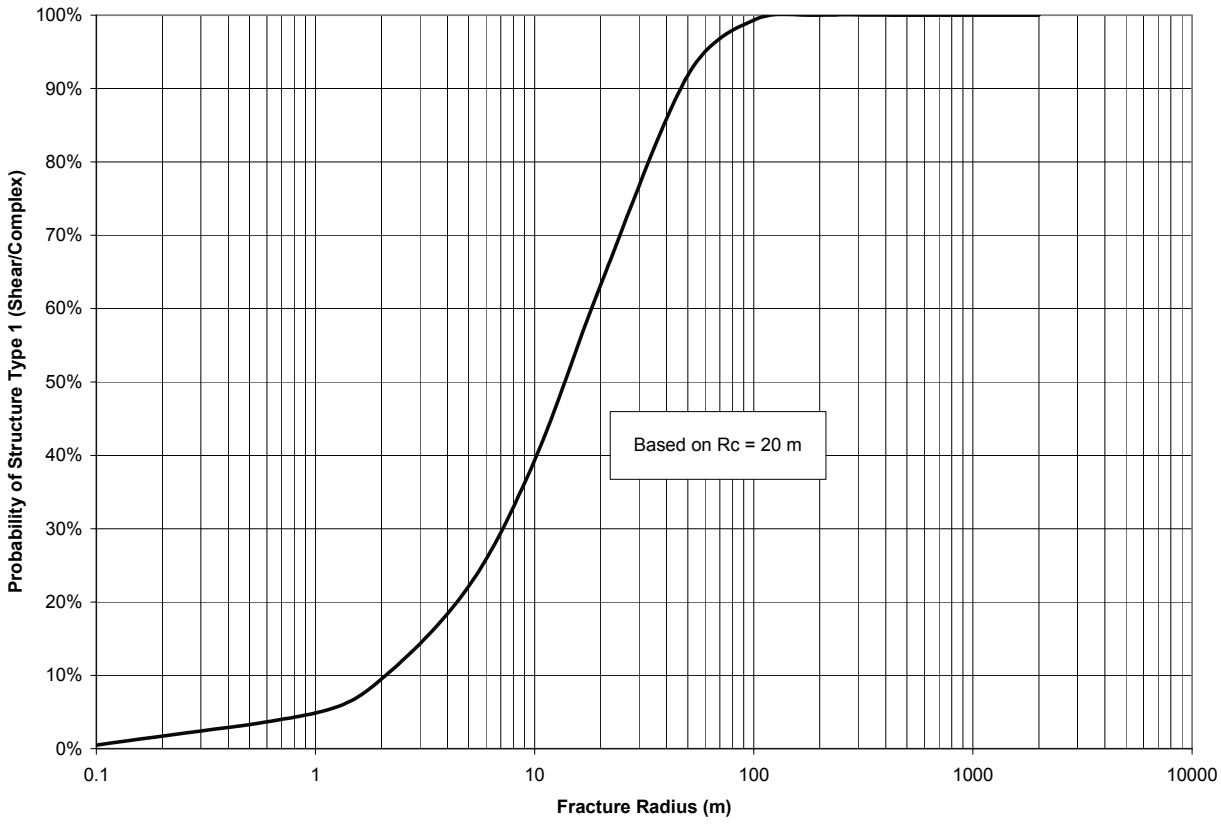

Figure A-8. *Assignment of Geological Structure Type (Type-1).*

Structural complexity is also related to fracture size – smaller fractures are generally Type 1 or 2, while larger structures tend to be more complex. However, the number of flow paths does not scale directly with fracture size – *in situ* transport experiments indicate that structures of 50-metre thickness can still be controlled by a few centimetre wide fractures.

In order to assign structural complexity to fractures, a *Complexity Factor* ranging from 1 to 5 was defined. The complexity factor was assigned to each of the deterministic 100-m scale structures based primarily on examination of BIPS logs.

Based on examination of BIPS logs, approximately 80% of background fractures are of Complexity Factor 1, and 20% are Complexity Factor 2. For the TRUE Block Scale deterministic structures, 64% are Complexity Factor 2 and 36% are Complexity Factor 3. The 1000-m scale structures are generally of Complexity Factor 3 to 5, although no detailed assignment has been made. This indicates some correlation between complexity and fracture size, although the correlation is definitely not one-to-one.

Figure A-9 illustrates the relationship between complexity and size for the TRUE Block Scale deterministic structures. For lengths less than 50-m, all of the structures are of Complexity Factor 2, such that the probability of Complexity Factor 3 is zero. As the size increases, more structures with Complexity Factor 3 structures are encountered, until the overall population percentage of Complexity Factor 3 (36%) is reached.

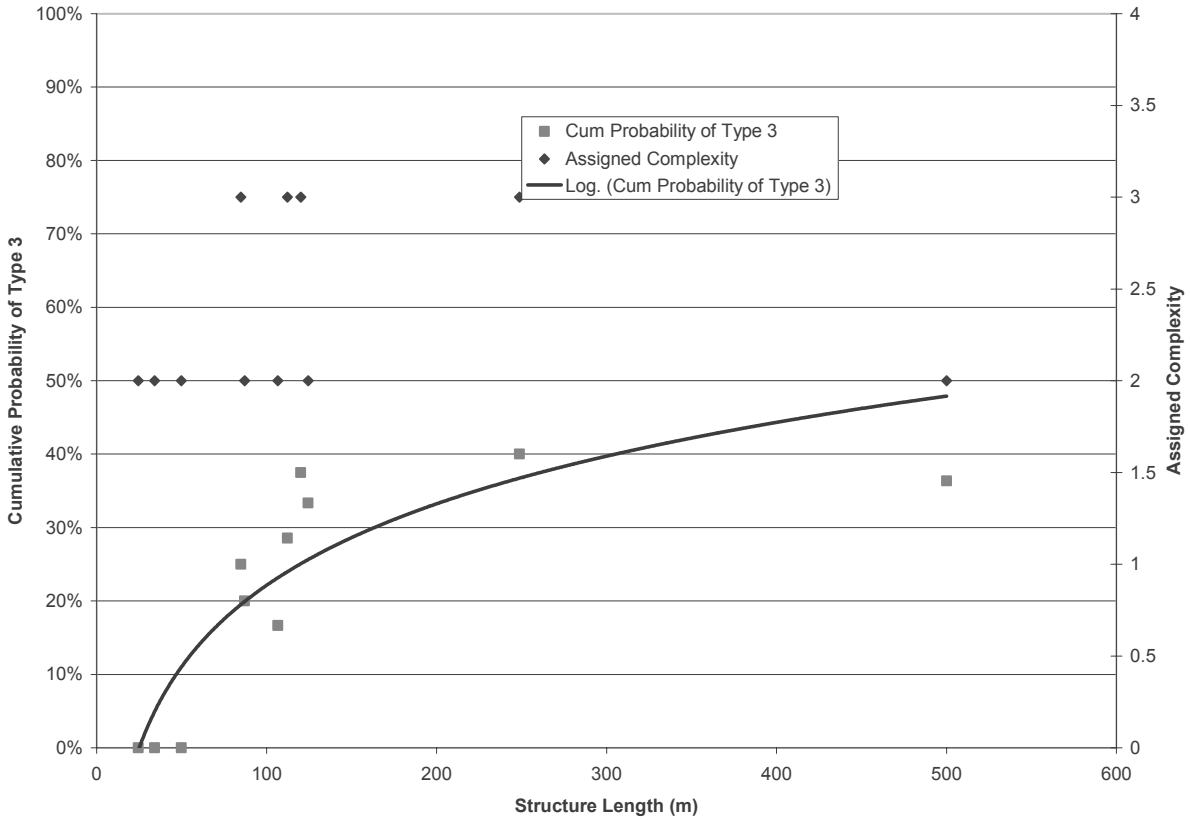

Figure A-9. *Complexity Factor and Size for 100-m Scale Structures.*

Figure A-9 includes a curve illustrating an exponential approximation to the observed percentage of Complexity Factor 3.

To assign complexity factors to background structures, a simple relationship of 80% Complexity Factor 1, and 20% Complexity Factor 2 was used. For the synthetic 100-m scale structures, the complexity factor was assigned correlated to length according to the relationship

$P[\text{Complexity Factor3}] = 1\text{-}e^{-S/So}$,

where S_0 is 200-meters and S is the structure length. The cumulative probability of Complexity Factor 3 for the synthetic structures is compared with the 100-m scale TRUE Block Scale structures is illustrated in Figure A-10.

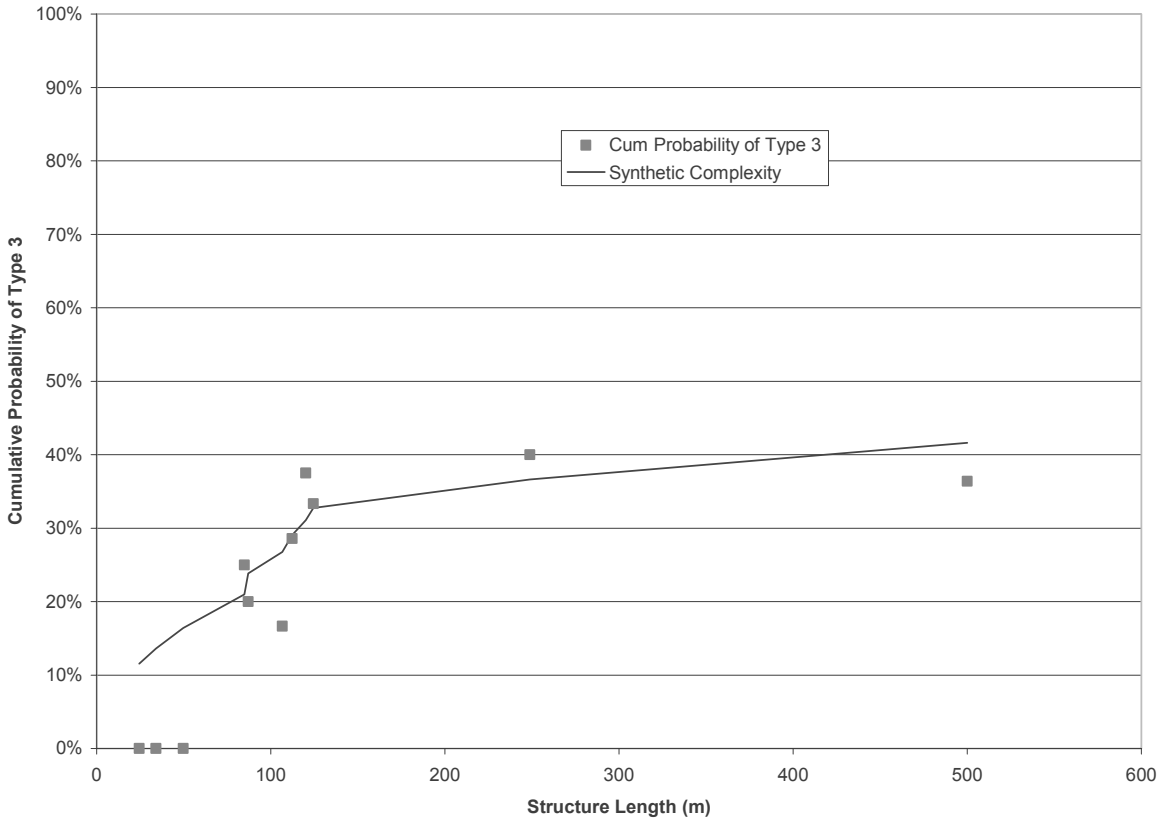

Figure A-10. *Assignment of Complexity Factor 3 to synthetic for 100-m scale structures.*

References

Dershowitz, W., Klise, K., Fox, A., Takeuchi, S. and M. Uchida (in prep). Channel Network and discrete fracture network analysis of hydraulic interference and transport experiments and prediction of Phase C experiments. Swedish Nuclear Fuel and Waste Management Company. Äspö Hard Rock Laboratory. International Progress Report IPR-02-29.

La Pointe, P.R, Cladouhos, T.T. and S. Follin 1999. Calculation of displacements on fractures intersecting canisters induced by earthquakes : Aberg, Beberg and Cberg examples. Swedish Nuclear Fuel and Waste Management Company. SKB Technical Report TR-99-03.

La Pointe, P.R, Cladouhos, T.T., Outters, N. and S. Follin 2000. Evaluation of the conservativeness of the methodology for estimating earthquake-induced movements of fractures intersecting canisters. Swedish Nuclear Fuel and Waste Management Company. SKB Technical Report TR-00-08.

Uchida, M., Doe, T., Dershowitz, W., Thomas, A., Wallmann, P. and A. Sawada, 1994. Discrete-fracture Modeling of the Äspo LPT-2, Large-Scale Pumping and Tracer Test. Swedish Nuclear Fuel and Waste Management Company, Äspö Hard Rock Laboratory, International Cooperation Report ICR 94-09.

Appendix B: Example assignment of properties to synthetic structures

B.1 Overview

The present report derives a number of new procedures to assign properties to synthetic structures. This appendix presents a simple demonstration of the use of these relationships. The following procedures are presented:

- Monte Carlo simulation of structure size
- Assignment of hydraulic and transport properties
- Assignment of geological properties and microstructural properties

B.2 Structure Length

Structure size is represented by a typical dimension, refereed to as length (L), or by the equivalent radius (R). Structure size for deterministic 100-m and 1000-m scale structures is provided as part of the hydrostructural model. For stochastic structures, the structure radius is calculated from a radius distribution as the structure is generated during Monte Carlo simulation.

For example, for stochastic 100-m scale structures, Table 3-7 defines the fracture radius as a Lognormal distribution with mean 108 m, and standard deviation 55 m. To generate a single synthetic structure, the radius would be selected from that Lognormal distribution by Monte Carlo simulation. For the current example, we will assume that a radius of 100 m was selected.

For a structure of 100 m radius, the fracture length depends on the orientation of the fracture. In general, the length is between 0.8 and 2 times the radius. For the current example, we generated the fracture stochastically, and calculated the length of the fracture as the trace in a horizontal plane. The length of the example synthetic structure is 170 m.

B.3 Hydraulic and transport properties

Fracture hydraulic properties are transmissivity T (m^2/s), hydraulic aperture (e_h), storativity S, and transport aperture (e_t).

The general form for correlation between fracture size (length-dimension, metres) and transmissivity (m^2/s) is:

$T = a\, L^b$

The transmissivity T (m^2/s) is related to length L (m) as (Figure 4-1 in report)

$T = 5\ 10^{-10}\ L^{\ 1.386}$

This relationship has a correlation coefficient ρ of 0.68, indicating significant scatter in the relationship between transmissivity and length. Therefore, transmissivity was assigned using Monte Carlo simulation to achieve a similar scatter. For each fracture, the fracture length is calculated as the trace in the horizontal plane. The fracture transmissivity is then assigned stochastically, using the relationship,

$T(L,r) = 5\ 10^{-10}\ L^{\ (1.386\ +0.3r)}$

where *r* is a uniform (-0.5,0.5) pseudo-random deviate. In this example the random deviate r was selected as r = -0.124, such that transmissivity T is assigned as 5.13×10^{-7} m^2/s.

Hydraulic aperture e_h, storativity S and transport aperture e_t are assigned directly correlated to structure transmissivity, using the relationships,

$e_h = a_h\ T^{\ b_h}$

$S = a_s\ T^{\ b_s}$

$e_t = a_t\ e_h$

where a and b are empirical constants. From Section 4.3 above, the constants a_h ,a_s and a_t are 0.5, 0.46 and 0.125 respectively. The constants b_h and b_s is 0.5.

Applying these equations with a transmissivity of 5.1×10^{-7} m^2/s,

$e_h = 3.58\ 10^{-4}$ m

$S = 3.3\ 10^{-4}$, and

$e_t = 4.48\ 10^{-5}$ m

B.4 Geological and Microstructural Properties

Geological and microstructural properties are defined in Chapter 2 in terms of Geological Structure Types and Complexity Factors.

Geological Structural Type is assigned using a correlation to length,

$$P[\text{Type 1}] = 1\text{-}e^{-0.7\ S/So},$$

where S_0 is 20 metres and S is the structure length/size. Given that our example structure has a length of 170 m, the probability that it is primarily of Geological Structure Type 1 is equal to 99.7%. Therefore, our example structure is of Type 1, provided the random Uniform (0,1) number r used to assign structure type is less than 0.997. The random number r selected was 0.567, and the example structure was therefore assigned as Geological Structure Type 1.

The variability of geological structure type in a given structure is specified by the complexity factor defined in Table 4-5 of the main report, cf. Table B-1.

Table B-1. Definition of Complexity Factor assigned to modelled structures, cf Table 4-3 for application to 100 m scale deterministic structures.

Complexity Factor	Number of (sub-parallel) conductive features/fractures per structure	Percent of primary geological structure type or combination of geological structure types (by area)
1	1	90-100%
2	1 to 2	70 to 100%
3	1 to 3	50 to 90%
4	3 to 10	50 to 90%
5	10+	50 to 90%

To assign complexity factors to background fractures, a simple relationship of 80% Complexity Factor 1, and 20% Complexity Factor 2 was defined in Chapter 4. For the synthetic 100 m scale structures, the Complexity Factor was assigned correlated to length according to the relationship

$$P[\text{Complexity Factor 3}] = 1\text{-}e^{-S/So},$$

where S_0 is 200 metres and S is the structure length/size. For the example 170 m scale structure, the probability of Complexity Factor 3 is equal to 57.3%. Therefore, if the random Uniform (0,1) number r used to assign complexity factor is less than 0.573, the structure would be assigned as Complexity Factor 3, and otherwise it would be assigned as Complexity Factor 2. In this case, r was generated as 0.896, and a Complexity Factor of 2 was therefore assigned to our example structure.

From Table 4-5 in the main report, the Complexity Factor of 2 corresponds to 1 to 2 subparallel conductive structures, with 70 to 100% of the primary geological structure type. For a simplified implementation, the example structure could therefore be implemented as a single structure of geological structure Type 1. For a more realistic model, the example structure might be a single discrete feature over 50% of its extent, and two discrete features over 50% of its extent. Where there were two discrete features, the second discrete feature would be of Geological Structural Type 1 over 70% of its length, and Geological Structural Type 2 over 30% of its length.

B.5 Microstructural Model Parameters

The microstructural model parameters for 100-m scale structures such as our example structure are provided in Section 4.4.3 of the main report. These parameters are applied to each of the discrete features that make up the structure. Where the discrete feature is of Geological Structure Type 1, the properties are given in Table 4-10, and where they are of Geological Structure Type 2, they are as given in Table 4-11.